
Study of Plutonium Oxide Powder Emissions from Simulated Shipping Container Leaks

Prepared by J. D. Yesso, W. J. Madia, G. H. Beatty, E. W. Schmidt,
L. C. Schwendiman, J. Mishima

Battelle Columbus Laboratories

Pacific Northwest Laboratory
Operated by
Battelle Memorial Institute

Prepared for
U.S. Nuclear Regulatory
Commission

NOTICE

This report was prepared as an account of work sponsored by an agency of the United States Government. Neither the United States Government nor any agency thereof, or any of their employees, makes any warranty, expressed or implied, or assumes any legal liability or responsibility for any third party's use, or the results of such use, of any information, apparatus product or process disclosed in this report, or represents that its use by such third party would not infringe privately owned rights.

Available from

GPO Sales Program
Division of Technical Information and Document Control
U. S. Nuclear Regulatory Commission
Washington, D. C. 20555

Printed copy price: \$4.25

and

National Technical Information Service
Springfield, Virginia 22161

Study of Plutonium Oxide Powder Emissions from Simulated Shipping Container Leaks

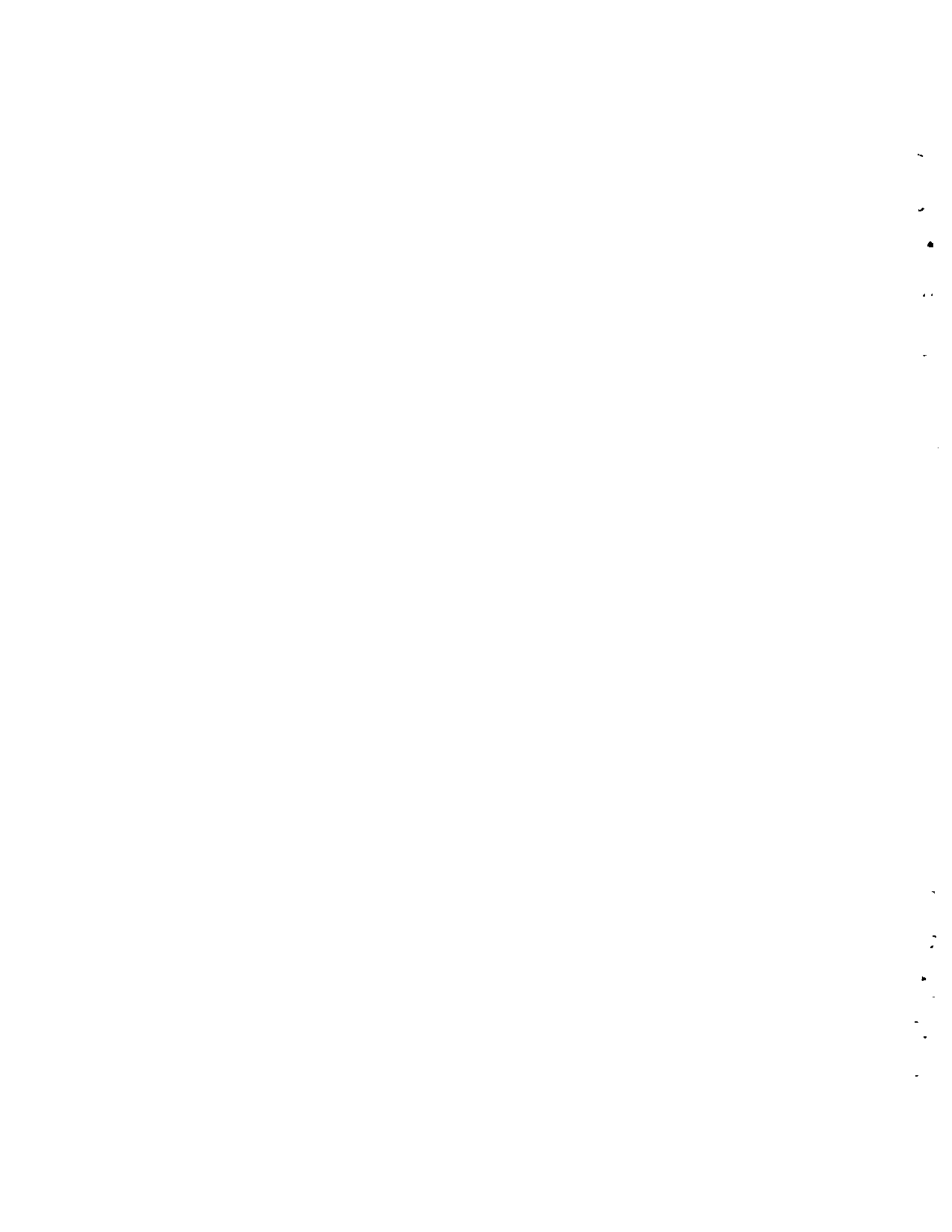
Manuscript Completed: May 1980
Date Published: August 1980

Prepared by
J. D. Yesso*, W. J. Madia*, G. H. Beatty*, E. W. Schmidt*,
L. C. Schwendiman**, J. Mishima**

* Battelle Columbus Laboratories
505 King Avenue
Columbus, OH 43201

** Pacific Northwest Laboratory
P.O. Box 999
Richland, WA 99352

Prepared for
Division of Safeguards, Fuel Cycle and Environmental Research
Office of Nuclear Regulatory Research
U.S. Nuclear Regulatory Commission
Washington, D.C. 20555
NRC FIN No. B2093



ABSTRACT

To provide data to facilitate the predictions of PuO₂ emissions through leaks in PuO₂ shipping containers under accident conditions, a series of experiments was conducted using PuO₂ powder and an experimental system designed to simulate a shipping container leak. Over two hundred experiments were completed. The experimental parameters investigated were the leak size/type, internal system pressure, agitation of the apparatus, leak orientation with respect to the powder location and the run time. No single parameter appeared to have any observable effect on the quantities of PuO₂ emitted. However, there was an apparent dependency on the interaction between the orifice area and the internal pressure. The dependency took the form of a function of $A\sqrt{P}$. Although this functional form was suggested by the data, the data were not sufficient to allow a more detailed function to be determined. The results of experiments in which the run time was variable produced the observation that changes in the run time did not result in changes in the quantities of PuO₂ emitted. This observation led to the conclusion that the majority of PuO₂ observed is emitted during the initial pressurization of the leak tube.

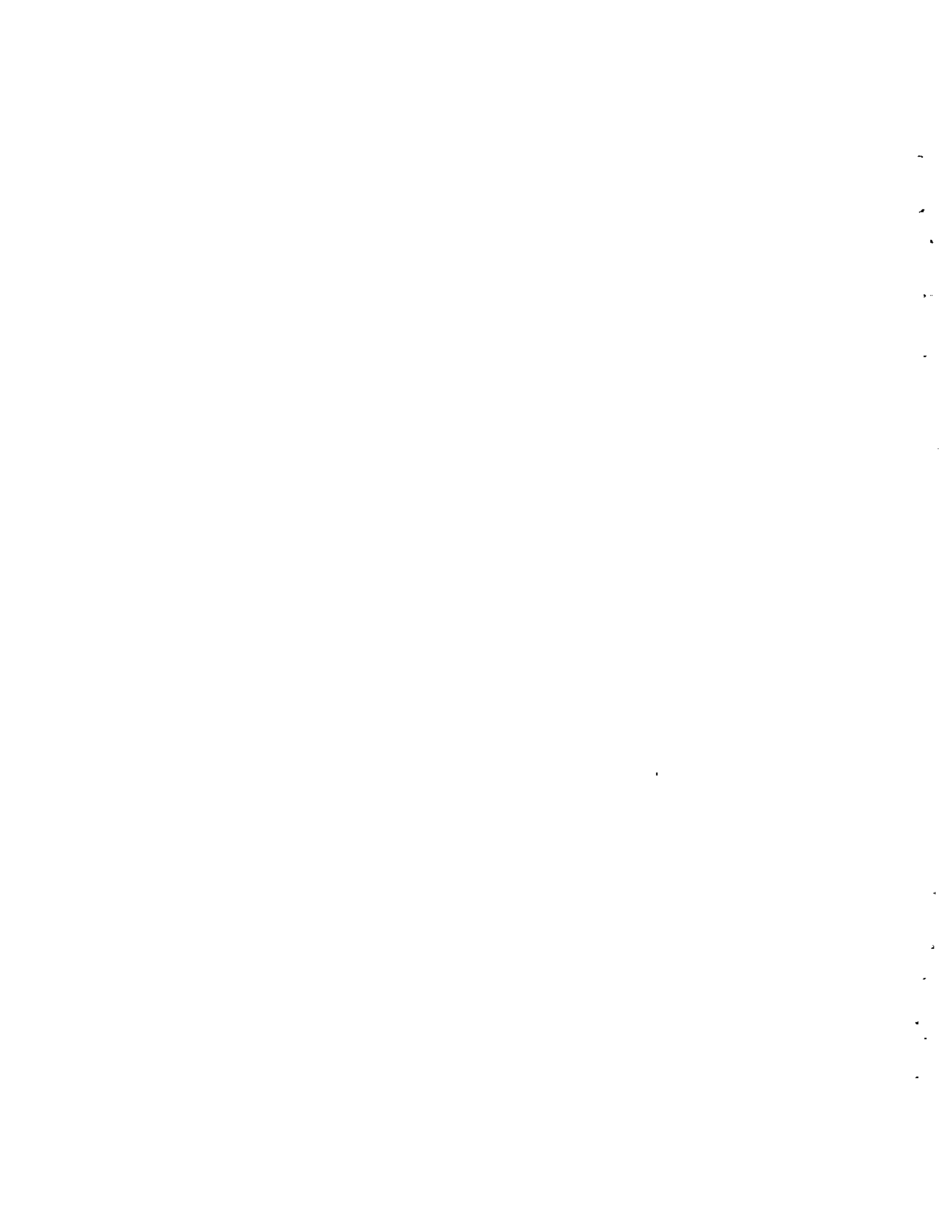


TABLE OF CONTENTS

| | <u>Page</u> |
|--|-------------|
| ABSTRACT | iii |
| FIGURES AND TABLES | vii |
| INTRODUCTION | 1 |
| OBJECTIVE | 3 |
| SUMMARY | 5 |
| EXPERIMENTAL | 7 |
| EXPERIMENTAL PROCEDURES | 17 |
| PARTICLE SIZING AND COMPARISONS | 17 |
| SPECIFIC ACTIVITY OF PuO ₂ POWDER | 17 |
| HELIUM FLOW RATES | 21 |
| RUN TECHNIQUE | 21 |
| ThO ₂ SIMULANT EXPERIMENTS | 31 |
| PuO ₂ EXPERIMENTS | 37 |
| EFFECT OF EXPERIMENTAL PARAMETERS ON THE SIZE DISTRIBUTION OF THE PuO ₂ EMISSION | 37 |
| CAPILLARY LEAK EXPERIMENTS | 44 |
| EFFECT OF EXPERIMENTAL PARAMETERS ON THE QUANTITY OF PuO ₂ EMISSION | 44 |
| EFFECT OF EXPERIMENTAL PARAMETERS ON THE SIZE DISTRIBUTION OF THE PuO ₂ EMISSION | 47 |
| SIMULATED CRACK EXPERIMENTS | 50 |
| PARAMETRIC DEPENDENCE OF PuO ₂ EMISSIONS THROUGH ORIFICES | 53 |
| VARIABILITY OF THE DATA | 54 |

TABLE OF CONTENTS
(CONTINUED)

| | <u>Page</u> |
|---|-------------|
| BACKGROUND SUBTRACTION | 54 |
| COLLECTION TIME DEPENDENCE | 55 |
| PARAMETRIC DEPENDENCY OF ORIFICE DATA | 56 |
| PuO ₂ MASS TO HELIUM FLOW CORRELATION | 72 |
| REFERENCES | 75 |
| APPENDIX A - LASER OPTICAL PARTICLE MONITORING SYSTEM (LOPMS) . . . | A-1 |
| EXPERIMENTAL | A-1 |
| PARTICLE LEAK RATE VERSUS TIME | A-4 |
| PARTICLE SIZE DISTRIBUTION | A-4 |
| CALIBRATION OF MCA | A-4 |
| MEASUREMENTS WITH ThO ₂ | A-8 |
| DISCUSSION | A-9 |
| CONCLUSIONS | A-10 |
| APPENDIX B - TABULATION OF LEAK RATE EXPERIMENTS DATA | B-1 |

FIGURES

| | <u>Page</u> |
|--|-------------|
| 1 SCHEMATIC DIAGRAM OF EXPERIMENTAL SET-UP USED FOR LEAK RATE EXPERIMENTS | 8 |
| 2 LEAK TUBE USED FOR THE PLUTONIA EXPERIMENTS | 9 |
| 3 SCHEMATIC DRAWING SHOWING ORIFICE END OF INCONEL 600 LEAK TUBE USED FOR THORIA SIMULANT EXPERIMENTS | 10 |
| 4 50- μ m-ID x 44-cm-LONG CAPILLARY LEAK | 12 |
| 5 CROSS SECTION OF 50- μ m-ID CAPILLARY TUBE | 13 |
| 6 ATOMIZATION OF SNOOP (A LIQUID LEAK DETECTOR) BY HELIUM FLOW THROUGH THE CAPILLARY LEAK ASSEMBLY | 15 |
| 7 SCHEMATIC SHOWING CONFIGURATION OF SIMULATED CRACK | 16 |
| 8 AERODYNAMIC SIZE DISTRIBUTIONS OF PuO ₂ and ThO ₂ POWDERS | 18 |
| 9 GEOMETRIC SIZE DISTRIBUTION OF PuO ₂ and ThO ₂ POWDER | 19 |
| 10 GEOMETRIC SIZE DISTRIBUTION OF PuO ₂ POWDER | 20 |
| 11 SCHEMATIC DEMONSTRATING CASCADE IMPACTOR OPERATION | 25 |
| 12 OUTSIDE VIEW OF CONTAINMENT BOX | 27 |
| 13 CUT-AWAY VIEW OF CONTAINMENT BOX | 28 |
| 14 SCHEMATIC SHOWING EXPERIMENTAL ARRANGEMENT | 30 |
| 15 EFFECT OF ORIFICE SIZE AND PRESSURE ON THE AVERAGE MEAN PARTICLE SIZE OF EMITTED PuO ₂ AT ROOM TEMPERATURE | 41 |
| 16 EFFECT OF TUBE POSITION ON THE AVERAGE MEAN PARTICLE SIZE OF PuO ₂ EMITTED THROUGH ORIFICES | 42 |
| 17 EFFECT OF VIBRATION ON THE EMISSION OF PuO ₂ POWDER THROUGH A 20- μ m ORIFICE | 43 |
| 18 EFFECT OF EXPERIMENTAL CONDITIONS ON THE AVERAGE EMISSION OF PuO ₂ POWDER THROUGH A 50- μ m-ID CAPILLARY AT ROOM TEMPERATURE | 46 |
| 19 PARTICLE SIZE DISTRIBUTION OF PuO ₂ EMISSION THROUGH A 50- μ m-ID x 4.4-cm-LONG CAPILLARY TUBE AT ROOM TEMPERATURE | 49 |

FIGURES
(CONTINUED)

| | <u>Page</u> |
|---|-------------|
| 20 DISTRIBUTION OF PLUTONIUM EMISSION (ON TRANSFORMED SCALE, Z) FOR EXPERIMENTAL REGION I ($A\sqrt{P} < 2000$) | 62 |
| 21 DISTRIBUTION OF PLUTONIUM EMISSION (ON TRANSFORMED SCALE, Z) FOR EXPERIMENTAL REGION II ($2000 \leq A\sqrt{P} < 20,000$) | 66 |
| 22 DISTRIBUTION OF PLUTONIUM EMISSION (ON TRANSFORMED SCALE, Z) FOR THREE EXPERIMENTAL REGIONS | 70 |
| A1 SYSTEM SETUP | A-2 |
| A2 LEAK TUBE USED FOR THE PLUTONIA EXPERIMENTS | A-3 |
| A3 RECORDING OSCILLOSCOPE TRACE OF PARTICLE EMISSION RATE | A-5 |
| A4 RELATIVE COUNTS VS. CHANNEL FOR 8- μ m MONODISPERSED DOP AEROSOL | A-6 |
| A5 RELATIVE COUNTS VS. CHANNEL FOR ThO ₂ TEST AEROSOL | A-7 |

TABLES

| | |
|--|----|
| 1 HELIUM LEAK RATES THROUGH ORIFICES AND CAPILLARIES | 11 |
| 2 SPECIFIC ACTIVITY OF THE PuO ₂ POWDER USED IN THE LEAK RATE EXPERIMENTS | 22 |
| 3 PLUTONIA ISOTOPIC COMPOSITION Pu LOT A-345 (ARHCO) ANALYZED BY TELEDYNE, INC. | 23 |
| 4 SUMMARY OF ROOM TEMPERATURE SIMULANT EXPERIMENTS USING ThO ₂ | 32 |
| 5 SUMMARY OF ELEVATED TEMPERATURE SIMULANT RUNS USING CASCADE IMPACTORS | 34 |
| 6 PARTICLE SIZE DISTRIBUTION OF PuO ₂ EMITTED THROUGH A 5- μ m ORIFICE AT ROOM TEMPERATURE | 38 |
| 7 PARTICLE SIZE DISTRIBUTION OF PuO ₂ EMITTED THROUGH A 10- μ m ORIFICE AT ROOM TEMPERATURE | 39 |

TABLES
(CONTINUED)

| | <u>Page</u> |
|---|-------------|
| 8 PARTICLE SIZE DISTRIBUTION OF PuO ₂ EMITTED THROUGH A 20- μ m ORIFICE AT ROOM TEMPERATURE | 40 |
| 9 SUMMARY OF PuO ₂ LEAK RATE EXPERIMENTS AT ROOM TEMPERATURE USING A 50- μ m-ID CAPILLARY | 45 |
| 10 PARTICLE SIZE DISTRIBUTIONS OF PuO ₂ EMISSION THROUGH A 50- μ m x 4.4-cm-LONG CAPILLARY TUBE AT ROOM TEMPERATURE | 48 |
| 11 PARAMETRIC MATRIX OF PuO ₂ EXPERIMENTS USING THE SIMULATED CRACK | 51 |
| 12 ARITHMETIC MEAN VALUE OF PuO ₂ POWDER LEAKED AND THE STANDARD DEVIATION FOR EACH EXPERIMENTAL CONDITION USING THE SIMULATED CRACK CONFIGURATION (MEAN/STANDARD DEVIATION) (in NEAREST ng) | 52 |
| 13 PARAMETRIC MATRIX OF PuO ₂ LEAK RATE EXPERIMENTS USING STANDARD ORIFICES | 57 |
| 14 PARAMETRIC MATRIX OF PuO ₂ LEAK RATE EXPERIMENTS USING STANDARD ORIFICES (DATA SET II) | 58 |
| 15 SUMMARY STATISTICS FOR REGION I, PHASE I | 61 |
| 16 SUMMARY STATISTICS FOR REGION I, PHASE II | 63 |
| 17 SUMMARY STATISTICS FOR REGION II, PHASE I | 64 |
| 18 SUMMARY STATISTICS FOR REGION II, PHASE II | 67 |
| 19 SUMMARY STATISTICS FOR REGION III, PHASE II | 68 |
| 20 SUMMARY STATISTICS FOR REGIONS I, II, AND III | 71 |
| 21 PLUTONIA MASS/HELIUM FLOW CORRELATION (μ g/cm ³) (PRESSURIZED LEAK TUBE) | 73 |
| B1 SUMMARY OF ROOM-TEMPERATURE PuO ₂ LEAK RATE EXPERIMENTS USING A SIMULATED CRACK | B-1 |
| B2 SUMMARY OF ROOM-TEMPERATURE PuO ₂ LEAK RATE EXPERIMENTS USING A SIMULATED CRACK; INITIAL HELIUM FLOW RATE EQUAL TO 9.8 cc/sec AT 1000 psi | B-2 |

TABLES
(CONTINUED)

| | <u>Page</u> |
|--|-------------|
| B3 SUMMARY OF ROOM-TEMPERATURE PuO ₂ LEAK RATE EXPERIMENTS USING A SIMULATED CRACK; INITIAL HELIUM FLOW RATE EQUAL TO 11.6 cc/sec AT 1000 psi | B-3 |
| B4 SUMMARY OF ROOM-TEMPERATURE PuO ₂ LEAK RATE EXPERIMENTS USING A SIMULATED CRACK; INITIAL HELIUM FLOW RATE EQUAL TO 13.2 cc/sec AT 1000 psi | B-4 |
| B5 SUMMARY OF ROOM-TEMPERATURE PuO ₂ LEAK RATE EXPERIMENTS USING A SIMULATED CRACK; WITH AN INITIAL He FLOW RATE OF 17.3 cc/sec AT 1000 psi | B-5 |
| B6 SUMMARY OF PuO ₂ LEAK RATE EXPERIMENTS USING A 20- m ORIFICE | B-6 |
| B7 SUMMARY OF PuO ₂ LEAK RATE EXPERIMENTS USING A 10- m ORIFICE | B-8 |
| B8 SUMMARY OF PuO ₂ LEAK RATE EXPERIMENTS USING A 5- m ORIFICE | B-9 |
| B9 SUMMARY OF PuO ₂ LEAK RATE EXPERIMENTS USING A 5- m ORIFICE | B-10 |
| B10 SUMMARY OF PuO ₂ LEAK RATE EXPERIMENTS USING A 10- m ORIFICE | B-11 |
| B11 SUMMARY OF PuO ₂ LEAK RATE EXPERIMENTS USING A 8- m ORIFICE | B-12 |
| B12 SUMMARY OF PuO ₂ LEAK RATE EXPERIMENTS USING A 20- m ORIFICE | B-13 |
| B13 SUMMARY OF PuO ₂ LEAK RATE EXPERIMENTS USING A 50- m ORIFICE | B-15 |
| B14 SUMMARY OF PuO ₂ LEAK RATE EXPERIMENTS USING A 50- m ORIFICE | B-16 |
| B15 SUMMARY OF PuO ₂ LEAK RATE EXPERIMENTS USING A 50- m ORIFICE | B-17 |

INTRODUCTION

Any increased use of plutonium in power production would result in a consequent increase in the number of shipments of nuclear materials. It is imperative that the shipping containers exhibit a high degree of leak tightness in order to insure that no significant amount of plutonium is released into the environment. In general, the leak tightness of shipping containers for radioactive materials is characterized by measurements of the rate of leakage of some tracer fluid, usually a gas, from the container.^(1,2) The maximum permissible gas leakage rate is a function of the specific radioactive nuclides to be transported in the container.⁽³⁾ It is anticipated that plutonium will be shipped in the form of a fine powder of PuO_2 which is not likely to leak at a rate typical of a gas. Consequently, the application of these criteria to PuO_2 shipping containers may result in unnecessarily restrictive standards for container leak tightness.

This document is a report on a Nuclear Regulatory Commission sponsored program which was designed to provide data to help establish a correlation between PuO_2 particulate leakage and helium gas leakage through simulated container leaks, thus providing a data base to allow for the development of a more realistic specification for the leak tightness of PuO_2 shipping containers. A primary concern is the quantity of PuO_2 which might be released under conditions expected to occur as a result of a transportation accident. The original leak tightness of the container may be used to estimate the PuO_2 emission.

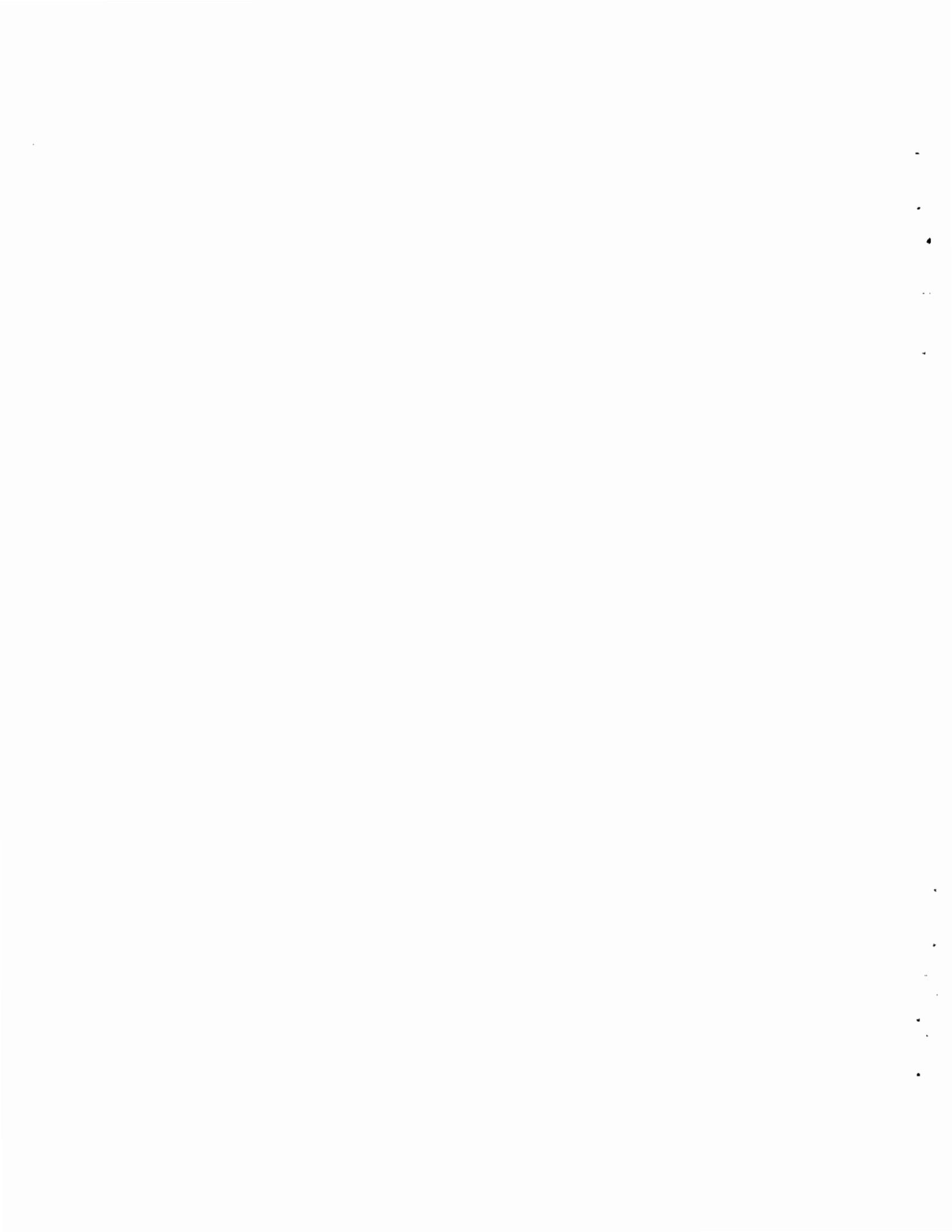
To provide information to aid in the evaluation of the behavior of PuO_2 particulate leakage, as it relates to gas leakage, under conditions to which a shipping container might be subjected, the effects of simulated container leaks were studied. The experiments were constrained to maximize the PuO_2 release. The leak types considered in this were: (1) "standard leak", consisting of a small orifice in a thin platinum disk, (2) a simulated crack made by machining a 220-microinch surface roughness in the mating faces of a split tapered disk and (3) 50- μm diameter capillary tubes 4.4 and 5.1 cm long. The experimental parameters investigated included internal gas pressure, leak orientation with respect to the powder location, agitation, run time and leak size/type.

As working with plutonium compounds presents certain practical handling difficulties, the approach taken was to divide the experimental effort into two distinct phases: (1) a simulant phase using ThO_2 powder, and (2) a "hot" phase using PuO_2 powder. The simulant phase served to: (1) allow experimental and apparatus design to be checked out prior to transfer to the glove box necessary for the safe handling of the PuO_2 , (2) allow development and check out of sample collection and measurement techniques, and (3) establish a preliminary data base.

This research was carried out by Battelle Columbus Laboratories as a part of a related services study contracted to Pacific Northwest Laboratory by the Office of Nuclear Regulatory Research.

OBJECTIVE

The objective of this study was to provide an experimental data base that will aid in the development of techniques to assess the potential releases of plutonia powder from shipping containers under conditions expected following a transportation accident.



SUMMARY

A series of experiments was conducted to investigate the dependence, upon various experimental parameters, of the emission of PuO_2 through small apertures. The experiments were designed around a four-parameter matrix: (1) internal gas pressure, (2) leak orientation with respect to the powder location, (3) agitation, and (4) leak size/type. For a few sets of experimental conditions the effect of the total run time was also considered. Leak types consisted of thin-plate orifices, simulated cracks consisting of split tapered disks with machined roughness on the mating surfaces and 50- μm -diameter capillary tubes. Nominal orifice sizes ranged from 5- μm to 50- μm in diameter, gas pressures ranged between ambient pressure and 1250 psig and run times ranged from "zero" to two hours. "Zero" run time refers to those experiments where the gas pressure in the experimental system was released immediately upon reaching operating pressure.

The data exhibited a high degree of irreproducibility which severely limited the ability to draw any firm conclusions concerning the parametric dependency of the data. Within the limits of the data, no apparent parametric dependence was observed for any single parameter; however, a weak dependency upon the interaction between the orifice area and the internal pressurization was observed. This is seen as an apparent functional relationship between a logarithmic transformation of the data, Z ($Z = \log_{10} (10 + 1000 X)$ where Z is the transformed variable and X is the PuO_2 emission in micrograms) and $\log_{10} A\sqrt{P}$ where A is the orifice area and P the internal pressure. Although the relationship is suggested by the data, the data are not sufficient to allow a more exact functional dependency to be determined.

The results of the experiments where the run time was variable showed that a change in the run time did not result in a change of the quantity of PuO_2 emitted. On the basis of this observation, it was concluded that the majority of the PuO_2 emission observed during an experiment occurs during the initial pressurization.

Correlations between the PuO_2 mass emitted during an experiments and the total helium flow produced values ranging between 3×10^{-8} and $5 \times 10^{-3} \mu\text{g of PuO}_2/\text{cm}^3$ of helium under internal pressurization of 500 to 1250 psig.



EXPERIMENTAL

The experimental setup used for both phases of the program is shown schematically in Figure 1. The essential components of the system are the leak tube, used to contain the ThO_2 or PuO_2 powder and support the leak assembly, a helium supply with pressure regulation, and a sampling device. The leak tube itself is constructed of Inconel Alloy 100, has an overall length of 12.7 cm and an ID of 0.64 cm. The reservoir volume is approximately 4 cc. Helium, to provide the necessary internal pressurization, is supplied through a 0.64-cm tube located at midlength. The leak tube used for the PuO_2 experiments is shown in Figure 2. The tube used for the simulant experiments was similar in design, but had the cap shown in Figure 3.

The leak assemblies were mounted in the end of the leak tube and sealed with stainless steel gaskets. The orifices used were prepared by the laser drilling of holes ranging between 5 and 50 μm in 0.10-mm platinum disks 9.5-mm in diameter. The orifices were examined microscopically prior to use to insure that the diameters were correct and the openings unobstructed. The flow rates of helium through 5-, 10-, 20- and 50- μm diameter orifices and a 50- μm ID capillary tube were measured using either the bubble-tube or pressure-drop method or both. The results of these measurements are presented in Table 1. These data apply to clean orifices installed in an empty leak tube; the actual leaks observed during the particle emission experiments vary from these somewhat.

Capillary leak assemblies were prepared by silver brazing type 304 stainless steel capillary tubing having an ID of 50 μm and an OD of 125 μm into a type 304 stainless steel support tube having an ID of 175 μm and OD of 1575 μm . This tubing assembly was brazed to a type 304 stainless steel disk sized to fit into the end of the leak tube. Assemblies of length 4.4 and 5.1 cm were prepared. The 4.4-cm-long assembly is shown in Figure 4. As might be expected, the inner surfaces of the capillary exhibit appreciable irregularity. Figure 5, a photomicrograph of a capillary cross section, clearly illustrates this irregularity.

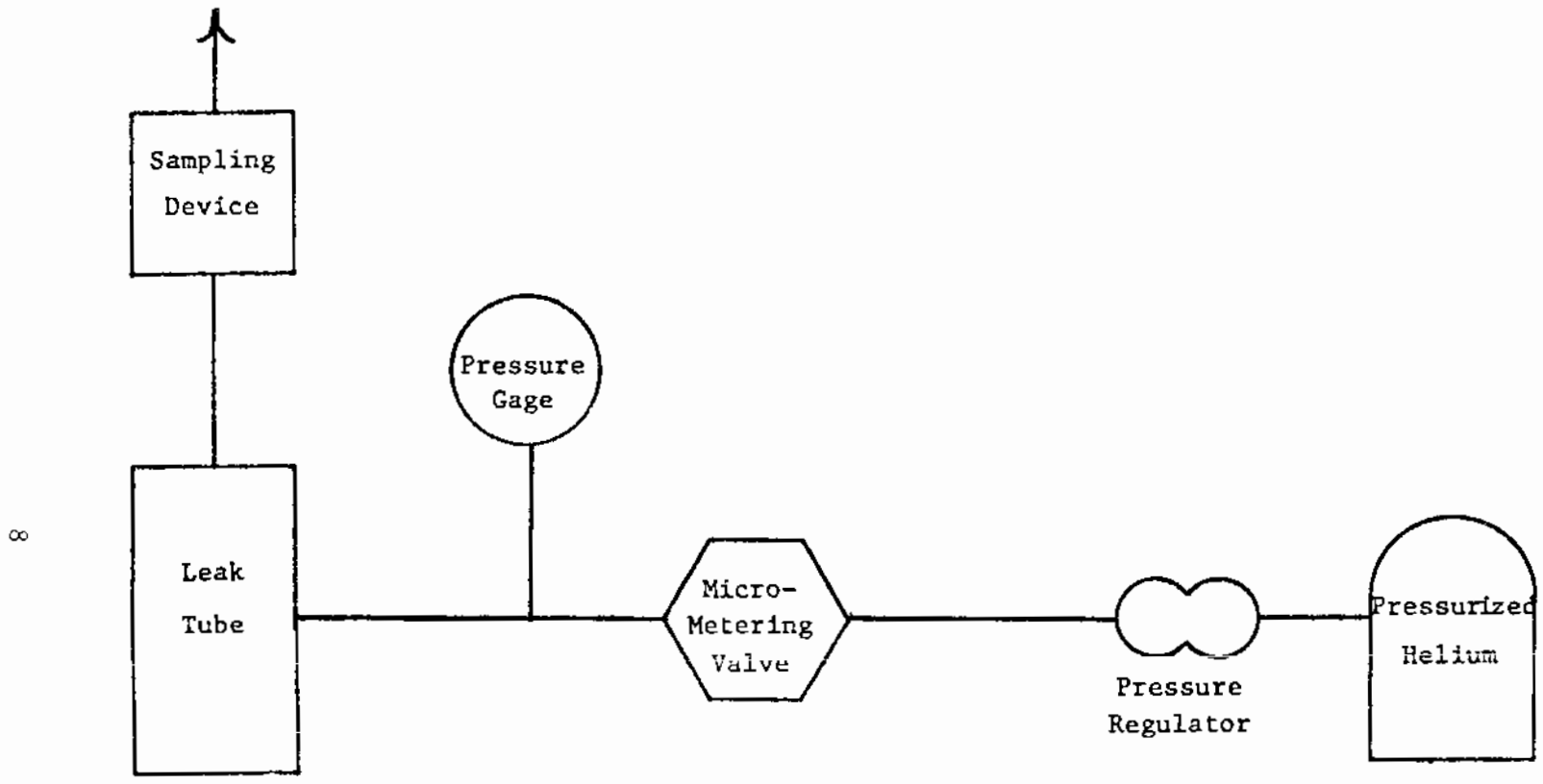


FIGURE 1. SCHEMATIC DIAGRAM OF EXPERIMENTAL SET-UP USED FOR LEAK RATE EXPERIMENTS

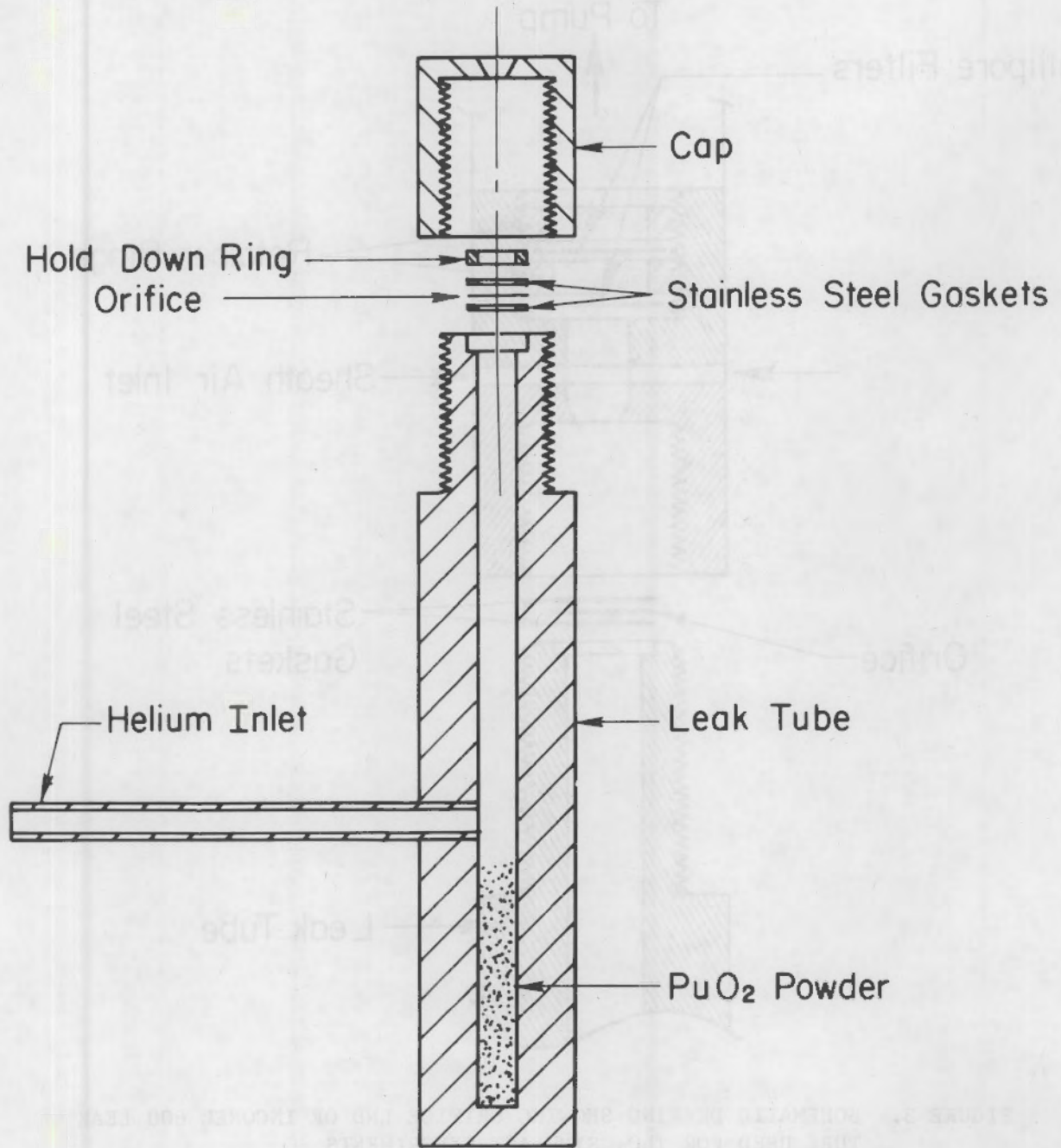


FIGURE 2. LEAK TUBE USED FOR THE PuO₂ EXPERIMENTS

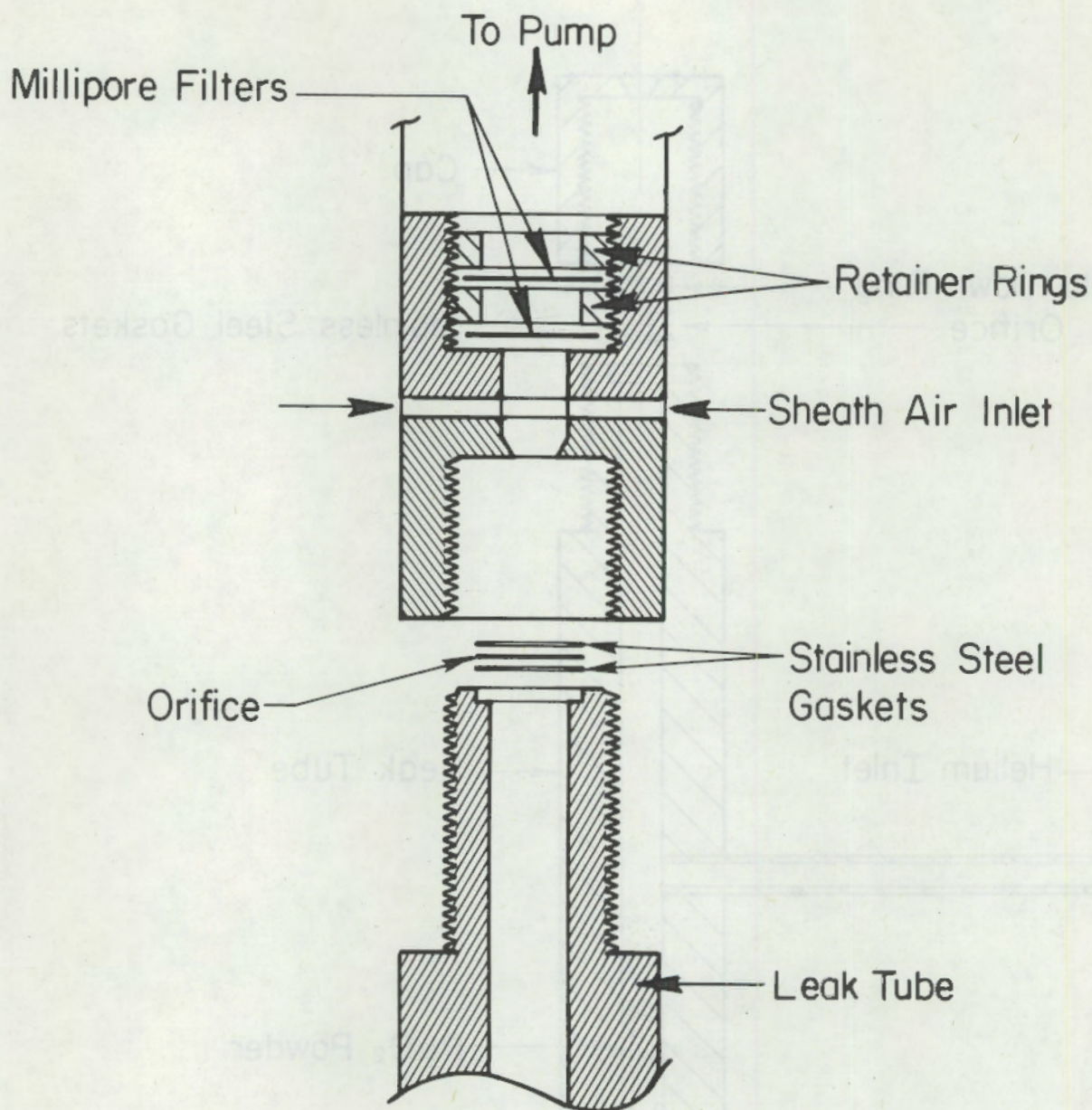


FIGURE 3. SCHEMATIC DRAWING SHOWING ORIFICE END OF INCONEL 600 LEAK TUBE USED FOR ThO_2 SIMULANT EXPERIMENTS

TABLE 1. HELIUM LEAK RATES THROUGH ORIFICES AND CAPILLARIES

| Type of Leak | Pressure, psig | Helium Leak Rate, std cc/sec |
|-----------------------|-------------------|------------------------------------|
| 5- μ m Orifice | 0 | 1.25×10^{-5} |
| " | 500 | 0.39 |
| " | 1000 | 0.77 |
| 10- μ m Orifice | 0 | 5.03×10^{-5} |
| " | 500 | 1.39 |
| " | 1000 | 2.89 |
| 20- μ m Orifice | 0 | 2.02×10^{-4} |
| " | 500 | 4.21 |
| " | 1000 | 8.09 |
| 50- μ m Orifice | 0 | 1.25×10^{-3} |
| " | 500 | - |
| " | 1000 | 58.0 |
| 50- μ m Capillary | 0 | 2.86×10^{-6} |
| " | 500 | 0.3 |
| " | 1000 | 0.8 |

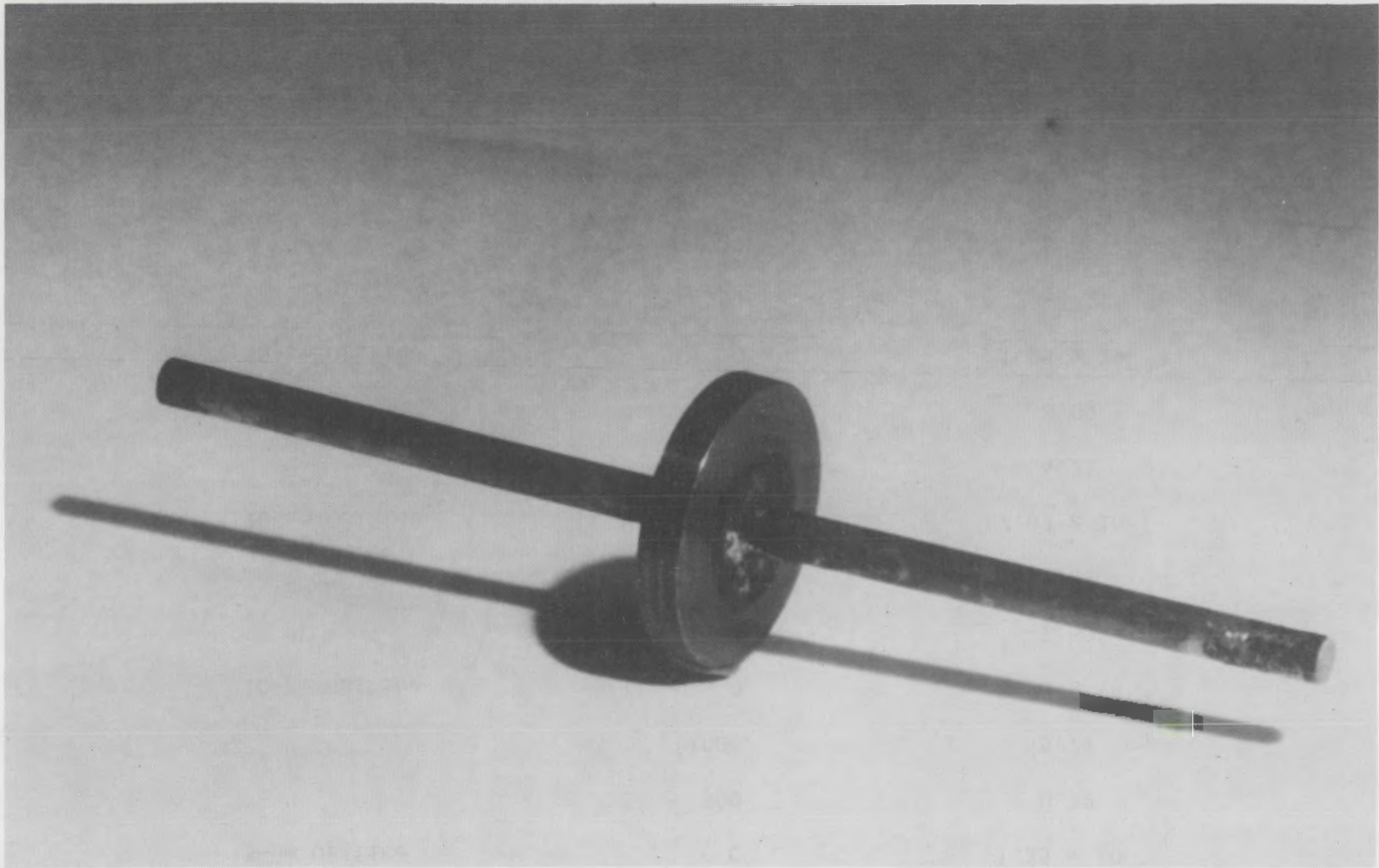


FIGURE 4. 50- μ m-ID x 4.4-cm-LONG CAPILLARY LEAK

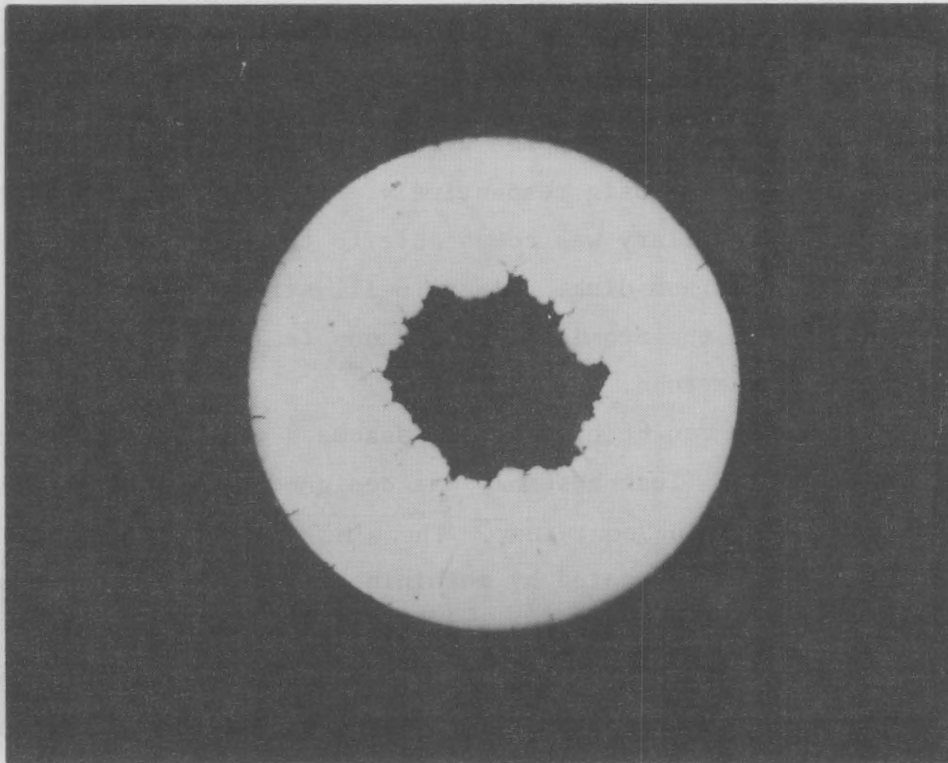


FIGURE 5. CROSS SECTION OF 50- μ m-ID CAPILLARY TUBE

The helium flow rate through the 4.4-cm-long capillary leak assembly was measured to be 0.82 and 0.30 cc/sec using the pressure decay method at pressures of 1000 and 500 psig respectively. At 1000 psig, the helium flow rate through the capillary was comparable to that observed for a 5- μ m orifice in a 0.10-mm platinum disk. Figure 6 illustrates the flow of helium through the capillary by the atomization of Snoop (a liquid leak detector) applied to the end of the tube.

As a leak path can be expected to assume a wide variety of configurations, an additional leak assembly was designed to simulate a crack in a plutonia powder shipping container. The simulated crack, shown schematically in Figure 7, was prepared by machining a surface roughness of 220 microinches on the mating faces of a split tapered disk. During machining, the disk was positioned such that the grooves would interlock when the disk pieces were placed together. The disk was designed to fit into a matching tapered ring that may be positioned at the end of the standard leak tube. The crack spacing, and consequently the helium leak rate, was adjusted by varying the amount of torque applied to the leak tube retaining nut. The observed leak rates varied between 6.1 and 17.3 cc/sec at 1000 psig and various applied torques.

Two types of sampling devices were used for the ThO_2 simulant experiments. Most of the experiments used the arrangement shown in Figure 2 where Millipore^(a) filters are mounted in the leak tube cap. The other sampling device which was also used for some of the PuO_2 experiments was a cascade impactor. This is a device which employs inertial deposition to collect aerosol particles and classify them according to size.

(a) Manufactured by Millipore Corp., Bedford, MA

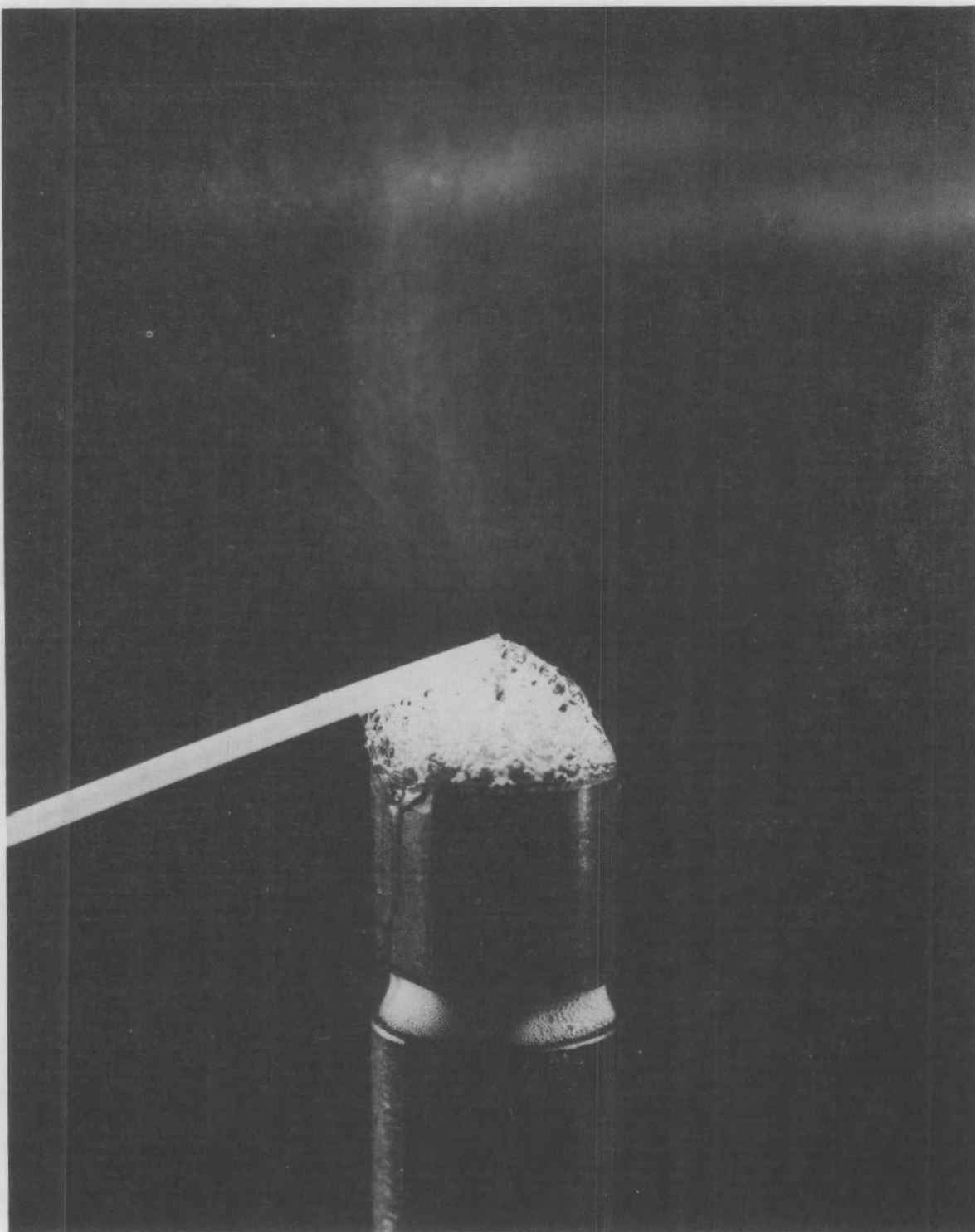


FIGURE 6. ATOMIZATION OF SNOOP (A LIQUID LEAK DETECTOR) BY HELIUM FLOW THROUGH THE CAPILLARY LEAK ASSEMBLY

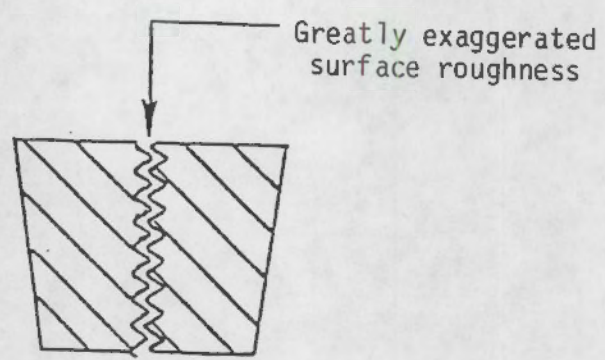
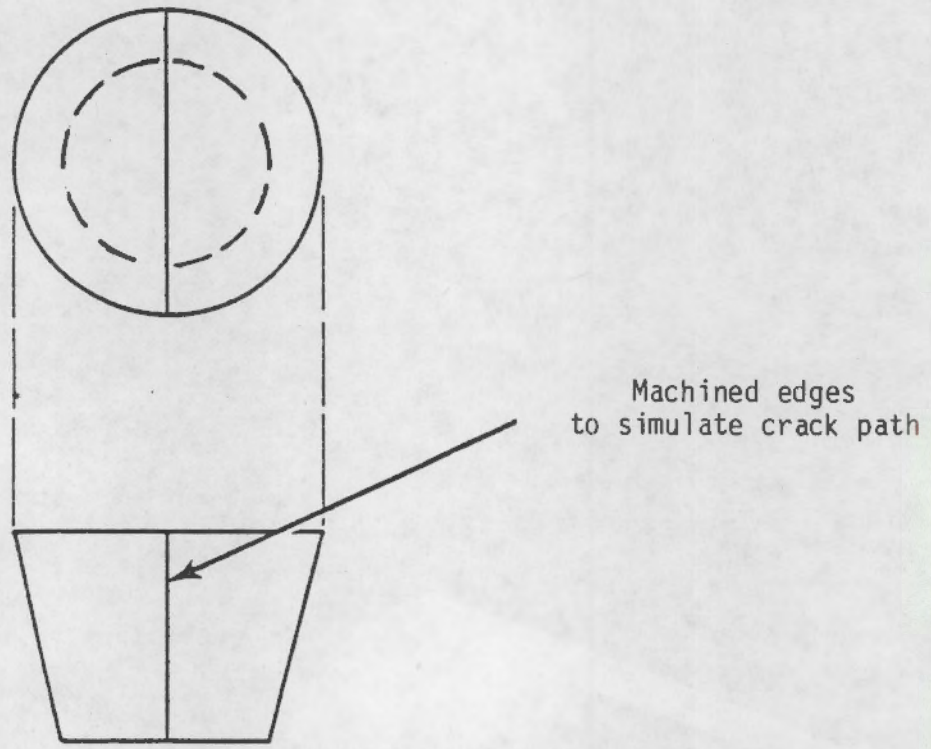


FIGURE 7. SCHEMATIC SHOWING CONFIGURATION OF SIMULATED CRACK

EXPERIMENTAL PROCEDURES

Particle Sizing and Comparisons

Prior to its final selection as the simulant material the ThO_2 particle size distribution was compared with that of the PuO_2 powder to ensure that the ThO_2 would be an appropriate simulant. The ThO_2 was first screened using the 325-mesh (44- μm) sieve to remove any large particles and then sized using the Battelle cascade impactor. Figure 8 shows the results of these measurements, as well as the nominal size distribution as obtained from Schwendiman⁽⁴⁾, of the PuO_2 powder for which the ThO_2 serves as a simulant. The agreement, though not exact, was adequate for this study with the mean diameters being 7.8- μm and 8.3- μm for ThO_2 and PuO_2 respectively.

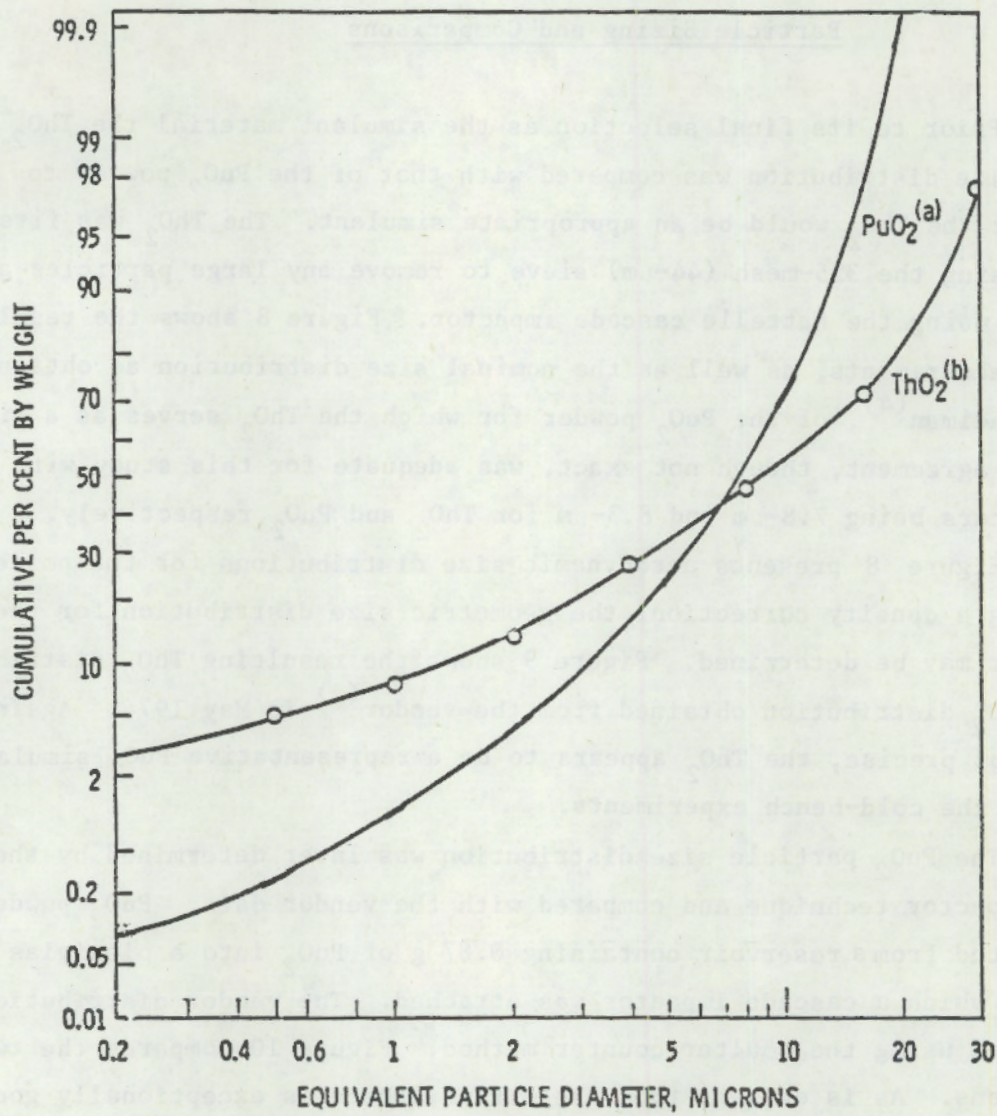
Figure 8 presents aerodynamic size distributions for the powders. By applying a density correction, the geometric size distribution for the ThO_2 powder may be determined. Figure 9 shows the resulting ThO_2 distribution and the PuO_2 distribution obtained from the vendor^(a) in May 1974. Again, although not precise, the ThO_2 appears to be a representative PuO_2 simulant for use in the cold-bench experiments.

The PuO_2 particle size distribution was later determined by the cascade impactor technique and compared with the vendor data. PuO_2 powder was aspirated from a reservoir containing 0.87 g of PuO_2 into a plexiglas chamber to which a cascade impactor was attached. The vendor distribution was obtained using the Coulter counter method. Figure 10 compares the two distributions. As is evident from the curves, there is exceptionally good agreement between the distributions determined by the two different techniques. Both sets of data indicate mean particle size of 2.5 μm .

Specific Activity of PuO_2 Powder

As only minute quantities of PuO_2 are expected to be emitted from the leak assemblies during the experiments, gravimetric analysis was felt to be impractical and chemical analysis too costly and time consuming. Con-

(a) Plutonium dioxide powder obtained from ARHCO (Atlantic Richfield Hanford Co.), Richland, WA.



- (a) Nominal PuO₂ size distribution (Schwendiman 1977)
 (b) Nominal ThO₂ size distribution (determined by L. Miga of Battelle Columbus Laboratories, December 18, 1976)

FIGURE 8. AERODYNAMIC SIZE DISTRIBUTIONS OF PuO₂ AND ThO₂ POWDERS

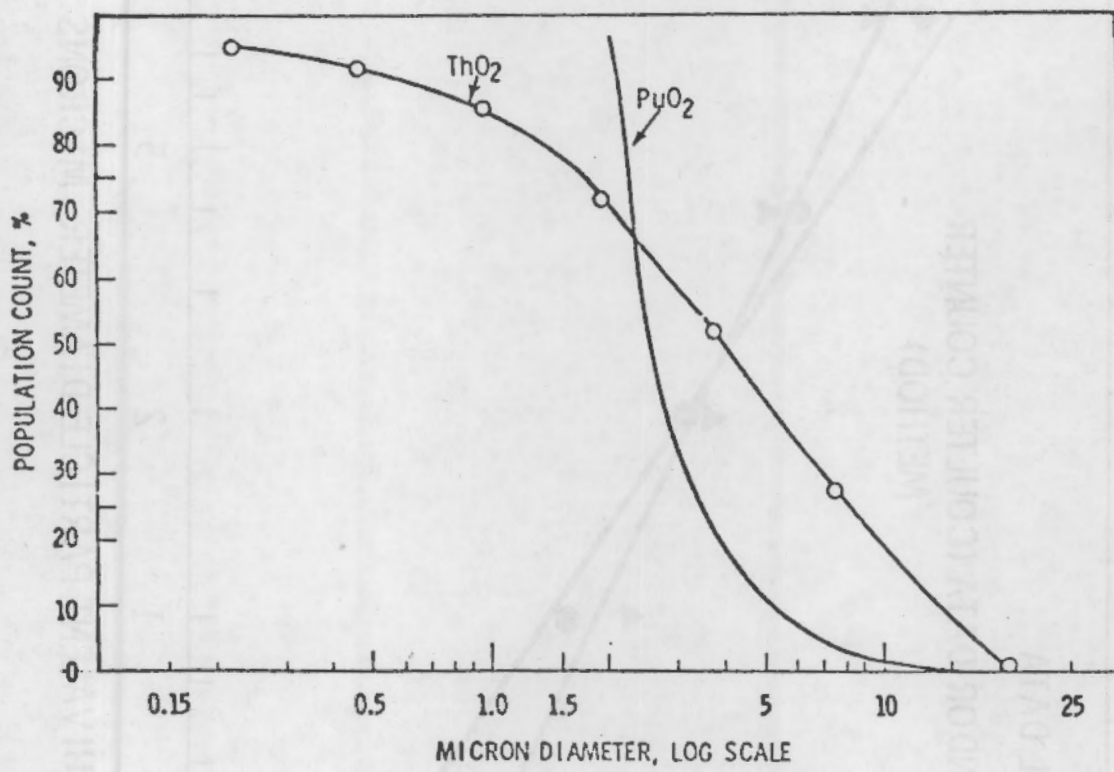


FIGURE 9. GEOMETRIC SIZE DISTRIBUTION OF PuO₂ AND ThO₂ POWDER

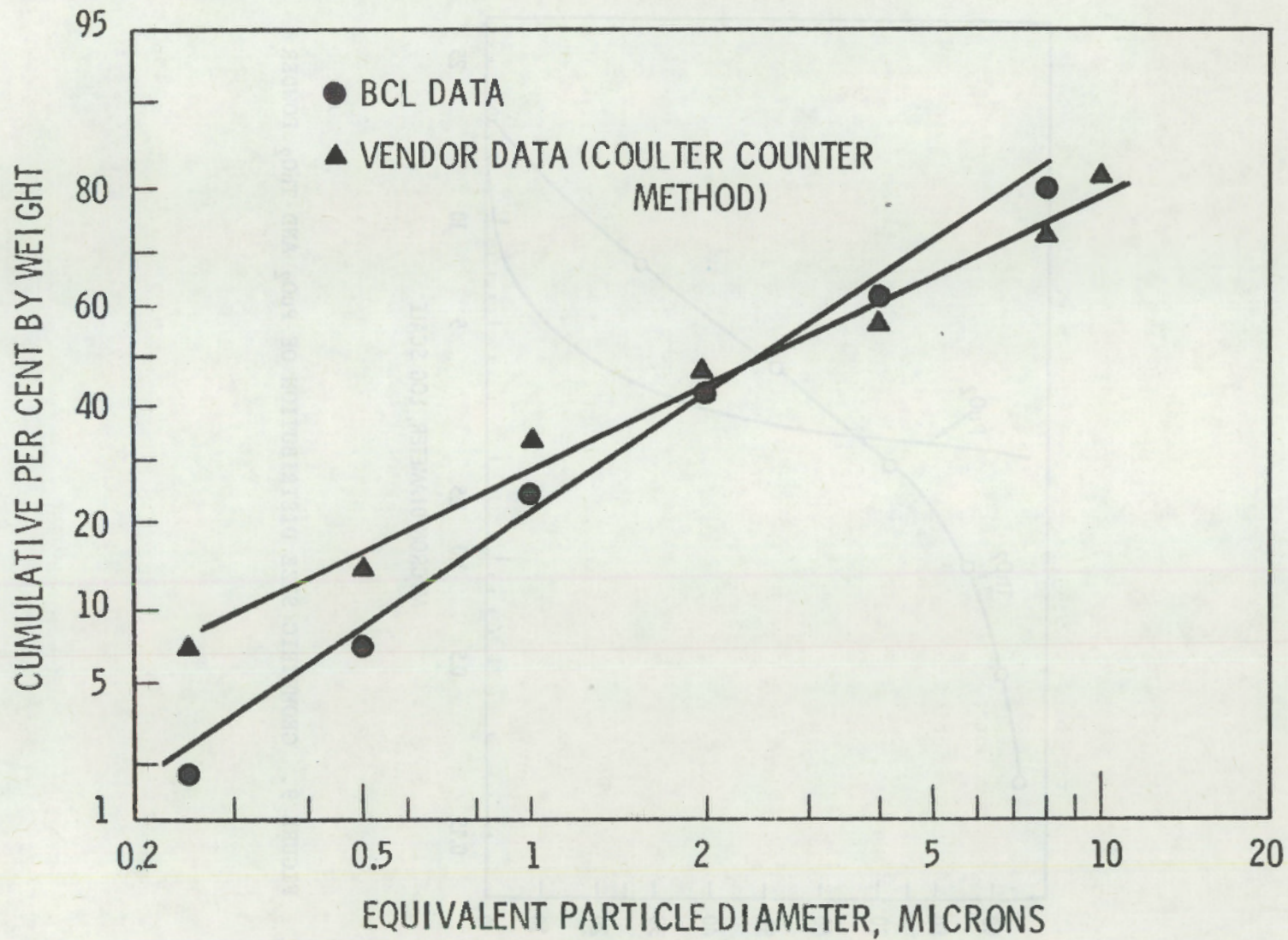


FIGURE 10. GEOMETRIC SIZE DISTRIBUTION OF PuO_2 POWDER

sequently, radioassay analysis was selected as the technique used to determine the quantities of PuO_2 collected.

The radioassay technique chosen employed the counting of the alpha particles emitted by the plutonium. This technique necessitates the correction of counting data for background, detection efficiency and the specific activity of the PuO_2 .

In order to obtain an actual specific activity of the PuO_2 powder being used in this study, three pairs of plutonium standards were prepared by dissolving the powder and depositing different quantities of the solution on small watch glasses. The solvent was evaporated by heating the watch glasses on a hot plate. The activity of these standards was measured and the specific activity was determined. The results are tabulated in Table 2. The isotopic composition of the powder as determined by Teledyne, Inc., is presented in Table 3. A specific activity calculated from these values is also shown in the table. As is apparent, the calculated value of 0.098 Ci/g is in excellent agreement with the measured activity of 0.096 ± 0.004 Ci/g.

Helium Flow Rates

Specifications for acceptable container leak sizes may be stated in terms of the quantity of helium leaked with respect to time. In order to provide any correlative information concerning particle emissions and gas flow, the flow rates must be adequately determined. Helium flow rates through the leak assemblies were determined by using either a bubble flow tube or calculations based on the system volume and the rate of decay of a closed (except for the leak assembly) system. This latter method is the proposed ANSI standard leak test on packages for shipment of radioactive materials, N-14.5 (12th draft).⁽¹⁾ For those runs conducted at ambient internal pressures, the approximate leak rate was calculated assuming molecular diffusion of helium into air.

Run Technique

All experiments, unless noted otherwise, were conducted with a nominal collection time of ten min. Notes collection times refer to the time during which a given set of experiments conditions are extant.

TABLE 2. SPECIFIC ACTIVITY OF THE
PuO₂ POWDER USED IN THE
LEAK RATE EXPERIMENTS

| <u>Standard Number</u> | <u>Specific Activity, Ci/g</u> |
|------------------------------|--------------------------------|
| 1A | 0.09 |
| 1B | 0.092 |
| 2A | 0.099 |
| 2B | 0.105 |
| 5A | 0.095 |
| 5B | <u>0.095</u> |
| Average = 0.096 ± 0.004 a.d. | |

As indicated above, the average specific activity of the standards is 0.096 ± 0.004 Ci/g.

TABLE 3. PLUTONIA ISOTOPIC COMPOSITION
 Pu LOT A-345 (ARHCO)
 ANALYZED BY TELEDYNE, INC.

| Isotope | Weight Percent |
|---------|----------------|
| Pu-238 | 0.108 |
| -239 | 86.881 |
| -240 | 11.359 |
| -241 | 1.432 |
| -242 | 0.220 |

Specific Activity: 0.098 Ci/g (Calculated)

0.096 \pm 0.004 Ci/g (Measured)

For all runs the leak tube was agitated for 1 min to disperse the powder and the sample collection device was operated for 1 min prior to pressurization and 1 min following depressurization in order insure that collection takes place during the entire period of particle flow.

At the mid-point of each run, the helium flow rate was determined using the pressure decay method.

The so-called "zero-time" runs were conducted such that the leak tube was pressurized for the minimum amount of time that was practical. This was accomplished by allowing the internal pressure to reach the desired value and then immediately isolating the leak tube from the high pressure line and releasing the helium through a bleed valve. The entire operation required approximately 1 min.

The impactor operates on the principle that particles moving in an airstream will strike a slide placed in their path if they possess sufficient inertia to overcome the drag exerted by the airstream which will pass around the slide. Figure 11 illustrates the operation of the impactor. As the aerosol approaches the slide after passing through the nozzle, the larger particles will impact on the slide while the smaller particles are carried along with the airstream. Because each jet is smaller than the preceding one, the velocity of the airstream will increase with each successive stage of the impactor and complete size classification is achieved. Those particles too small to be collected in the fifth and final stage are collected on a high-efficiency membrane filter.

When size classification was not desired for the plutonium experiments, the impactor was replaced with a device similar in configuration, but containing a membrane filter only to provide complete particle collection.

When desired, agitation may be applied to the leak tube through a mechanical vibrator^(a) directly coupled to the leak tube. The purpose of the vibration, when used, was to maximize the aerosolization of the powder during experiments.

(a) Scripto Vibratool®, 120 cps, 1/32-in displacement, uncoupled.

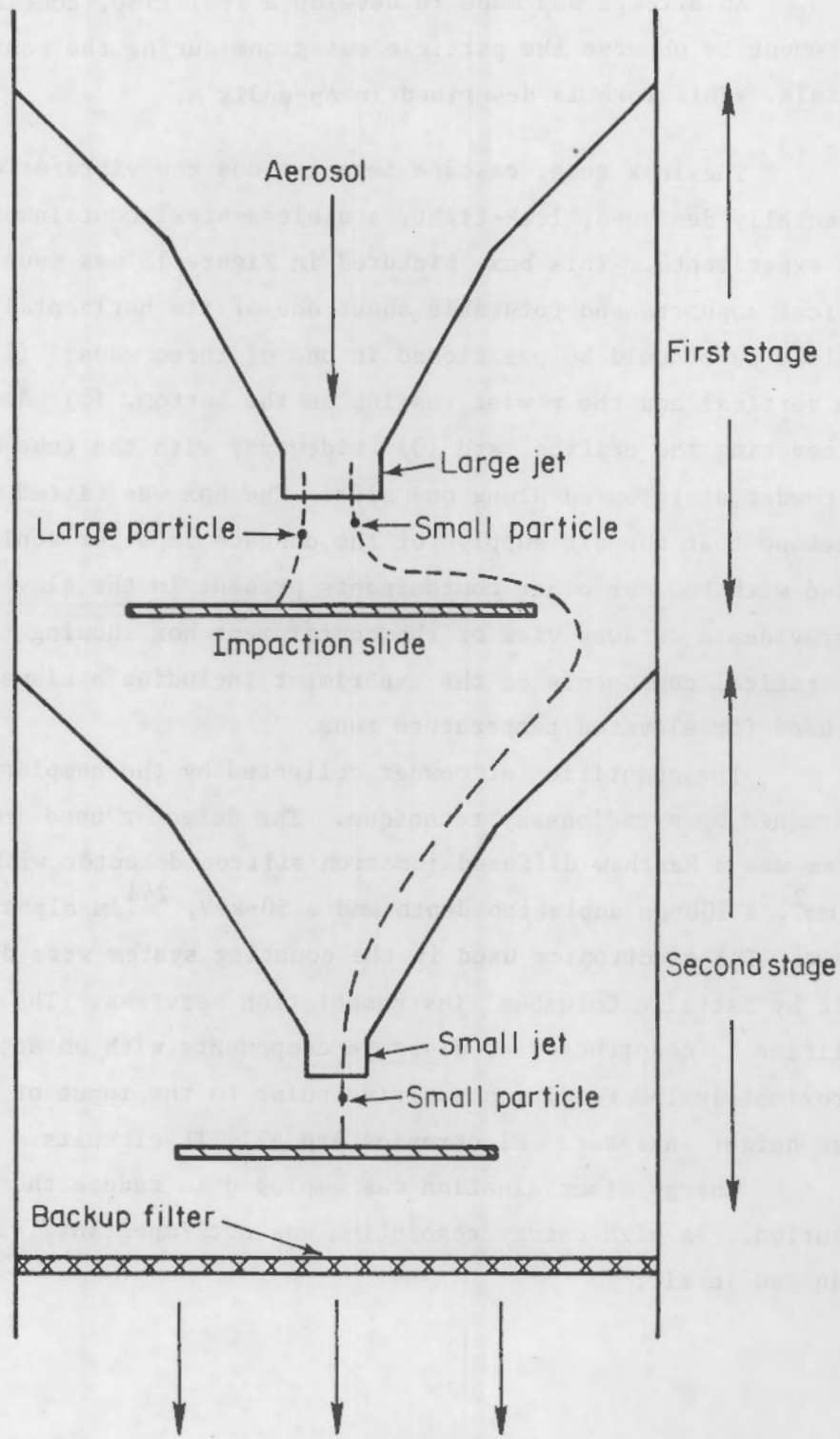


FIGURE 11. SCHEMATIC DEMONSTRATING CASCADE IMPACTOR OPERATION

An attempt was made to develop a real-time, continuous monitoring instrument to observe the particle emissions during the course of the experiments. This work is described in Appendix A.

The leak tube, cascade impactor and the vibrator were mounted in a specially designed, leak-tight, stainless-steel containment box for the PuO_2 experiments. This box, pictured in Figure 12 was mounted on two vertical supports and rotatable about one of its horizontal axes such that the leak tube could be positioned in one of three ways: (1) up, with the tube vertical and the powder resting on the bottom, (2) down, with the powder covering the orifice, and (3) sideways, with the tube horizontal and the powder distributed along one side. The box was fitted with an absolute filter so that the air supply for the cascade impactor would not be contaminated with PuO_2 or other contaminants present in the glove box. Figure 13 provides a cutaway view of the containment box showing the placement of the critical components of the experiment including a clamshell-type furnace used for elevated temperature runs.

The quantities of powder collected by the sampling device were determined by a radioassay technique. The detector used in the counting system was a Harshaw diffused junction silicon detector with a surface area of 450 mm^2 , a $100\text{-}\mu\text{m}$ depletion depth and a 50-keV , ^{241}Am alpha resolution in vacuum. The electronics used in the counting system were designed and built by Battelle Columbus' instrumentation services. The preamplifier-amplifier is constructed of discrete components with an adjustable gain of approximately 150 feeding a positive pulse to the input of the single channel pulse height analyzer. Electronics are all TTL circuits.

Energy discrimination was employed to reduce the background contribution. As high-energy resolution was not important, all counting was conducted in air.

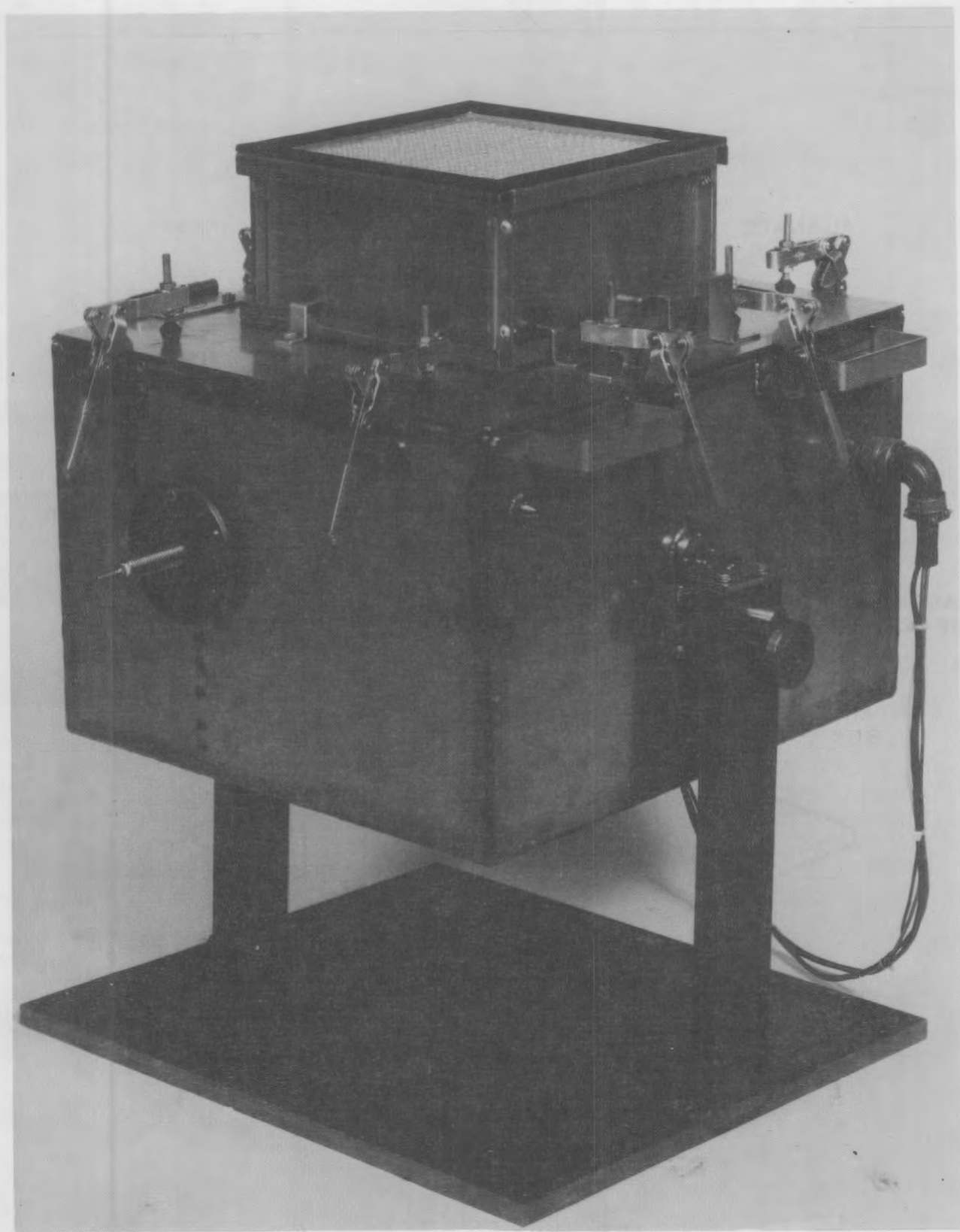


FIGURE 12. OUTSIDE VIEW OF CONTAINMENT BOX

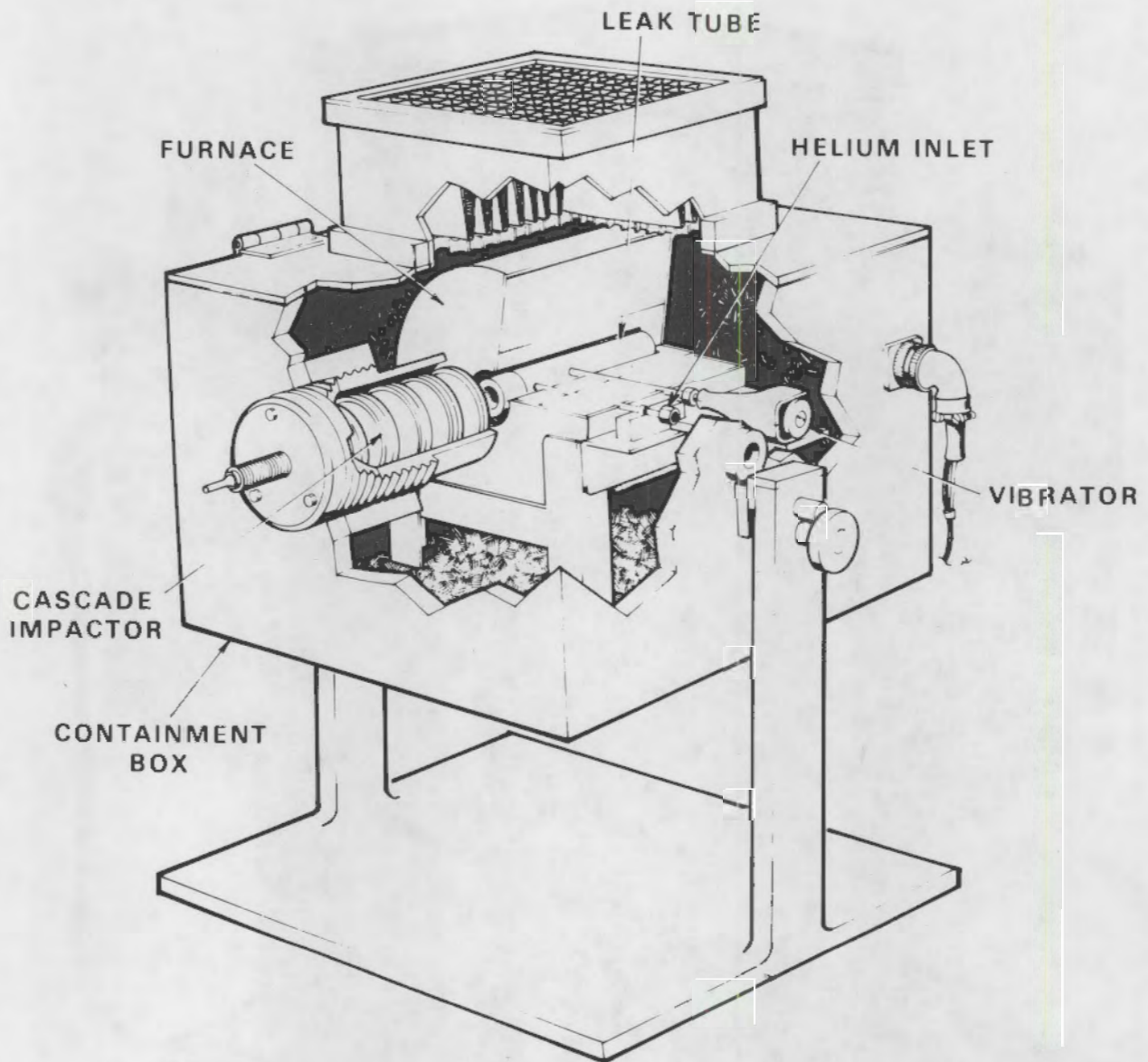


FIGURE 13. CUT-AWAY VIEW OF CONTAINMENT BOX

The entire experimental system was housed in a stainless steel glove box^(a) for the experiments using PuO₂ powder. Prior to use, the glove box was pressurized with helium and leak tested with a helium mass spectrometer type leak detector. No detectable leakage was observed with the leak detector set on the 1×10^{-8} torr range. Figure 14 shows, schematically, the arrangement of the experimental system in the glove box. To allow monitoring of the helium flow, an "Omniflow"[®] turbine flow-meter^(b) was installed in the experimental system. The "Omniflow" is an in-line flow metering device which provides digital flow information. The flow rates obtained are in terms of the actual pressures, they must be converted to standard flow rates. The flow-meter was calibrated in the experimental system using the pressure decay method to insure that flow rate information could be related to previous runs. Thirty data points were used in the calibration and were fitted to a straight line with a linear correlation coefficient of 0.995. The calibration curve reveals that the minimum flow which can be reliably measured by the flow-meter is approximately 0.1 acc/sec.



(a) Obtained from Stainless Engineering Company, Boulder, CO

(b) Obtained from Flow Technology, Inc., P.O. Box 21346, Phoenix, AR

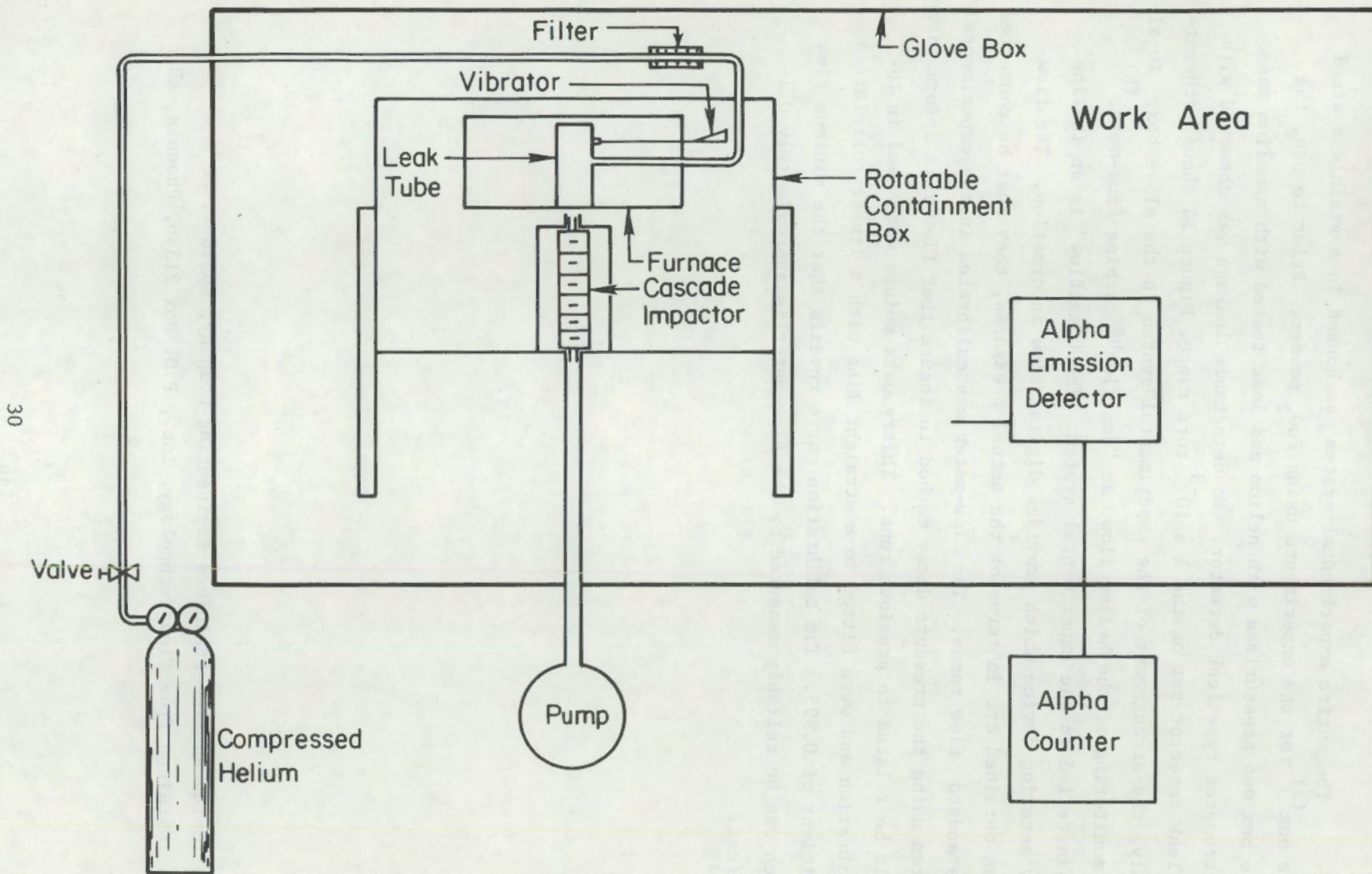


FIGURE 14. SCHEMATIC SHOWING EXPERIMENTAL ARRANGEMENT

ThO₂ SIMULANT EXPERIMENTS

Preliminary bench-top experiments were conducted using ThO₂ powder as a simulant for the PuO₂ powder. The objective of these experiments was to allow the check-out and development of the experimental system and technique prior to initiation of the PuO₂ experiments and to establish a preliminary data base concerning the effects of orifice size, leak-tube orientation, internal system pressure and agitation on the emission of powders through the leak assemblies.

The simulant experiments were conducted at nominal pressures of 500 and 1000 psi, temperatures of ambient, 400° C and 815° C using orifices of 5, 10, 20 and 50- μ m diameters. The ThO₂ emissions were collected on membrane filters mounted in the leak tube cap for the ambient temperature runs. The cascade impactor was used during the elevated temperature runs. The exact conditions for each experiment, along with the results, are presented in Tables 4 and 5. The quantities of ThO₂ collected were determined using either an alpha radioassay technique or X-ray fluorescence.

On the basis of this rather limited set of data, the following observations have been made:

- (1) With a few exceptions, no ThO₂ release was noted for orifices less than 50 μ m in diameter under any conditions. This does not mean that no release occurred, but that it was not readily detectable with the ThO₂ simulant.
- (2) At room temperature, more ThO₂ was emitted through a 50- μ m orifice with the orifice in the down position and without vibrating the leak tube as compared to a similar experiment with vibration (see Th 14 and Th 17).
- (3) Based on the results of Runs 17, 17a, 17b, and 17c, the emission of ThO₂ through a 50- μ m orifice at room temperature was reproducible within a factor of about 2 for the leak-down position.
- (4) Results with respect to position and vibration are rather ambiguous. For example, considerable ThO₂

TABLE 4. SUMMARY OF ROOM TEMPERATURE SIMULANT EXPERIMENTS USING ThO₂

| Run No. | Orifice Diameter, μm | Tube Position | Nominal Helium Pressure psig | Temperature C | Length of Run, hr | Vibration | Sheath Air | Grounded | $\mu\text{g ThO}_2$ | | | |
|---------|---------------------------------|---------------|------------------------------|---------------|-------------------|-------------------|------------|----------|---------------------|---------------------|------------------------|--------------------|
| | | | | | | | | | 1st Filter | 2nd Filter | Orifice ^(a) | Walls |
| Th 1 | 10 | Up | 1000 ^(b) | 20 | 1/10 | No | No | No | ND | Not used | - | - |
| Th 2 | 10 | Up | 1000 ^(b) | 21 | 1/10 | Yes | No | No | ND | Not used | - | - |
| Th 3 | 10 | Down | 1000 ^(b) | 22 | 4 | No ^(c) | No | No | ND | Not used | - | - |
| Th 4 | 20 | Up | 1000 ^(b) | 19 | 1/12 | No | No | No | ND | Not used | - | - |
| Th 5 | 20 | Sideways | 1000 | 19 | 1/6 | Yes | No | No | ND | Not used | - | - |
| Th 6 | 20 | Sideways | 1000 | 19 | 4 | Yes | No | No | 1.0 ^(d) | Not used | - | - |
| Th 6a | 20 | Sideways | 1000 | 21 | 5 | Yes | No | No | 10 ^(d) | Not used | 50 | - |
| Th 7 | 20 | Sideways | 1000 | 21 | 2 | No | No | No | 1.5 ^(d) | <1.0 ^(d) | <50 | 1.5 ^(d) |
| Th 8 | 20 | Sideways | 1000 | 21 | 2 | Radial | No | No | <1.0 ^(d) | 3.0 ^(d) | <50 | 4.0 ^(d) |
| Th 9 | 20 | Sideways | 1000 | 23 | 2-1/3 | No | No | Yes | ND ^(d) | ND ^(d) | <50 | <50 |
| Th 10 | 20 | Sideways | 1000 | 23 | 2 | Radial | Yes | No | ND ^(d) | Not used | <50 | <50 |
| Th 11 | 20 | Down | 1000 | 21 | 2 | Radial | Yes | No | <1.0 ^(d) | Not used | <50 | <50 |
| Th 11a | 20 | Down | 1000 | 21 | 2 | Radial | Yes | No | 1.0 ^(d) | Not used | <50 | <50 |
| Th 11b | 20 | Down | 1000 | 21 | 2 | Radial | Yes | No | <1.0 ^(d) | Not used | <50 | <50 |
| Th 12 | 5 | Down | 1000 | 21 | 2 | Radial | Yes | No | <1.0 ^(d) | Not used | <50 | <50 |
| Th 13 | 20 | Down | 1000 | 21 | 2 | Axial | Yes | No | <1.0 ^(d) | Not used | <50 | <50 |
| Th 14 | 50 | Down | 1000 | 21 | 2 | Radial | Yes | No | 1.5 ^(d) | Not used | <50 | <50 |
| Th 15 | 50 | Sideways | 1000 | 21 | 2 | Radial | Yes | No | <1.0 ^(d) | Not used | <50 | <50 |
| Th 16 | 50 | Sideways | 1000 | 24 | 2 | Radial | Yes | No | 35.0 ^(f) | Not used | <50 | 60 |
| Th 17 | 50 | Down | 1000 | 26 | 2 | No | Yes | No | 85.0 ^(f) | Not used | 96 | 96 |
| Th 18 | 50 | Sideways | 1000 | 26 | 2 | No | Yes | No | <1.0 ^(d) | Not used | <50 | <50 |
| Th 19 | 50 | Sideways | 1000 | 29 | 2 | Radial | Yes | No | <1.0 ^(d) | Not used | <50 | <50 |
| Th 20 | 50 | Up | 1000 | 26 | 2 | Radial | Yes | No | 20.0 ^(d) | Not used | <50 | <50 |

TABLE 4. SUMMARY OF ROOM TEMPERATURE SIMULANT EXPERIMENTS USING ThO₂ (Continued)

| Run No. | Orifice Diameter, μm | Tube Position | Nominal Helium Pressure psig | Temperature C | Length of Run, hr | Vibration | Sheath Air | Grounded | 1st Filter | 2nd Filter | Orifice ^(a) | Walls |
|---------|---------------------------------|---------------|------------------------------|---------------|-------------------|-----------|------------|----------|---------------------|------------|------------------------|-------|
| Th 21 | 50 | Up | 1000 | 22 | 2 | No | Yes | No | 1.0 ^(d) | Not used | <50 | <50 |
| Th 22 | 10 | Down | 1000 | 17 | 2 | Radial | Yes | No | Failed | Not used | <50 | <50 |
| Th 22a | 10 | Down | 1000 | 20 | 2 | Radial | Yes | No | Failed | Not used | - | - |
| Th 22b | 10 | Down | 1000 | 18 | 2 | Radial | Yes | No | 45.0 ^(d) | Not used | <50 | <50 |
| Th 23 | 20 | Down | 1000 | 23 | 2 | No | Yes | No | 3.0 ^(d) | Not used | ND | ND |
| Th 17a | 50 | Down | 1000 | 24 | 2 | No | Yes | No | 46.0 ^(d) | Not used | 107 | 225 |
| Th 17b | 50 | Down | 1000 | 24 | 2 | No | Yes | No | 28.0 ^(d) | Not used | 113 | 266 |
| Th 17c | 50 | Down | 1000 | 23 | 2 | No | Yes | No | 65.0 ^(d) | Not used | 87 | <50 |
| Th 24 | 50 | Down | 1000 | 22 | 2 | No | No | No | 60.0 ^(d) | Not used | 64 | 168 |
| Th 12a | 5 | Down | 1000 | 16 | 2 | Radial | Yes | No | 25.0 ^(d) | Not used | ND | <50 |

(a) Downstream face.

(b) Pressure was allowed to decay.

(c) The leak tube was vibrated for first 6 months.

(d) These results are based on X-ray fluorescence analysis. Other data are the results of radioassay alpha counting which has a detection limit of 50 μg of ThO₂. ND = Not Detected.

TABLE 5. SUMMARY OF ELEVATED TEMPERATURE SIMULANT RUNS USING CASCADE IMPACTORS (a)

| Run No. | Pressure, psig | Temperature, C | Quantity of ThO ₂ Detected ^(b) for Indicated Maximum Particle Size, μg | | | | | | Total |
|----------------------|----------------|----------------|--|------|------|------|------|--------|--------|
| | | | Inlet Nozzle Residue | 8 μm | 4 μm | 2 μm | 1 μm | 0.5 μm | |
| Th 25 | 1000 | 400 | 358 | 127 | N.D. | <50 | <50 | <50 | 485 |
| Th 26 | 500 | 400 | <50 | <50 | <50 | N.D. | <50 | <50 | <50 |
| Th 27 | 1000 | 815 | 1766 | 647 | 153 | 73 | <50 | 53 | 2692 |
| Th 28 | 500 | 815 | 940 | 220 | 60 | <50 | <50 | <50 | 1220 |
| Th 31 ^(c) | 1000 | 815 | <50 | 686 | 80 | <50 | <50 | 107 | 873 |
| Th 32 ^(c) | 1000 | 815 | 111 | 2226 | 303 | <50 | <50 | <50 | 2640 |
| Th 33 ^(d) | 1000 | 815 | 2886 | 7846 | 893 | 180 | 73 | 80 | 11,958 |

(a) All runs with 50-μm-diameter orifice disc, in down position, for 2 hr, with no vibration.

(b) Data are the results of radioassay alpha counting which has a detection limit of 50 μg of ThO₂.

(c) The cascade impactor used in this run has a calibrated airflow rate of 13 l/min. In the other runs, the cascade impactor having a calibrated airflow rate of 1 l/min was used.

(d) Examination of the orifice after this run showed that the orifice was cracked, which explains why the ThO₂ emission was so great.

was released one time in the sideways and up position with vibration (see Experiments 16 and 20). On the other hand, little or no release occurred in one case of the up position with no vibration (Experiment 21) and numerous runs in the sideways position both with and without vibration (Experiments 7-10, 15, 18, 19).

- (5) At 920 psig, considerably more ThO_2 is emitted through a 50- μm orifice at 815°C than at 400°C (see Th 25 and Th 27).
- (6) At 400°C, more ThO_2 is emitted through a 50- μm orifice at 920 psig than at 440 psig (see Th 25 and Th 26).
- (7) At 815°C, the data indicate that considerably more ThO_2 is emitted at a pressure of 920 psig than at 440 psig.
- (8) The use of an impactor with a sheath airflow rate of 13 l/min, compared to one with a flow rate of 1 l/min, reduced the stray deposition of ThO_2 at 815°C with a 50- μm orifice.
- (9) A general comparison of the ThO_2 leak rate through a 50- μm orifice at room temperature and an internal pressure of 920 psig to the helium leak rate indicates that the emission of ThO_2 is less than that of helium by a factor of about 10^8 on an atom per molecule basis.

was released one time in the sideways and up position
with vibration (see experiments 18 and 20). On the
other hand, little or no release occurred in one case
of the up position with no vibration (experiment 11)
and a serious time in the sideways position both with and
without vibration (experiments 1, 10, 13, 18, 19).

(5) At 930 gals, considerably more IMU is emitted through
a 30-in orifice at 81°C than at 800 gals (see IM 22 and
T 23).

(6) At 800 gals, more IMU is emitted through a 30-in orifice
at 910 gals than at 800 gals (see IM 22 and T 23).

(7) At 815°C, the data indicate that considerably more
IMU is emitted at a pressure of 930 gals than at 800 gals.

(8) The use of an orifice with a specific flow rate of
13 l/min, compared to one with a flow rate of 1 l/min,
reduced the steady deposition of IMU at 815°C with a
30-in orifice.

(9) A general comparison of the 100% leak rate through a
30-in orifice at room temperature and an internal pressure
of 810 gals to the helium flow rate indicates that the
emission of IMU is less than that of helium by a
factor of about 10 on an atom per molecule basis.

PuO₂ EXPERIMENTS

Effect of Experimental Parameters on the Size Distribution of the PuO₂ Emission

The effects of orifice size, helium pressure, leak-tube position, and vibration on the particulate size distribution of the PuO₂ emissions are summarized in Table 6 through 8 and illustrated in Figures 15 through 17.

In about half the experiments carried out with 10- and 20- μm orifices, the average particle size distribution of the leaked PuO₂ powder paralleled that of the starting powder. In the case of the 5- μm orifice, however, the emission particle size distribution did not parallel that of the starting powder and generally was skewed toward sizes smaller than about 1 μm . In most of the other runs with 10- and 20- μm orifices, the particulate distribution was skewed toward sizes greater than 2 μm .

Size measurements for several runs indicate a shift to a mean emitted particle size larger than that of the starting powder. In general, this may be accounted for by biased measurements of the initial size distribution. Both the Battelle measurements and the comparable ARHCO measurements were done on suspended and dispersed PuO₂ particles. The measurement techniques used would tend to break up or discriminately lose any large agglomerates, thus indicating a smaller than representative mean particle size. Many of the experimental runs may not have this same biasing mechanism. The parametric effects on the emitted PuO₂ particle size are discussed below.

- Orifice Size. The effect of orifice size on the average mean particle size of the PuO₂ emission is shown in Figure 15. These data indicate that the mean size of the emission decreased with a decrease in orifice size at helium pressures of 440 and 920 psig. The average mean particle size was 1.5, 2.2, and 5.3 μm for the 50-, 10-, and 20- μm orifices, respectively. This may be accounted for by increasing shear stress with decreasing orifice size resulting in breakup of agglomerates. Another factor to be considered is the likelihood of the increased

TABLE 6. PARTICLE SIZE DISTRIBUTION OF PuO₂ EMITTED THROUGH A 5- μ m ORIFICE AT ROOM TEMPERATURE^(a)

| Run Number | Tube Position | Nominal Helium Pressure ^(b) , psig | Vibration | Particle Size Distribution Cumulative Percent | | | | | | Mean Particle Size, μ m |
|-----------------|---------------|---|-----------|---|------------|------------|------------|--------------|---------------|-----------------------------|
| | | | | <8 μ m | <4 μ m | <2 μ m | <1 μ m | <0.5 μ m | <0.25 μ m | |
| Starting Powder | - | - | - | 80.0 | 61.0 | 42.0 | 23.0 | 7.0 | 1.7 | 2.5 |
| 28 | Down | 1000 | No | - | 33.4 | 23.2 | 17.5 | 7.8 | 4.9 | 4.7 |
| 29 | Sideways | 1000 | Yes | - | 89.1 | 84.9 | 60.2 | 56.4 | 8.5 | 0.57 |
| 30 | Up | 1000 | Yes | - | 87.1 | 86.6 | 82.0 | 30.4 | 4.6 | 0.60 |
| 31 | Down | 500 | Yes | - | 89.7 | 59.8 | 59.8 | 47.7 | 12.2 | 0.88 |
| 32 | Sideways | 500 | Yes | - | 86.2 | 68.4 | 56.9 | 8.6 | 6.9 | 1.25 |
| 33 | Up | 500 | Yes | - | 87.7 | 65.8 | 57.5 | 31.5 | 4.1 | 1.07 |

(a) All runs were for 10 min

(b) Actual pressures were 920 and 440 psig.

TABLE 7. PARTICLE SIZE DISTRIBUTION OF PuO₂ EMITTED THROUGH A 10- μ m ORIFICE AT ROOM TEMPERATURE^(a)

| Run Number | Tube Position | Nominal Helium Pressure ^(b) , psig | Vibration | Particle Size Distribution, Cumulative Percent | | | | | | Mean Particle Size, μ m |
|-----------------|---------------|---|-----------|--|------------|------------|------------|--------------|---------------|-----------------------------|
| | | | | <8 μ m | <4 μ m | <2 μ m | <1 μ m | <0.5 μ m | <0.25 μ m | |
| Starting Powder | - | - | - | 80.0 | 61.0 | 42.0 | 23.0 | 7.0 | 1.7 | 2.5 |
| 19 | Down | 1000 | No | - | 91.2 | 89.9 | 89.3 | 87.8 | 84.5 | <0.25 |
| 20 | Sideways | 1000 | Yes | - | 80.2 | 63.2 | 43.7 | 37.6 | 8.7 | 1.3 |
| 21 | Up | 1000 | Yes | - | 52.5 | 4.7 | 0.58 | 0.10 | 0 | 4.9 |
| 22 | Down | 500 | Yes | - | 44.5 | 26.1 | 12.6 | 1.9 | 0 | 3.3 |
| 23 | Sideways | 500 | Yes | - | 78.2 | 67.3 | 40.4 | 25.6 | 19.9 | 1.2 |
| 24 | Up | 500 | Yes | - | 90.3 | 15.4 | 8.2 | 4.6 | 0 | 2.0 |

(a) All runs were for 10 min

(b) Actual pressures were 920 and 440 psig.

TABLE 8. PARTICLE SIZE DISTRIBUTION OF PuO₂ EMITTED THROUGH A 20- μ m ORIFICE AT ROOM TEMPERATURE^(a)

| Run Number(s) | Position | Nominal Helium Pressure ^(b) , psig | Vibration | Particle Size Distribution, Cumulative Percent | | | | | | Average Mean Particle Size, μ m |
|-----------------------|----------|---|-----------|--|------------|------------|------------|--------------|---------------|-------------------------------------|
| | | | | <8 μ m | <4 μ m | <2 μ m | <1 μ m | <0.5 μ m | <0.25 μ m | |
| Starting Powder | - | - | - | 80.0 | 61.0 | 42.0 | 23.0 | 7.0 | 1.7 | 2.5 |
| Pu 1, Pu 1a | Down | 1000 | Yes | - | 60.6 | 27.5 | 9.9 | 3.3 | 2.0 | 5.1 |
| Pu 2, Pu 2a | Down | 1000 | No | - | 65.9 | 50.9 | 40.2 | 12.1 | 1.9 | 2.7 |
| Pu 3, Pu 3a | Sideways | 1000 | No | - | 46.8 | 15.9 | 5.2 | 3.7 | 1.0 | 4.4 |
| Pu 4, Pu 4a | Sideways | 1000 | Yes | - | 50.2 | 14.2 | 6.0 | 5.1 | 4.7 | 7.4 |
| Pu 5, Pu 5a | Up | 1000 | No | - | 61.8 | 21.7 | 2.6 | 0.6 | 0.2 | 3.5 |
| Pu 6, Pu 6a, Pu 6b | Up | 1000 | Yes | - | 41.4 | 10.3 | 1.3 | 0.12 | 0.01 | 5.2 |
| Pu 7, Pu 7a | Down | 500 | No | - | 17.7 | 2.9 | 0.5 | 0.13 | 0.01 | 11.0 |
| Pu 8, Pu 8a | Down | 500 | Yes | - | 28.9 | 5.8 | 0.4 | 0.02 | 0.01 | 8.0 |
| Pu 9, Pu 9a, Pu 9b | Sideways | 500 | Yes | 66.4 ^(c) | 52.5 | 37.4 | 27.2 | 16.6 | 4.1 | 5.7 |
| Pu 14, Pu 14a | Sideways | 500 | No | - | 61.1 | 41.5 | 29.6 | 21.2 | 6.0 | 4.5 |
| Pu 10, Pu 10a | Up | 500 | Yes | - | 81.9 | 12.7 | 2.6 | 1.2 | 0.15 | 3.4 |
| Pu 15, Pu 15a | Up | 500 | No | - | 80.7 | 31.7 | 2.6 | 0.6 | 0.25 | 2.8 |
| Pu 11, Pu 11a, Pu 11b | Down | Ambient | No | - | 74.2 | 51.5 | 32.6 | 16.3 | 7.2 | 1.8 |
| Pu 16 | Down | Ambient | Yes | - | 87.5 | 77.1 | 65.6 | 16.7 | 13.5 | 0.9 |
| Pu 12 | Sideways | Ambient | Yes | - | 59.4 | 49.0 | 17.4 | 10.1 | 2.6 | 2.6 |
| Pu 17 | Sideways | Ambient | No | - | 88.3 | 72.3 | 62.8 | 48.9 | 37.2 | 0.5 |
| Pu 13 | Up | Ambient | Yes | - | 79.3 | 67.5 | 22.0 | 17.2 | 1.9 | 1.6 |
| Pu 18 | Up | Ambient | No | - | 66.7 | 59.6 | 46.5 | 28.3 | 0 | 1.2 |

(a) All runs were for 10 min
 (b) Actual pressures were 920 and 440 psig.
 (c) Data for Run Pu 9 only.

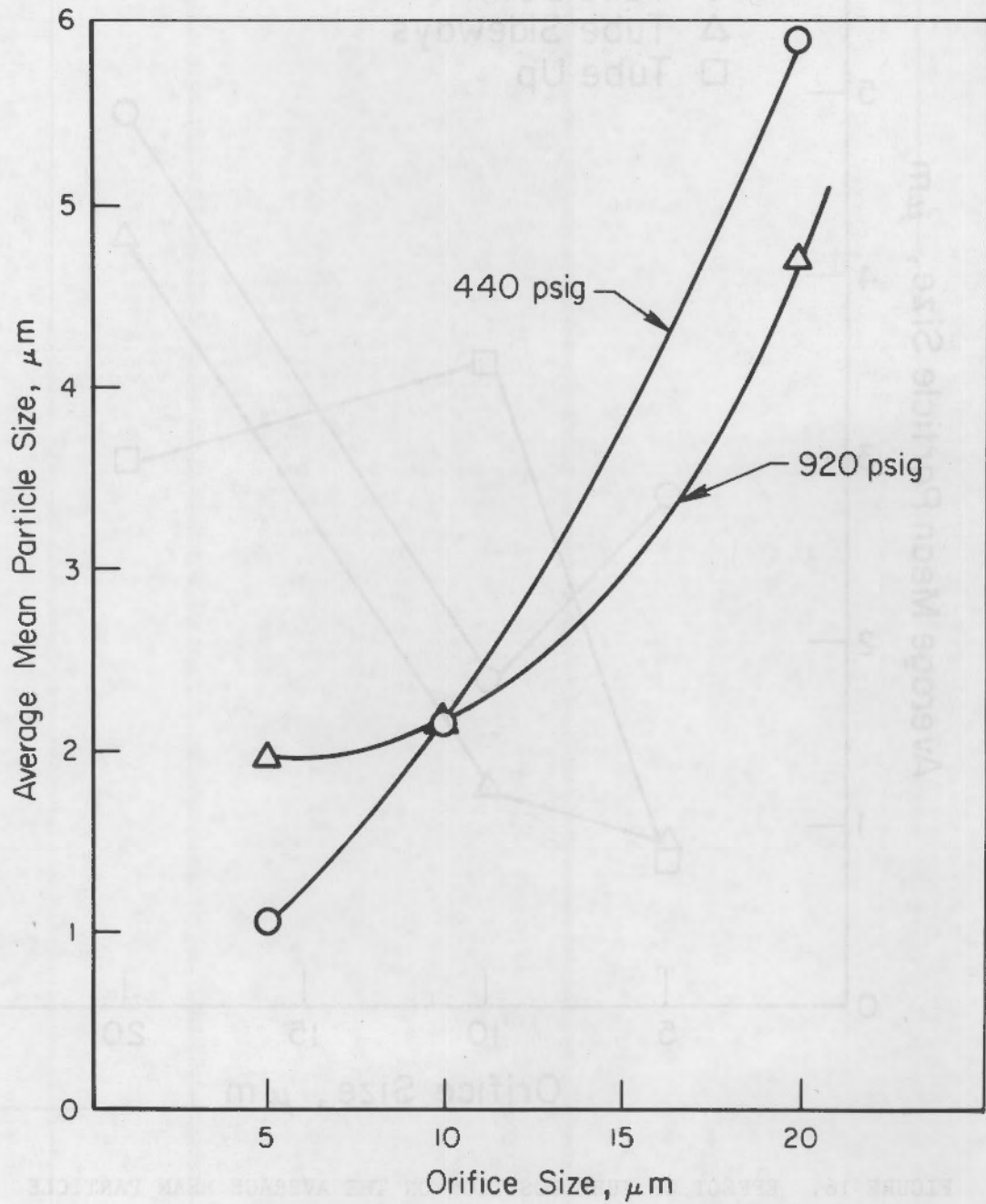


FIGURE 15. EFFECT OF ORIFICE SIZE AND PRESSURE ON THE AVERAGE MEAN PARTICLE SIZE OF EMITTED PuO_2 AT ROOM TEMPERATURE

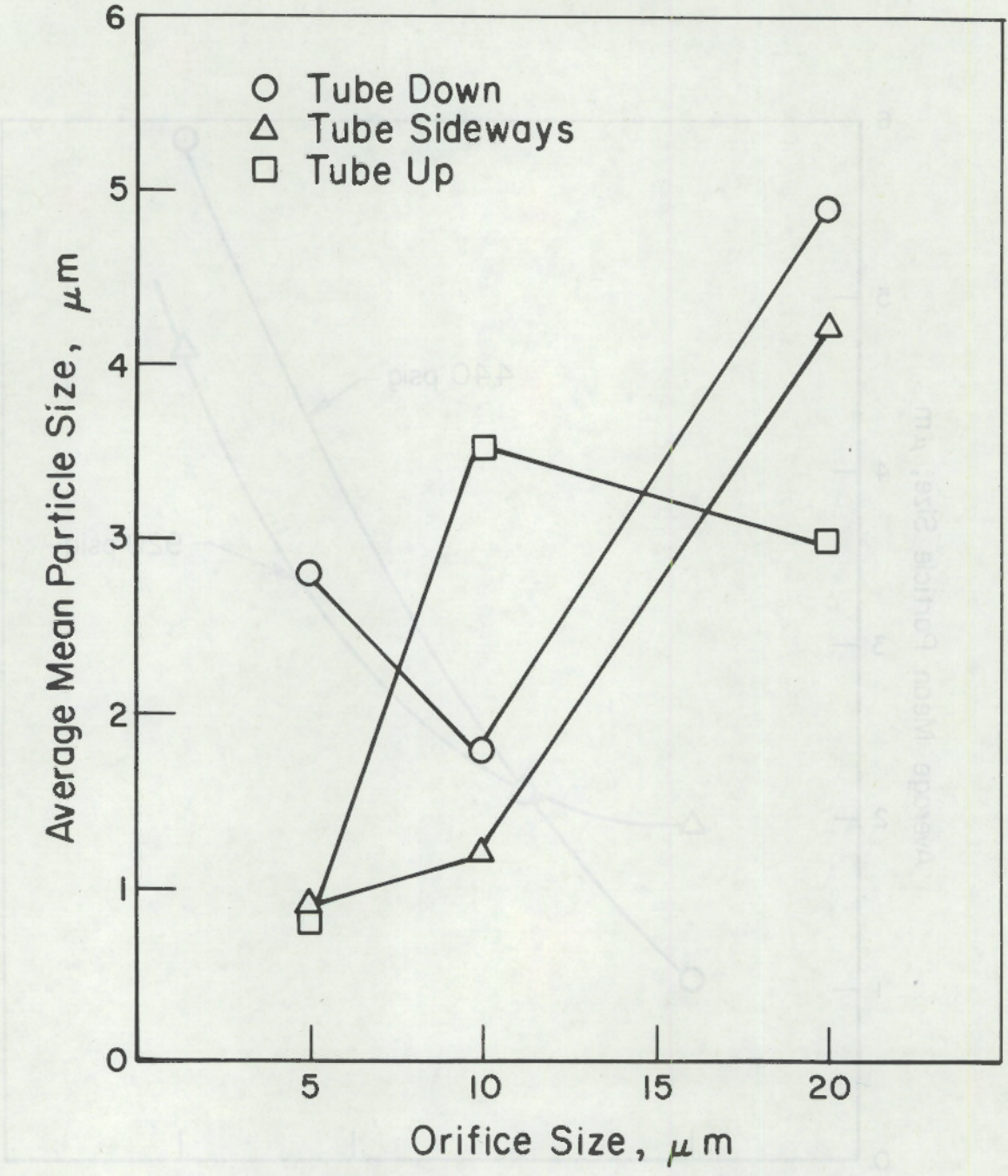


FIGURE 16. EFFECT OF TUBE POSITION ON THE AVERAGE MEAN PARTICLE SIZE OF PuO₂ EMITTED THROUGH ORIFICES

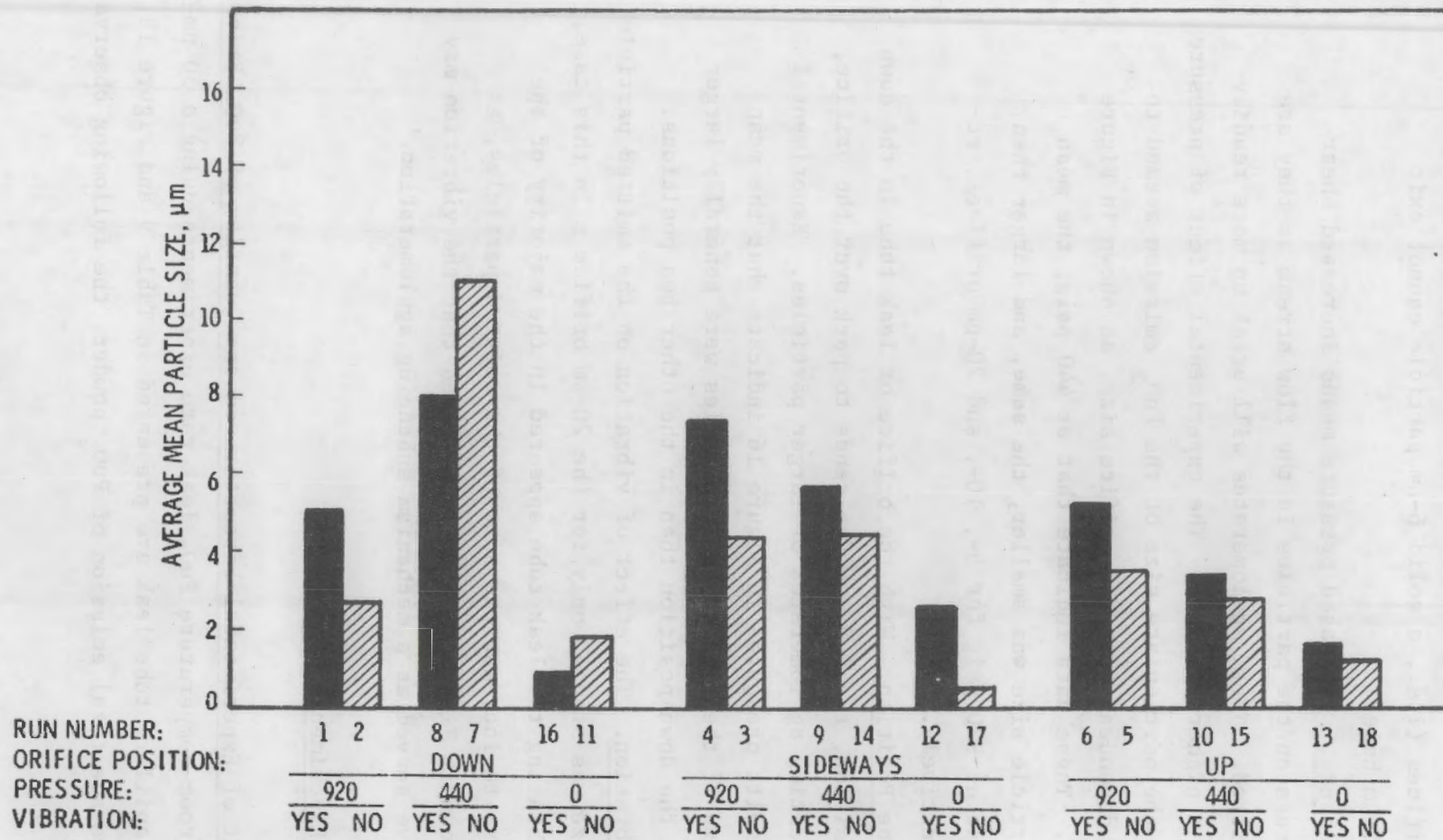


FIGURE 17. EFFECT OF VIBRATION ON THE EMISSION OF PuO_2 POWDER THROUGH A 20- μm ORIFICE

effect of simple sieving collection in the smaller orifices (i.e., a solid 6- μm particle cannot exit a 5- μm hole).

- Pressure. Increased pressure means increased shear stress on the particles in the flow stream as they are emitted. Thus, agglomerates will break up more readily at a higher pressure. The experimental effect of pressure on the particulate size of the PuO_2 emission seemed to be dependent upon the orifice size, as shown in Figure 15. These data indicate that at 440 psig, the mean particle size was smaller, the same, and larger than that at 920 psig for 5-, 10-, and 20- μm orifices, respectively.
- Tube Position. With the orifice or leak tube in the down position, the PuO_2 powder tends to pack over the orifice, creating agglomerates of larger particles. Experimental results presented in Figure 16 indicate that the mean size of the emitted PuO_2 particles were generally larger in the down position than in the other two positions.
- Vibration. The effect of vibration on the emitted particle size was studied only for the 20- μm orifice. In this case, vibrating the leak tube appeared in the majority of the runs to increase the size of the emitted particles, as shown in Figure 17. It is believed that the vibration may have served as a mechanism enhancing agglomeration.

Capillary Leak Experiments

Effect of Experimental Parameters on the Quantity of PuO_2 Emission.

Results of the room-temperature PuO_2 leak rate experiments using a 50- μm -ID x 4.4-cm-long capillary tube leak are presented in Table 9 and Figure 18. Based on the average total emission of PuO_2 powder, the following observations are made.

TABLE 9. SUMMARY OF PuO₂ LEAK RATE EXPERIMENTS AT ROOM TEMPERATURE USING A 50- μ m-ID CAPILLARY^(a)

| Run Number | Tube Position | Pressure, psig | Vibration | Quantity of PuO ₂ Detected for Indicated Particle Size, μ g ^(b) | | | | | | | | Total ^(c) | Helium Leak Rate, cc/sec |
|-----------------------|---------------|----------------|-----------|---|------------|-------------|-------------|---------------|------------------|---------------|-----------------|----------------------|--------------------------|
| | | | | Inlet Nozzle | >4 μ m | 4-2 μ m | 2-1 μ m | 1-0.5 μ m | 0.5-0.25 μ m | <0.25 μ m | Filter, μ m | | |
| Pu 39 | Down | 1000 | No | 0.0076 | 0.0006 | 0.0003 | 0.0013 | 0.0004 | 0.0006 | 0.0001 | - | 0.0073 | 0.87 |
| Pu 39a ^(e) | Down | 1000 | No | 0.0025 | - | - | - | - | - | - | 0.0005 | -0.0011 | 14.1 |
| Pu 40 | Up | 1000 | Yes | 0.0032 | 0.0019 | 0.0025 | 0.0013 | 0.0069 | 0.0006 | - | - | 0.0129 | 27.4 |
| Pu 40a ^(e) | Up | 1000 | Yes | 0.0050 | - | - | - | - | - | - | 0.0001 | 0.001 | 26.1 |
| Pu 41 | Down | 500 | Yes | 0.0057 | 0.0025 | 0.0000 | 0.0006 | 0.0005 | 0.0004 | 0.0003 | - | 0.0060 | 3.9 |
| Pu 41a ^(e) | Down | 500 | Yes | 0.0013 | - | - | - | - | - | - | 0.0013 | -0.0015 | 0.86 |
| Pu 42 | Up | 500 | Yes | 0.0025 | - | - | - | - | - | - | - | 0.0041 | 4.8 |
| Pu 42a ^(e) | Up | 500 | Yes | 0.0139 | - | - | - | - | - | - | 0.0001 | 0.0098 | 5.6 |
| Pu 43 ^(e) | Down | Ambient | No | 0.0063 | - | - | - | - | - | - | 0.0397 | 0.0419 | - |
| Pu 43a ^(e) | Down | Ambient | No | 0.0044 | - | - | - | - | - | - | 0.0006 | 0.0010 | - |
| Pu 44 ^(e) | Up | Ambient | Yes | 0.0013 | - | - | - | - | - | - | 0.0025 | -0.0000 | - |
| Pu 44a ^(e) | Up | Ambient | Yes | 0.0032 | - | - | - | - | - | - | 0.0013 | 0.0003 | - |

(a) All runs were for 10 min

(b) Based on the specific activity of 0.096 Ci/g for Pu.

(c) The average box background for these experiments was 0.0041 μ g PuO₂ for a ten-min collection. This quantity was subtracted from the total emission, but not from the emissions for each size range.

(d) The leak rate was determined by the pressure decay method at the midpoint of the run. In an empty leak tube, the He leak rate was 0.8 and 0.3 cc/sec at 920 and 440 psig, respectively. Thus, leak rates higher than those are presumably indicative of leak in He supply line to the leak tube.

(e) The sizing stages of the cascade impactor were replaced with a tube and all of the PuO₂ emission was collected on the final filter located at the entrance end.

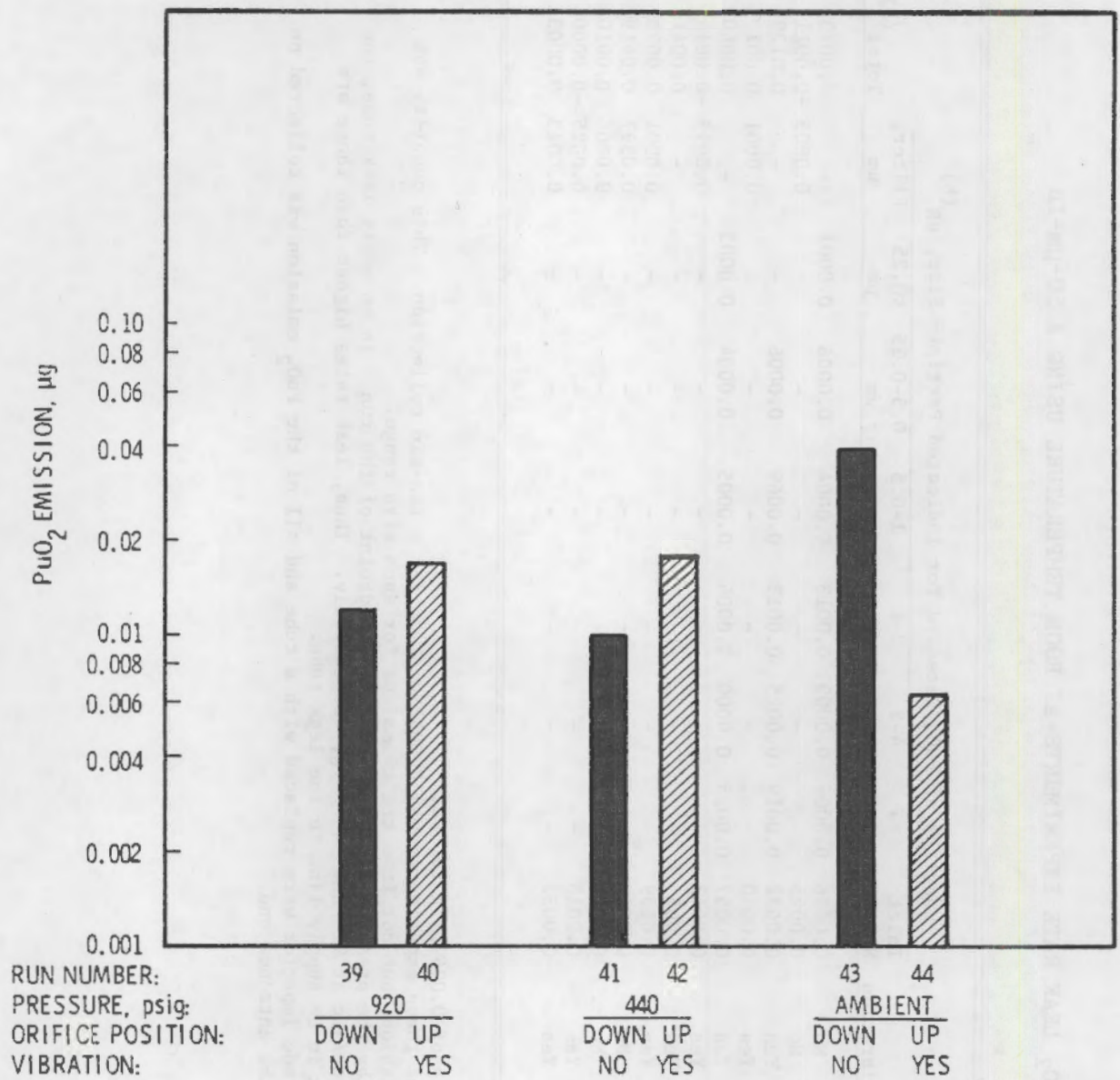


FIGURE 18. EFFECT OF EXPERIMENTAL CONDITIONS ON THE AVERAGE EMISSION OF PuO_2 POWDER THROUGH A 50- μm -ID CAPILLARY AT ROOM TEMPERATURE

- The greatest emission occurred at ambient pressure with the leak tube in the down position. The He:PuO₂ leak rate ratio was 4.9×10^2 in this experiment.
- The PuO₂ emission was slightly greater with the leak tube in the up position at helium pressures of 920 and 440 psig. However, at ambient pressure, the emission was greater in the down position.
- In general, pressure appeared to have little effect on the PuO₂ emission.
- The PuO₂ emission through the 50- μ m-ID capillary was comparable to that through the 5- μ m orifice at helium pressures of 920 and 400 psig and at ambient pressure. Helium leak rates were similarly comparable under all conditions.

Effect of Experimental Parameters on the Size Distribution of the

PuO₂ Emission. Particle-size data on the room-temperature capillary leak experiments are presented in Table 10 and Figure 19. The average mean particle size of PuO₂ emission was about 1.3 μ m and 2.3 μ m at helium pressures of 920 and 440 psig, respectively. The overall average mean particle size was 1.8 μ m, which is comparable to that for the 5- μ m orifice. The largest mean particle size of leaked particles was 3.9 μ m, which occurred at 440 psig with the leak tube down and vibrated.

The particle-size distribution of the emission for Run Pu 41 was similar to that of the starting powder. For the other runs, there was a general displacement of the size distribution toward emission of smaller particles. Run Pu 42 showed an unusually large percentage of particles smaller than 0.25 μ m.

TABLE 10. PARTICLE SIZE DISTRIBUTION OF PuO₂ EMISSION THROUGH A 50- μ m x 4.4-cm-LONG
CAPILLARY TUBE AT ROOM TEMPERATURE^(a)

| Number | Position | Nominal Helium Pressure ^(b) , psig | Vibration | Particle Size Distribution, Cumulative Percent | | | | | | Mean Particle Size |
|-----------------|----------|--|-----------|---|------|------|------|------|-------|--------------------------|
| | | | | <8 | <4 | <2 | <1 | <0.5 | <0.25 | |
| Starting Powder | - | - | - | 80.0 | 61.0 | 42.0 | 23.0 | 7.0 | 1.7 | 2.5 |
| Pu 39 | Down | 1000 | No | - | 78.3 | 70.3 | 31.9 | 21.0 | 2.9 | 1.3 |
| Pu 40 | Up | 1000 | Yes | - | 86.0 | 68.1 | 59.5 | 6.5 | 0 | 1.2 |
| Pu 41 | Down | 500 | Yes | - | 44.0 | 43.5 | 25.1 | 14.7 | 6.8 | 3.9 |
| Pu 42 | Up | 500 | Yes | - | 84.3 | 65.9 | 60.7 | 45.0 | 41.5 | 0.6 |

(a) All runs were for 10 min.

(b) Actual pressures were 920 and 440 psig.

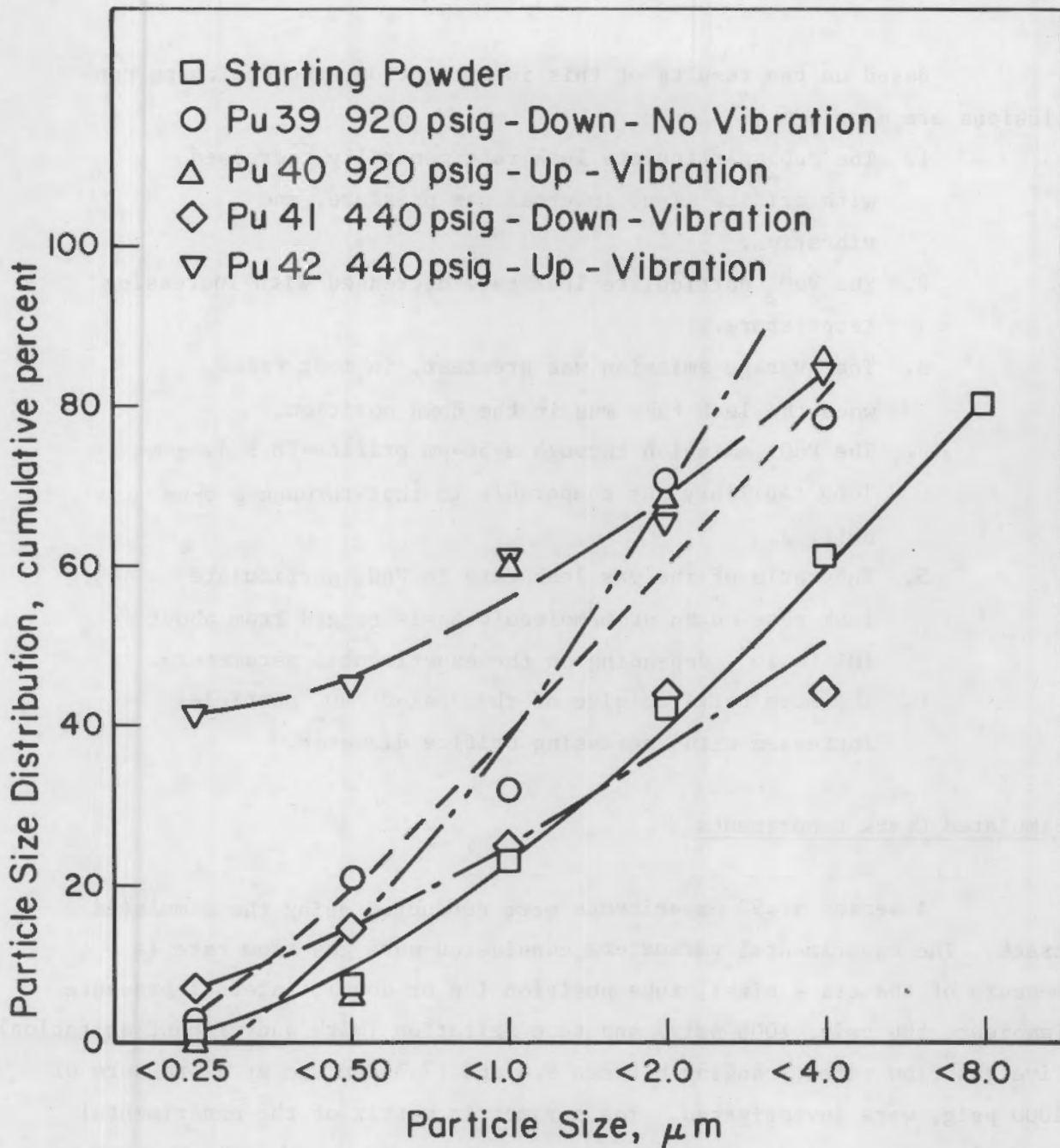


FIGURE 19. PARTICLE SIZE DISTRIBUTION OF PuO_2 EMISSION THROUGH A 50- μm -ID x 4.4-cm-LONG CAPILLARY TUBE AT ROOM TEMPERATURE

Based on the results of this investigation, the following conclusions are made:

1. The PuO_2 particulate leak rate generally increased with orifice size, internal gas pressure, and vibration.
2. The PuO_2 particulate leak rate decreased with increasing temperature.
3. The average emission was greatest, in most cases, when the leak tube was in the down position.
4. The PuO_2 emission through a 50- μm orifice-ID x 4.4-cm-long capillary was comparable to that through a 5- μm orifice.
5. The ratio of the gas leak rate to PuO_2 particulate leak rate on an atom/molecule basis ranged from about 10^3 to 10^9 , depending on the experimental parameters.
6. The mean particle size of the leaked PuO_2 particles increased with increasing orifice diameter.

Simulated Crack Experiments

A series of 92 experiments were conducted using the simulated crack. The experimental parameters considered were gas flow rate (a measure of the crack size), tube position (up or down), internal pressure (ambient, 500 psig, 1000 psig) and tube agitation (with and without agitation). Five gas flow rates, ranging between 9.8 and 17.3 scc/sec at a pressure of 1000 psig, were investigated. The parametric matrix of the experimental conditions presented in Table 11 serves as a summary of the 92 experiments conducted.

The results of the experiments are presented in Appendix B, Tables B1 through B5.

Inspection of the data tables reveals the extreme variability exhibited by the data. This observation is more clearly demonstrated in Table 12 which presents the arithmetic mean value of the PuO_2 emissions

TABLE 11. PARAMETRIC MATRIX OF PuO₂ EXPERIMENTS
USING THE SIMULATED CRACK

| Leak Rate (scc/sec) | Vibration | Pressure: Position: | Ambient | | 500 psig | | 1000 psig | |
|---------------------------|-----------|------------------------|---------|------|----------|------|-----------|------|
| | | | Up | Down | Up | Down | Up | Down |
| 9.8 | Y | | 2 | 2 | 3 | 2 | 2 | - |
| 9.8 | N | | - | 2 | - | - | 2 | 2 |
| 11.4 | Y | | 2 | - | 3 | 2 | 2 | - |
| 11.4 | N | | - | 2 | - | - | 2 | 2 |
| 11.6 | Y | | 2 | - | 2 | 4 | 4 | - |
| 11.6 | N | | - | 2 | - | - | 4 | 6 |
| 13.2 | Y | | 2 | - | 4 | 2 | 2 | - |
| 13.2 | N | | - | 4 | - | - | 4 | 2 |
| 17.3 | Y | | 2 | - | 2 | 2 | 4 | - |
| 17.3 | N | | - | 2 | - | - | 2 | 2 |

(a) Leak rate at 1000 psig using pressure decay method; determined prior to runs.

TABLE 12. ARITHMETIC MEAN VALUE OF PuO_2 POWDER LEAKED AND THE STANDARD DEVIATION FOR EACH EXPERIMENTAL CONDITION USING THE SIMULATED CRACK CONFIGURATION (MEAN/STANDARD DEVIATION) (IN NEAREST ng)

| Leak Rate (scc/sec) | Vibration | Pressure: Position: | Ambient | | 500 psig | | 1000 psig | |
|---------------------|-----------|---------------------|---------|-------|----------|---------|-----------|------------|
| | | | Up | Down | Up | Down | Up | Down |
| 9.8 | Y | | 3/3 | -1/0 | 1/2 | 66/44 | 5/5 | - |
| 9.8 | N | | - | 0/1 | - | - | 4/0 | 2/1 |
| 11.4 | Y | | 1/0 | - | 0/0 | 0/0 | -1/0 | - |
| 11.4 | N | | - | -1/1 | - | - | -1/1 | -1/0 |
| 11.6 | Y | | -1/0 | - | -2/1 | 469/851 | 441/872 | - |
| 11.6 | N | | - | 0/1 | - | - | 180/265 | 5955/14127 |
| 13.2 | Y | | -1/1 | - | 1/2 | 570/114 | 5/2 | - |
| 13.2 | N | | - | 37/73 | - | - | 28/50 | 41/17 |
| 17.3 | Y | | 0/0 | - | 5/1 | 553/134 | 57/97 | - |
| 17.3 | N | | - | 9/10 | - | - | 42/21 | 24/2 |

and the standard deviation for each experimental condition. For many but not all conditions the variability is such that the standard deviation associated with a series of experiments carried out under identical conditions is greater than the mean value of those experiments. Such extreme variability would be expected to mask all but the most obvious parametric effects.

A visual examination of the data in Tables B1 through B5 or the average values of Table 12 reveals no consistent pattern of dependence of the quantity of PuO_2 emitted on the experimental parameters. For the sake of thoroughness, the data were analyzed by standard test of statistical significance. Prior to the analysis the data were transformed logarithmically to the form

$$Z = \log (1000 X + 10)$$

where X is the total PuO_2 emission in micrograms. This transformation was suggested by a plot of the standard deviation versus the average PuO_2 emission for a given set of conditions which demonstrated that the standard deviation is directly proportional to the quantity of PuO_2 emitted. This transformation served to somewhat stabilize the variability of the data and reduce the skewness. Although this transformation was not ideal, attempts to provide a better one were unsuccessful. This logarithmic transformation was used for the subsequent data analysis. Using standard tests of statistical significance, the data were examined for effects of the internal gas pressure, leak size, tube position, and agitation of the powder. Within the limits imposed by the variability of the data no consistent parametric dependence could be discerned.

Parametric Dependence of PuO_2 Emissions Through Orifices

A total of 250 experiments were conducted using orifices ranging from 5 through 50 μm in diameter. The experimental parameters investigated were orifice size, internal pressure, tube position and powder agitation. The results of these experiments and the actual conditions under which they were conducted are presented in Tables B6 through B17 of Appendix B.

Variability of the Data

The experimental results for the orifice experiments exhibit an extreme degree of variability. Repeated runs (i.e., several runs conducted under identical experimental conditions) often differed from one another by several orders of magnitude. This variability is probably a consequence of the small quantity of PuO_2 being emitted. In many cases, the differences observed between a series of identical runs are no greater than what would be expected by the addition or subtraction of a single large particle of plutonia powder. In fact, in some cases, the entire quantity of PuO_2 detected could be attributed to one powder particle. In the original powder, 20 percent of the particles had diameters of greater than $8 \mu\text{m}$, which corresponds to a PuO_2 mass of approximately 25 nanograms per particle. It is easy to see how one particle could affect the emission. When working with such small numbers of particles, it is not surprising to see the severe variability of the data.

Due to the small quantities of PuO_2 emitted and the high sensitivity of the radioassay technique, it would not be expected that the reproducibility of the data would be exact. However, these data may be evidence that the PuO_2 emissions are influenced by some undefined factor. One such factor considered is possible plugging and unplugging of the leak during the course of a run. A digital flow meter was installed in the system to study this. Flow rate data were accumulated during each run and examined for changes of flow. The data showed that although there was considerable fluctuation in the flow rates between runs, there was no significant change during any given run. The indications were that those incidents which resulted in flow rate changes had to occur during the initial pressurization or final depressurization of the leak tube, when the flow rate cannot be measured.

Background Subtraction

The containment box background measurements appear to exhibit a lack of reproducibility similar to that observed for the actual run measurements. It was therefore felt that it would be more appropriate to use an

average value for the background rather than to rely upon a single measurement associated with a series of runs. The earlier experiments Pu 1 through Pu 36 exhibited a consistently higher background than the later runs Pu 82 through Pu 131 so the background averages used for these two sets of runs differed. For the earlier runs, the background for the runs was 0.0030 μg , while the latter set of background was 0.0013 μg with subtraction was greater than that associated with the counting of the PuO_2 emitted. Consequently, only the background error will contribute significantly to the error associated with the net total emissions.

Collection Time Dependence

To determine the effects of the collection time, a series of experiments with varying collection times was conducted. The time effect was investigated for both 20- μm and 50- μm -diameter orifices. The results of these experiments are included in the tables of Appendix B. For the 20- μm -diameter orifices, the experiments were all conducted at 1000 psig pressure, in the upright position and with no vibration. The 20- μm -orifice runs were compared and their collection times were Pu 107 through Pu 107n (10 min), Pu 108 through Pu 108d (60 min), Pu 109 through Pu 109d ("zero time") and Pu 110 through Pu 110d (120 min). For the 50- μm -diameter orifice runs, the conditions were 1000 psig, up position, with vibration. These experiments and collection times are labelled Pu 119 through Pu 119e (10 min), Pu 128 through Pu 128d ("zero time"), Pu 129 through Pu 129d (60 min). The "zero time" designation refers to those experiments conducted with the collection time and the time during which the tube is fully pressurized kept to the most practical minimum. This was accomplished by rapidly pressurizing the leak tube and immediately after achieving the desired pressure, shutting off the helium supply and releasing the pressure through a bleed valve. The entire operation requires somewhat less than 1 min.

Prior to analysis, the data were subjected to a logarithmic transformation designed to eliminate negative numbers and zeros and help minimize skewness and stabilize the variance. The transformed data were

examined for effects of the collection time using standard tests for statistical significance (F - test, Students t-test). No consistent run time dependence was observed for either orifice size examined.

Parametric Dependency of Orifice Data

The experiments may be considered as consisting of two sets of data. The two sets were both conducted using essentially identical equipment (only minor changes made between sets) but were separated by an extended time period. The first set (Phase I) was completed early in the experimental program. The second set (Phase II) was conducted several months later, and was designed to augment the original experimental design in a way that would either confirm or refute the existence of certain effects that were suggested by the results of the Set I experiments. It was also anticipated that the Phase II data would improve the estimate of experimental error computed from the Phase I data.

The orifice experiments conducted, including those of both Phase I and Phase II, is summarized in Tables 13 and 14. Inasmuch as each experimental run is expensive and time consuming, the number of runs had to be limited to the most important treatment combinations. This accounts for the empty cells in the matrix, which preclude a simple, unified analysis.

Because of the extreme heteroschedasticity (lack of uniform variability as experimental conditions change) and positive skewness (a concentration of low values, along with a few extremely large values) exhibited by the raw data, a transformation of the data seemed advisable in order to make use of standard parametric statistical techniques.

The mean and standard deviation of various cells in the matrix of experimental treatments were noticeably correlated, which led us to consider a logarithmic transformation. The difficulty of dealing with cumbersome decimal fractions and negative observations (which cannot be converted to logarithms) was eliminated by increasing the product 1000×10 , for every X. The transformation equation thus took the form

TABLE 13. PARAMETRIC MATRIX OF PuO₂ LEAK RATE EXPERIMENTS USING STANDARD ORIFICES

DATA SET

| Orifice Size | Vibration | Pressure: Position: | Ambient | | | 500 psig | | | 1000 psig | | |
|--------------|-----------|---------------------|---------|------|----------|----------|------|----------|-----------|------|----------|
| | | | Up | Down | Sideways | Up | Down | Sideways | Up | Down | Sideways |
| 5 | Y | | 2 | - | 2 | 2 | 2 | 2 | 2 | - | 2 |
| 5 | N | | - | 2 | - | - | - | - | - | 4 | - |
| 10 | Y | | 2 | - | 2 | 2 | 2 | 2 | 3 | - | 2 |
| 10 | N | | - | 2 | - | - | - | - | - | 2 | - |
| 20 | Y | | 2 | 2 | 3 | 4 | 2 | 3 | 3 | 2 | 2 |
| 20 | N | | 2 | 3 | 2 | 2 | 2 | 2 | 2 | 2 | 2 |

TABLE 14. PARAMETRIX MATRIX OF PuO₂ LEAK RATE EXPERIMENTS USING STANDARD ORIFICES

DATA SET II

| Orifice Size | Vibration | Pressure: Position : | Ambient | | 500 psig | | 1000 psig | | | 1250 psig | |
|--------------|-----------|----------------------|---------|------|----------|------|-----------|------|----------|-----------|------|
| | | | Up | Down | Up | Down | Up | Down | Sideways | Up | Down |
| 5 | Y | | - | 4 | - | 2 | - | 2 | - | - | - |
| 5 | N | | 2 | - | - | 6 | - | 6 | - | - | - |
| 8 | Y | | - | - | - | - | 4 | 4 | 4 | 2 | 2 |
| 8 | N | | - | - | - | - | - | 4 | - | - | 4 |
| 10 | Y | | - | - | - | 4 | - | - | - | - | - |
| 10 | N | | - | - | 4 | 4 | - | - | - | - | - |
| 20 | Y | | 2 | 2 | - | - | 4 | 4 | - | - | - |
| 20 | N | | 2 | 2 | - | - | 32 | 2 | - | - | - |
| 50 | Y | | 2 | 2 | 4 | 5 | 20 | 5 | - | 4 | 4 |
| 50 | N | | - | - | 2 | 2 | 15 | - | - | 2 | 2 |

$$Z = \log_{10} (1000 X + 10) ,$$

where

X = net quantity of PuO_2

Z = new variate after transformation

Although this transformation was somewhat effective in stabilizing the variance and reducing the skewness, it fell short of being the ideal solution. However, we were unsuccessful in trying to improve upon it. So, despite its shortcomings, this transformation was used in conjunction with all the data analysis.

Through the use of standard statistical tests of significance (the F-test and the T-test), selectively applied, it was concluded that tube position and vibration have no consistent effect on powder emission. Accordingly, these variables were eliminated from further analysis, and the primary effort was concentrated on ascertaining the effects of orifice size and helium pressure.

Analysis of similar data by Pacific Northwest Laboratory⁽⁵⁾ suggested that powder emission is related to $A\sqrt{P}$, where A is the cross-sectional area of the orifice and P is helium pressure. Consequently, we explored the effect of this quantity on the net emission of plutonium oxide powder in the Battelle-Columbus experiments. The first step was to construct a scatter plot showing emission (on transformed scale) versus $A\sqrt{P}$. On the basis of this plot, the data were separated into groups for further study. The first separation was based upon the value of $A\sqrt{P}$, and resulted in three experimental regions. Region I consisted of all data for which the value of $A\sqrt{P}$ was less than 2,000. Region II consisted of all data for which the value of $A\sqrt{P}$ was greater than or equal to 2,000, but smaller than 20,000. Region III consisted of all data for which the value of $A\sqrt{P}$ was greater than or equal to 20,000. The data within each region were further separated into two groups corresponding to Phase I and Phase II of the experimental program. In total, this cross-classification resulted in five groups of orifice data, each of which was analyzed separately.

The data corresponding to Region I and Phase I, as defined above, consists of 46 measurements of PuO_2 emissions. These measurements represent six combinations of orifice size and helium pressure, each combination

constituting a separate subgroup, as shown in Table 15 in order of increasing values of $A\sqrt{P}$. Summary statistics for each of these subgroups are presented in the table, in both original units and transformed units. These statistics support the assumption of negligible differences among subgroups. Accordingly, all six subgroups were combined to produce the histogram in Figure 21A and the overall statistics in Table 15. Taking into account the effect of sampling error and sample size, the histogram has the sort of shape to be expected from a homogeneous set of data. It is reasonable to suppose that it represents a random sample from a unimodal distribution which is slightly skewed toward the right.

The data corresponding to Region I, Phase II, consists of 58 measurements of plutonium oxide emissions. These measurements represent six combinations of orifice size and helium pressure, as shown in Table 16 in order of increasing values of $A\sqrt{P}$. Summary statistics for each of these subgroups are presented in the table. These statistics support the assumption of negligible differences among subgroups. Accordingly, all six subgroups were combined to produce the histogram in Figure 20B and the summary statistics in the last column of Table 16. As before, the histogram has the sort of shape to be expected from a homogeneous set of data.

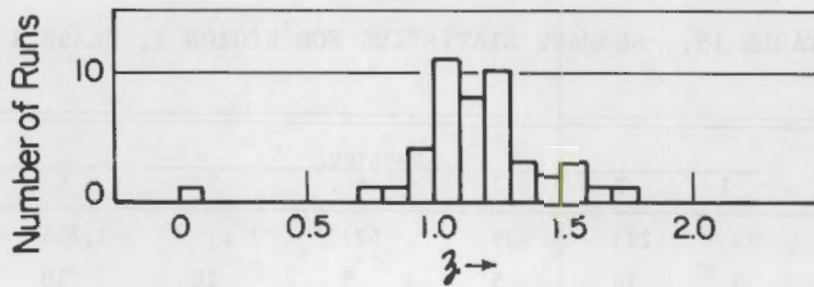
From visual inspection, it appears that the two histograms in Figures 20A and 20B represent random samples from the same population. This conclusion is supported by standard parametric tests of statistical significance^(a). Accordingly, the two histograms were pooled to obtain the histogram in Figure 20C.

The data corresponding to Region II, Phase I, consists of 35 measurements of plutonium oxide emissions. These measurements represent three combinations of orifice size and helium pressure, as shown in Table 17 in order of increasing values of $A\sqrt{P}$. These statistics support the assumption of negligible differences among subgroups. Accordingly, all

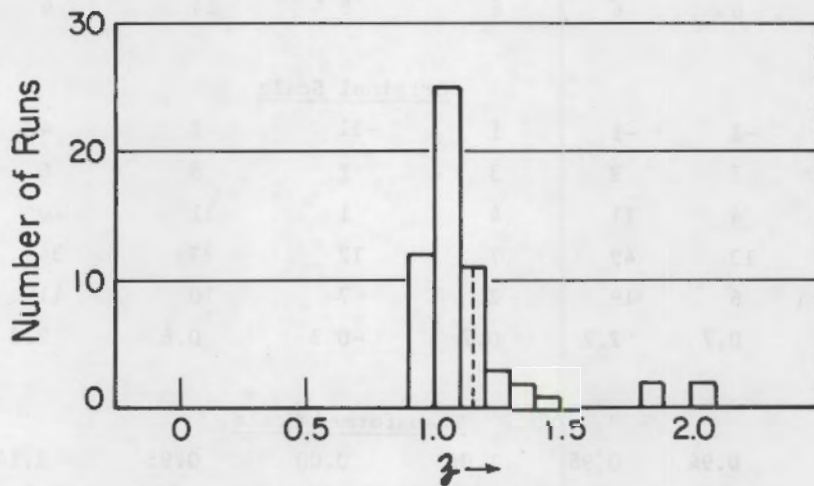
(a) Student's t-test shows no significant difference between the means of the two histograms, and Fisher's F-test shows no significant difference between the variances.

TABLE 15. SUMMARY STATISTICS FOR REGION I, PHASE I

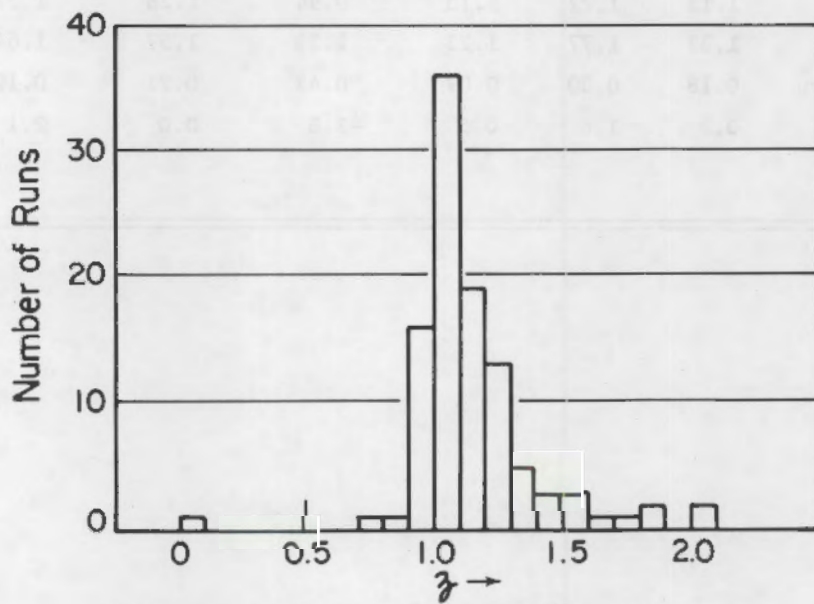
| Statistics | Subgroup | | | | | | Total Sample |
|-------------------------|--------------------------|------|------|-------|-------|-------|--------------|
| | 1 | 2 | 3 | 4 | 5 | 6 | |
| A \sqrt{P} | 73 | 294 | 439 | 621 | 1,175 | 1,756 | |
| Diameter, μm | 5 | 10 | 5 | 5 | 20 | 10 | |
| Pressure, psi | 14 | 14 | 500 | 1,000 | 14 | 500 | |
| Number of Runs | 6 | 6 | 6 | 8 | 14 | 6 | 46 |
| | <u>Original Scale</u> | | | | | | |
| Minimum | -1 | -1 | 1 | -11 | -1 | 4 | -11 |
| Median | 3 | 3 | 3 | 1 | 8 | 6 | 5 |
| Average | 4 | 11 | 4 | 1 | 11 | 10 | 7 |
| Maximum | 13 | 49 | 7 | 12 | 27 | 34 | 49 |
| Standard Deviation | 6 | 19 | 2 | 7 | 10 | 11 | 11 |
| Skewness | 0.7 | 2.2 | 0.7 | -0.3 | 0.6 | 2.3 | 1.9 |
| | <u>Transformed Scale</u> | | | | | | |
| Minimum | 0.94 | 0.98 | 1.06 | 0.00 | 0.95 | 1.14 | 0.00 |
| Median | 1.12 | 1.10 | 1.11 | 1.06 | 1.26 | 1.21 | 1.16 |
| Average | 1.13 | 1.22 | 1.13 | 0.94 | 1.28 | 1.27 | 1.17 |
| Maximum | 1.37 | 1.77 | 1.23 | 1.33 | 1.57 | 1.64 | 1.77 |
| Standard Deviation | 0.18 | 0.30 | 0.07 | 0.42 | 0.21 | 0.19 | 0.27 |
| Skewness | 0.2 | 1.6 | 0.5 | -1.8 | 0.0 | 2.1 | -1.4 |



A. Phase I



B. Phase II



C. Phase I and Phase II Combined

FIGURE 20. DISTRIBUTION OF PLUTONIUM EMISSION (ON TRANSFORMED SCALE, z) FOR EXPERIMENTAL REGION I ($A\sqrt{P} < 2000$)

TABLE 16. SUMMARY STATISTICS FOR REGION I, PHASE II

| Statistics | Subgroup | | | | | | Total Sample |
|-------------------------|--------------------------|-------|-------|-------|-------|-------|--------------|
| | 1 | 2 | 3 | 4 | 5 | 6 | |
| \overline{AvP} | 73 | 621 | 1,175 | 1,590 | 1,756 | 1,777 | |
| Diameter, μm | 5 | 5 | 20 | 8 | 10 | 8 | |
| Pressure, psi | 14 | 1,000 | 14 | 1,000 | 500 | 1,250 | |
| Number of Runs | 6 | 8 | 8 | 16 | 12 | 7 | 58 |
| | <u>Original Scale</u> | | | | | | |
| Minimum | 3 | -1 | -1 | -2 | -1 | -1 | -2 |
| Median | 7 | 1 | 1 | 1 | 1 | 0 | 1 |
| Average | 22 | 2 | 2 | 16 | 3 | 1 | 8 |
| Maximum | 99 | 12 | 6 | 110 | 10 | 2 | 110 |
| Standard Deviation | 37 | 4 | 2 | 33 | 3 | 1 | 22 |
| Skewness | 2.4 | 2.4 | 1.5 | 2.1 | 1.0 | 1.0 | 3.7 |
| | <u>Transformed Scale</u> | | | | | | |
| Minimum | 1.11 | 0.96 | 0.97 | 0.92 | 0.95 | 0.98 | 0.92 |
| Median | 1.22 | 1.04 | 1.04 | 1.04 | 1.05 | 1.01 | 1.05 |
| Average | 1.36 | 1.06 | 1.06 | 1.22 | 1.09 | 1.02 | 1.14 |
| Maximum | 2.04 | 1.34 | 1.20 | 2.08 | 1.31 | 1.09 | 2.08 |
| Standard Deviation | 0.35 | 0.12 | 0.07 | 0.37 | 0.11 | 0.04 | 0.25 |
| Skewness | 2.0 | 2.0 | 1.1 | 1.6 | 0.6 | 0.9 | 2.7 |

TABLE 17. SUMMARY STATISTICS FOR REGION II, PHASE I

| Statistic | Subgroup | | | Total Sample |
|-------------------------|--------------------------|-------|--------|--------------|
| | 1 | 2 | 3 | |
| $\bar{A}\sqrt{P}$ | 2,484 | 7,025 | 9,935 | |
| Diameter, μm | 10 | 20 | 20 | |
| Pressure, psi | 1,000 | 500 | 1,000 | |
| Number of Runs | 7 | 15 | 13 | 35 |
| | <u>Original Scale</u> | | | |
| Minimum | -1 | 5 | 2 | -1 |
| Median | 27 | 103 | 60 | 87 |
| Average | 126 | 276 | 1,870 | 838 |
| Maximum | 420 | 1,617 | 17,590 | 17,590 |
| Standard Deviation | 163 | 411 | 5,000 | 3,090 |
| Skewness | 1.2 | 2.7 | 3.1 | 5.1 |
| | <u>Transformed Scale</u> | | | |
| Minimum | 0.98 | 1.16 | 1.07 | 0.98 |
| Median | 1.56 | 2.05 | 1.85 | 1.98 |
| Average | 1.78 | 2.06 | 2.07 | 2.01 |
| Maximum | 2.63 | 3.21 | 4.25 | 4.25 |
| Standard Deviation | 0.64 | 0.66 | 0.95 | 0.76 |
| Skewness | 0.2 | 0.0 | 1.4 | 1.0 |

three subgroups were combined to produce the histogram in Figure 21A and the summary statistics in the last column of Table 17. This histogram contrasts sharply with the histogram for Region I, but the difference may simply be due to the erratic nature of small samples.

The data corresponding to Region II, Phase II, consists of 46 measurements of plutonium oxide emissions. These measurements represent two combinations of orifice size and helium pressure, as shown in Table 18 in order of increasing values of $A\sqrt{P}$. These statistics support the assumption of negligible differences among subgroups. Accordingly, both subgroups were combined to produce the histogram in Figure 22B and the summary statistics in the last column of Table 18. This histogram is fairly conventional in shape.

From visual inspection, it appears that the two histograms in Figures 21A and 21B represent random samples from totally different populations. This conclusion is supported by a standard nonparametric test of statistical significance^(b). Nevertheless, the two histograms were pooled to obtain the histogram in Figure 21C, in order to visualize the consequences of a different approach. From the standpoint of predicting future performance, it makes sense to combine Phase I and Phase II data, even though they don't agree. What are the alternatives? It is difficult to come up with a sensible rationale for two separate populations. Even if such a rationale could be found, it would involve the risk of underestimating the experimental error.

The data corresponding to Region III, Phase II, consists of 65 measurements of plutonium oxide emissions (Region III is devoid of any Phase I data). These measurements represent three combinations of orifice size and helium pressure, as shown in Table 19 in order of increasing values of $A\sqrt{P}$. These statistics support the assumption of negligible differences among subgroups. Accordingly, all three subgroups were combined to produce the summary statistics in the last column of Table 19.

(b) The Wilcoxon-Mann-Whitney test.

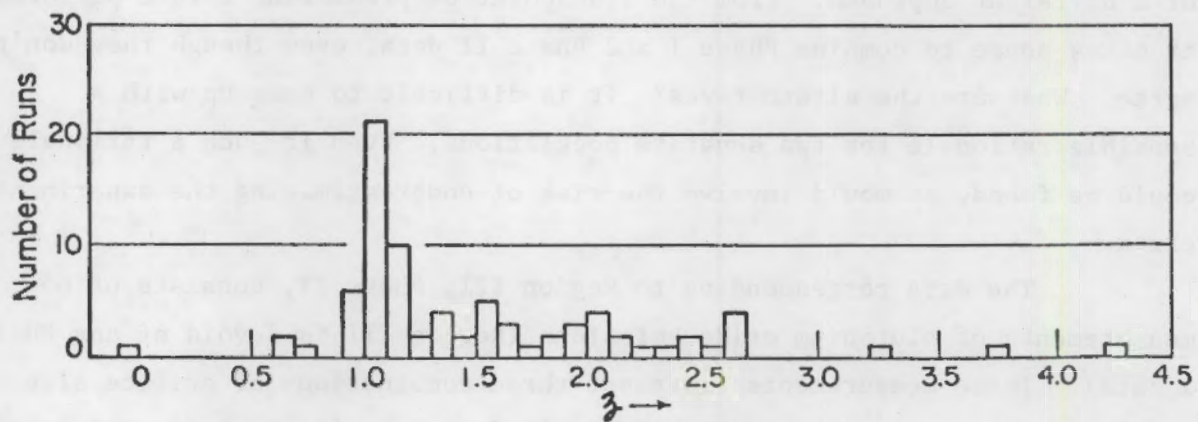
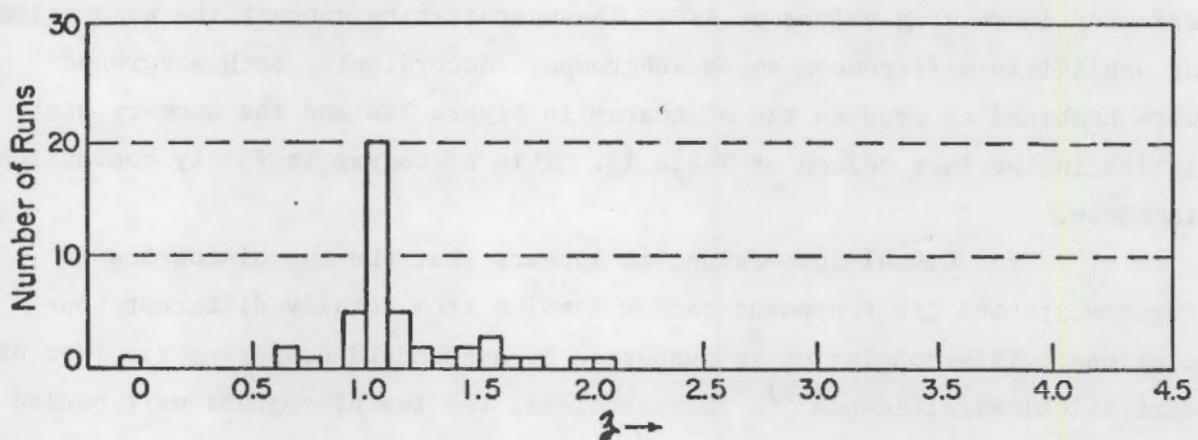
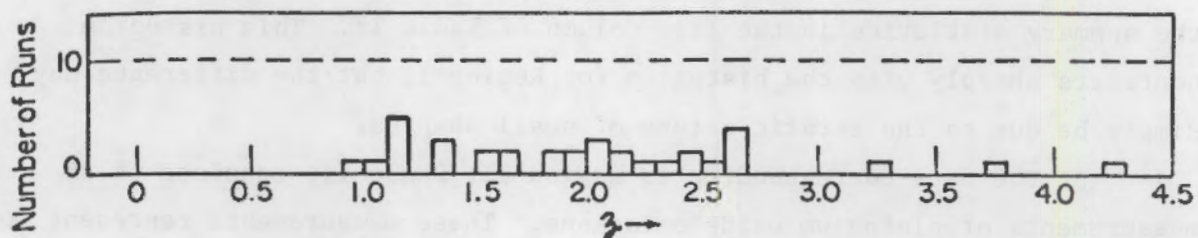


FIGURE 21. DISTRIBUTION OF PLUTONIUM EMISSION (ON TRANSFORMED SCALE, Z) FOR EXPERIMENTAL REGION II ($2000 \leq A\sqrt{P} < 20,000$)

TABLE 18. SUMMARY STATISTICS FOR REGION II, PHASE II

| Statistics | 1 | 2 | Total Sample |
|-------------------------|--------------------------|-------|--------------|
| $A\sqrt{P}$ | 7,347 | 9,935 | |
| Diameter, μm | 50 | 20 | |
| Pressure, psi | 14 | 1,000 | |
| Number of Runs | 4 | 42 | 46 |
| | <u>Original Scale</u> | | |
| Minimum | -1 | -9 | -9 |
| Median | 1 | 1 | 1 |
| Average | 1 | 9 | 8 |
| Maximum | 5 | 96 | 96 |
| Standard Deviation | 2 | 21 | 20 |
| Skewness | 1.5 | 2.9 | 3.1 |
| | <u>Transformed Scale</u> | | |
| Minimum | 0.98 | -0.10 | -0.10 |
| Median | 1.03 | 1.03 | 1.03 |
| Average | 1.05 | 1.13 | 1.12 |
| Maximum | 1.16 | 2.03 | 2.03 |
| Standard Deviation | 0.08 | 0.36 | 0.34 |
| Skewness | 1.4 | -0.1 | -0.1 |

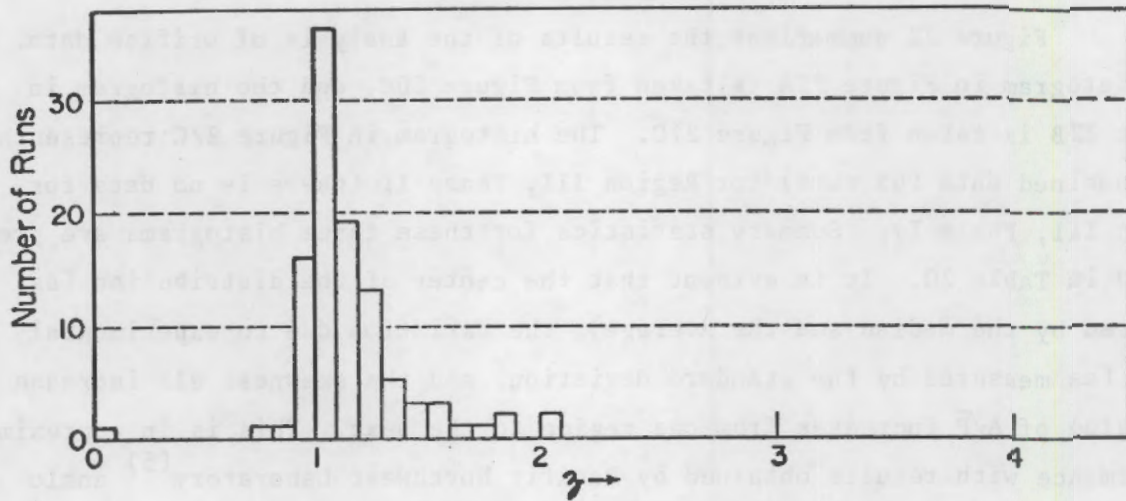
TABLE 19. SUMMARY STATISTICS FOR REGION III, PHASE II

| Statistic | Subgroup | | | Total Sample |
|--------------------|----------|--------------------------|--------|--------------|
| | 1 | 2 | 3 | |
| A _V P | 43,905 | 62,091 | 69,420 | |
| Diameter, μm | 50 | 50 | 50 | |
| Pressure, psi | 500 | 1,000 | 1,250 | |
| Number of Runs | 13 | 40 | 12 | 65 |
| | | <u>Original Scale</u> | | |
| Minimum | -2 | -1 | -1 | -2 |
| Median | 1 | 13 | 36 | 13 |
| Average | 1,070 | 970 | 2,980 | 1,361 |
| Maximum | 7,973 | 12,800 | 30,060 | 30,060 |
| Standard Deviation | 2,354 | 2,963 | 8,593 | 4,437 |
| Skewness | 2.5 | 3.5 | 3.4 | 5.0 |
| | | <u>Transformed Scale</u> | | |
| Minimum | 0.98 | 0.96 | 0.97 | 0.93 |
| Median | 1.03 | 1.36 | 1.66 | 1.36 |
| Average | 1.67 | 1.76 | 2.00 | 1.79 |
| Maximum | 3.90 | 4.11 | 4.48 | 4.43 |
| Standard Deviation | 1.12 | 0.91 | 1.15 | 0.99 |
| Skewness | 1.4 | 1.4 | 1.2 | 1.3 |

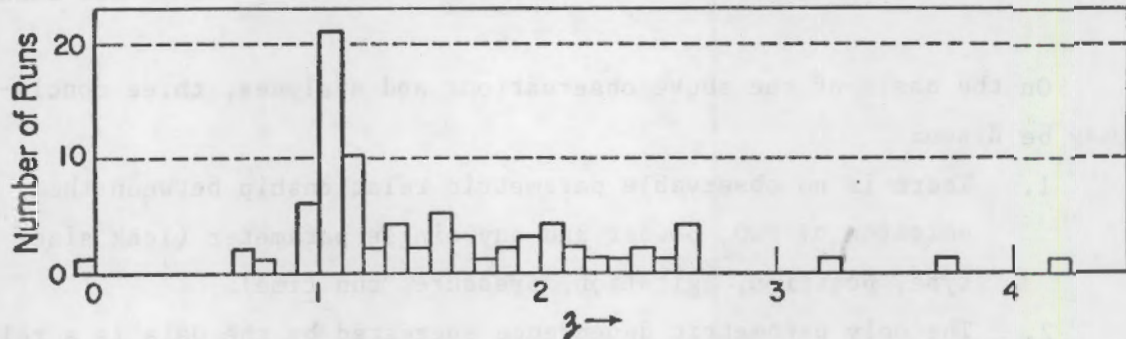
Figure 22 summarizes the results of the analysis of orifice data. The histogram in Figure 22A is taken from Figure 20C, and the histogram in Figure 22B is taken from Figure 21C. The histogram in Figure 22C represents the combined data (65 runs) for Region III, Phase II (there is no data for Region III, Phase I). Summary statistics for these three histograms are presented in Table 20. It is evident that the center of the distribution (as measured by the median and the average), the variation due to experimental error (as measured by the standard deviation) and the skewness all increase as the value of $A\sqrt{P}$ increases from one region to the next. This is in approximate comformance with results obtained by Pacific Northwest Laboratory⁽⁵⁾ analogous data. Although a trend is indicated by the results shown in Figure 22, the form of the relationship cannot be determined from the present data bank.

On the basis of the above observations and analyses, three conclusions may be drawn:

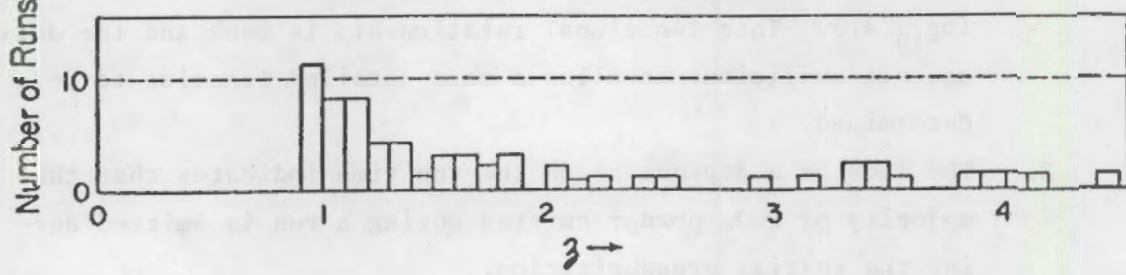
1. There is no observable parametric relationship between the emission of PuO_2 powder and any single parameter (leak size/type, position, agitation, pressure, run time).
2. The only parametric dependence suggested by the data is a relationship between the logarithmic transformation of the data and $\log_{10} A\sqrt{P}$. This functional relationship is weak and the data are not sufficient to allow a more detailed function to be determined.
3. The lack of a dependence on the run time indicates that the majority of PuO_2 powder emitted during a run is emitted during the initial pressurization.



A. Region I ($A\sqrt{P} < 2000$)



B. Region II ($2000 \leq A\sqrt{P} < 20,000$)



C. Region III ($A\sqrt{P} \geq 20,000$)

FIGURE 22. DISTRIBUTION OF PLUTONIUM EMISSION (ON TRANSFORMED SCALE, Z) FOR THREE EXPERIMENTAL REGIONS

TABLE 20. SUMMARY STATISTICS FOR REGIONS I, II, AND III

| Statistic | Region | | |
|--------------------|--------------------------|--------|--------|
| | I | II | III |
| Number of Runs | 104 | 81 | 65 |
| | <u>Original Scale</u> | | |
| Minimum | -11 | -9 | -2 |
| Median | 2 | 6 | 13 |
| Average | 8 | 367 | 1,361 |
| Maximum | 110 | 17,590 | 30,060 |
| Standard Deviation | 18 | 2,057 | 4,437 |
| Skewness | 4.0 | 7.8 | 5.0 |
| | <u>Transformed Scale</u> | | |
| Minimum | 0.00 | -0.10 | 0.93 |
| Median | 1.08 | 1.20 | 1.36 |
| Average | 1.15 | 1.51 | 1.79 |
| Maximum | 2.08 | 4.25 | 4.48 |
| Standard Deviation | 0.26 | 0.71 | 0.99 |
| Skewness | 0.7 | 1.4 | 1.3 |

PuO₂ Mass to Helium Flow Correlation

A correlation between the mass of PuO₂ emitted during an experiment and the total helium flow could be useful in determining leak specifications for shipping containers. Further, it was agreed upon with Pacific Northwest Laboratory personnel that all the topical reports associated with the plutonium oxide leak rate experiments would present the data in terms of total helium flow and PuO₂ emitted. To this end, columns six, eight and nine are included in the tables of Appendix B. These columns are, respectively, total helium flow in scc, net total mass of plutonia detected, and the plutonia mass to helium flow ratio in µg/cc. The maximum and minimum mass to flow ratios observed for the pressurized orifice experiments are presented in Table 21. As inspection of the table reveals, the maximum value observed was 5×10^{-3} µg/cc and the minimum observed value 3×10^{-8} µg/cc.

TABLE 21. PLUTONIA MASS/HELIUM FLOW CORRELATION ($\mu\text{g}/\text{cm}^3$)
(PRESSURIZED LEAK TUBE)

| Orifice Size (μm) | Mass/Flow | |
|-----------------------------------|--------------------|--------------------|
| | Minimum | Maximum |
| 5 | 9×10^{-8} | 2×10^{-5} |
| 8 | 3×10^{-8} | 4×10^{-5} |
| 10 | 1×10^{-7} | 2×10^{-4} |
| 20 | 3×10^{-8} | 4×10^{-3} |
| 50 | 1×10^{-7} | 5×10^{-3} |

Only positive non-zero value included

REFERENCES

- (1) ANSI-N14-5, Leakage Tests on Packages for Shipment of Radioactive Materials, November, 1974.
- (2) Regulatory Guide 7.4, Leakage Tests on Packages for Shipment of Radioactive Materials, U.S. Nuclear Regulatory Commission, June, 1975.
- (3) IAEA Safety Series No. 6, Regulations for the Safe Transport of Radioactive Materials, Table VII, 1973 ed.
- (4) L. C. Schwendiman, Supporting Information for the Estimation of Plutonium Oxide Leak Rates Through Very Small Apertures, BNWL-2198, Pacific Northwest Laboratory, 1977.
- (5) Sutter, S. L., J. W. Johnson, J. Mishima, P. C. Owzarski, L. C. Schwendiman and G. B. Long, Depleted Uranium Dioxide Powder Flow Through Very Small Openings, NUREG/CR-1099, PNL-3177, Pacific Northwest Laboratory, Richland, WA, 1980.*

* Available for purchase from the NRC/GPO Sales Program, U.S. Nuclear Regulatory Commission, Washington, DC 20555, and the National Technical Information Service, Springfield, VA 22161.

REFERENCES

- (1) ANSI-M14-7, Leakage Tests on Packages for Shipment of Radioactive Materials, November, 1974.
- (2) Laboratory Guide 7-A, Leakage Tests on Packages for Shipment of Radioactive Materials, U.S. Nuclear Regulatory Commission, June, 1975.
- (3) ICA Safety Series No. 6, Regulations for the Safe Transport of Radioactive Materials, Table VII, 1973 ed.
- (4) J. C. Schwendeman, Specific Information for the Evaluation of Minimum Gaseous Leak Rates Through Very Small Apertures, NRC-1198, Seattle Northwest Laboratory, 1977.
- (5) G. J. S. J., W. Johnson, J. Mathias, F. C. Quisenberry, J. C. Schwendeman and C. M. Long, Degraded Uranium Dioxide Powder Flow Through Very Small Apertures, NRC-1197, Seattle Northwest Laboratory, Richland, WA, 1977.

Available for purchase from the NTIS/STI Sales Program, U.S. Government Printing Office, Washington, DC 20540, and the National Technical Information Service, Springfield, VA 22161.

APPENDIX A

LASER OPTICAL PARTICLE MONITORING SYSTEM (LOPMS)

APPENDIX A

LASER OPTICAL PARTICLE MONITORING SYSTEM (LOPMS)

A real-time, continuous monitoring instrument would be highly useful in characterizing particulate leaks from small cracks. The number of particles emitted from a given leak, the particulate leak rate, the change in the leak rate with time, and the particle size distribution are the desired data. To obtain this information, the development of a laser optical particle monitoring system was undertaken.

The system was designed to detect light scattered by leak particles as they pass through a uniform plane of laser light intercepting the leak path. A schematic representation of the system is shown in Figure A1. As a particle passes through the plane of laser light it scatters light in all directions. The light scattered at a fixed solid angle in the forward direction is collected by a fiber optics bundle and transmitted to a photomultiplier tube (PMT). The associated voltage pulse generated by the PMT is classified according to its magnitude and stored using a multichannel analyzer (MCA). In principle, each detected light pulse corresponds to a leaked particle and the magnitude of the voltage pulse is related to the particle size. By monitoring the counts with time, the total number of particles leaked, the leak rate, and the change in leak rate are measured. Also obtained are the number of counts in each of several intensity classifications, thus indicating a relative particle size distribution.

Experimental

A series of particle leak rate and size distribution experiments were conducted using a leak tube having a 50- μm orifice (Figure A2). Helium gas, at a constant pressure of 500 psig, was supplied to the leak tube during testing. The leak tube was oriented in the upright position, i.e., emitting particles in the upward direction. ThO_2 powder was used as a simulant for PuO_2 in the experiments.

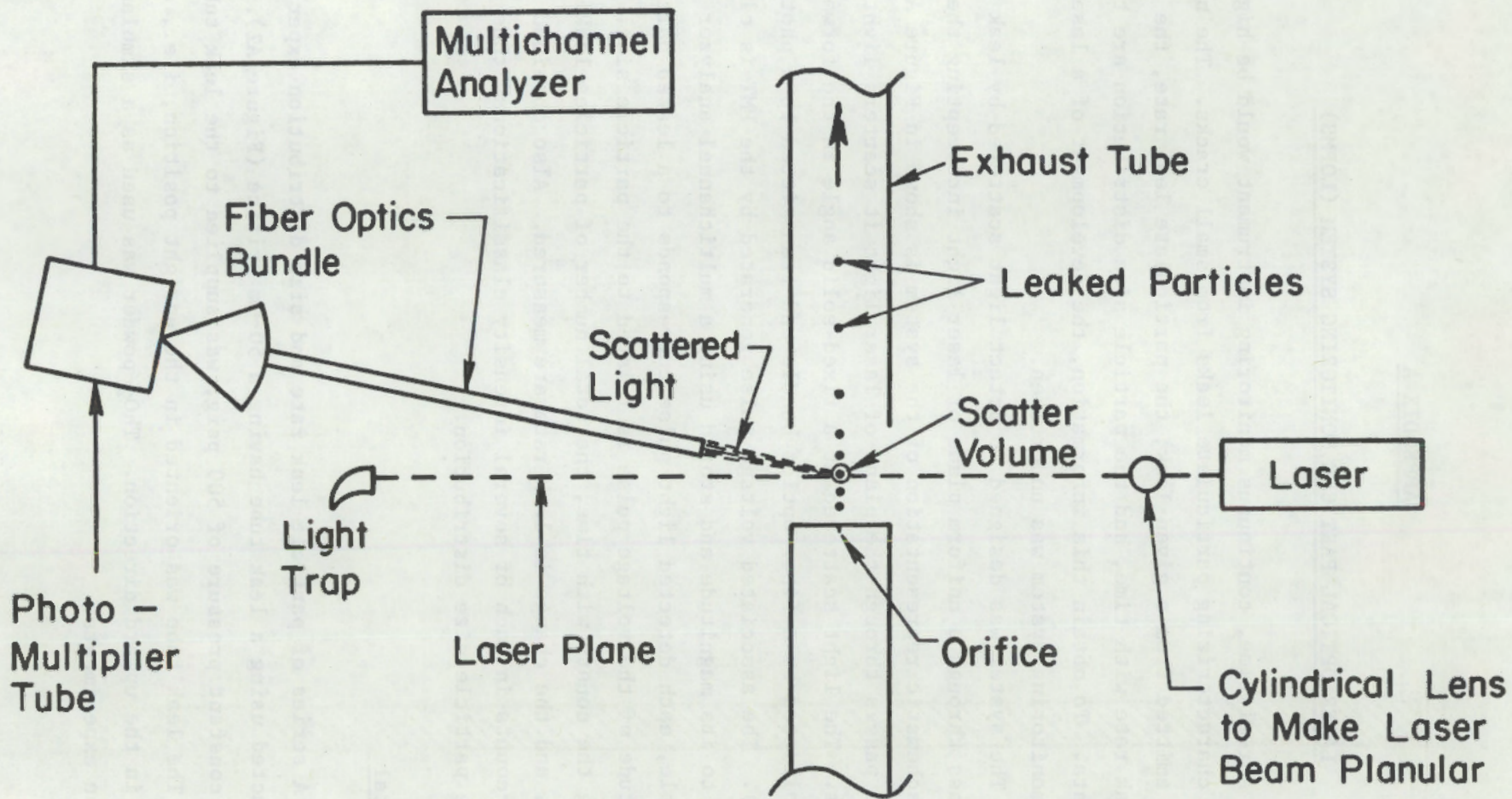


FIGURE A1. SYSTEM SETUP

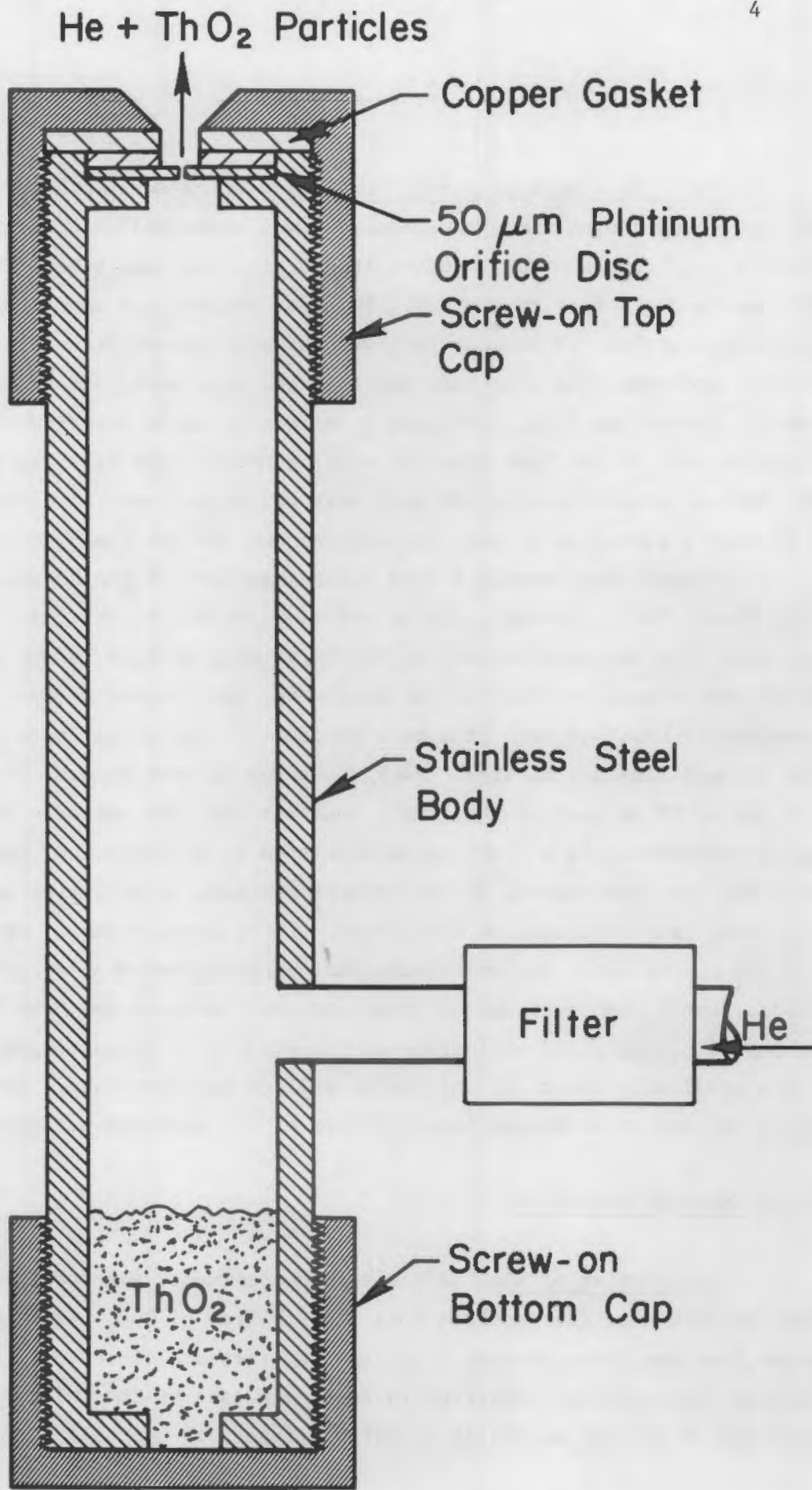


FIGURE A2. LEAK TUBE USED FOR THE PLUTONIA EXPERIMENTS

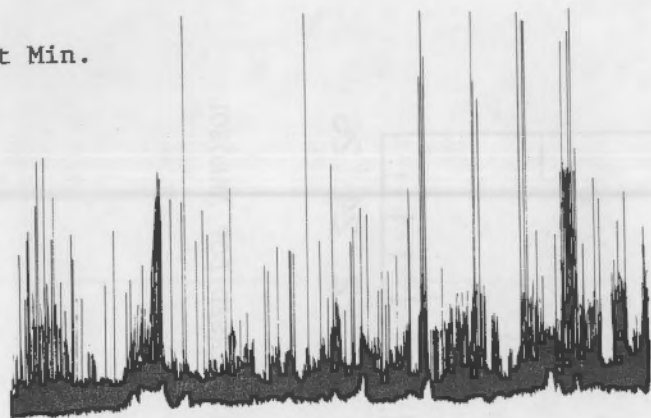
Particle Leak Rate Versus Time. To determine if the ThO_2 particle leak rate changed with time, an experiment was conducted using a high-speed recording oscillograph (RO) to chart the particulate leak rate. The RO was connected to the output of the PMT. In order to simulate conditions in which a shipping container of nuclear fuel was suddenly jarred or tumbled in a transportation accident, the leak tube was agitated vigorously before being connected to the helium line. Presumably, agitation would distribute ThO_2 over the inside wall of the leak tube and suspend some of the finer particles. The leak tube was pressurized to 500 psig with helium and data were taken using the RO over a period of 11 min, cycling the RO: on for 1 min, off for 1 min.

Figures A3a through f show typical section of the RO chart for the first, third, fifth, seventh, ninth, and eleventh min of the run. The particle leak rate was greatest during the first min, decayed to ~ 10 to 20 percent of the initial rate during the third min, and finally decayed to an approximately constant rate of 1 to 5 percent of the initial rate for the fifth through eleventh minutes. Background due to room aerosol was determined to be ~ 10 to 20 percent of the final, constant particle emission rate. Each peak was assumed to be a light pulse generated by a single ThO_2 particle traversing the laser plane, but no efforts was made to determine absolute particle count rate or detection efficiency. It is interesting to note that from the fifth minute until the end of the run, particle emission appears somewhat periodic rather than continuous. Such periodic emission may have been caused by repeated plugging and unplugging of the orifice or by particles merely being periodically swept off the inside wall of the leak tube. Additional study is needed to determine the mechanism of the apparent periodic emission.

Particle Size Distribution

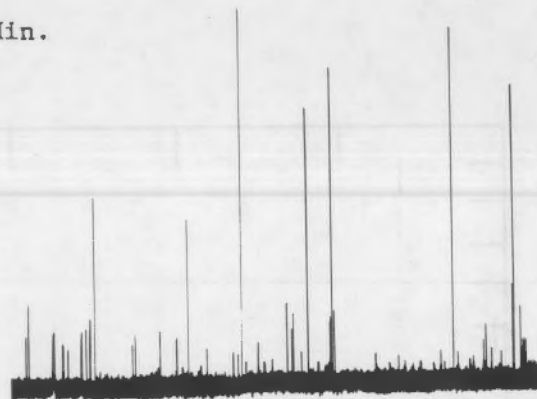
Calibration of MCA. A series of experiments were conducted in an effort to determine the particle size distribution of ThO_2 particles being emitted from the 50- μm orifice at a constant pressure of 500-psig helium. Scattered light pulses, converted to voltage pulses by the PMT, were classified in the MCA according to pulse height.

1st Min.



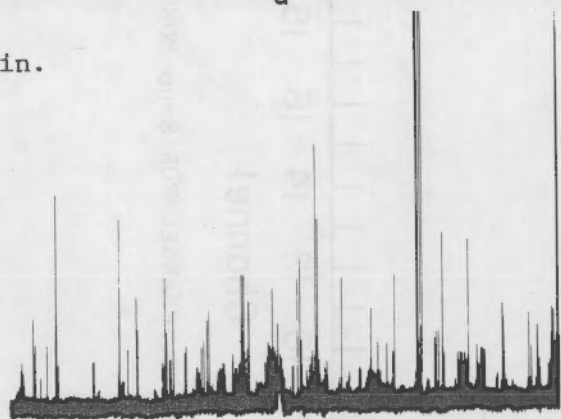
a

7th Min.



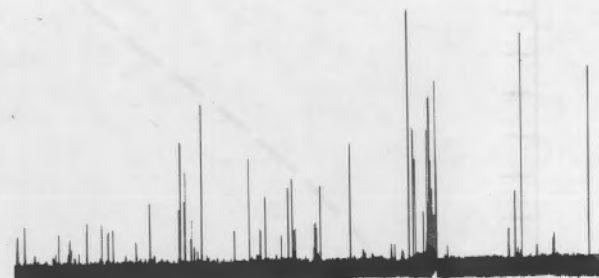
d

3rd Min.



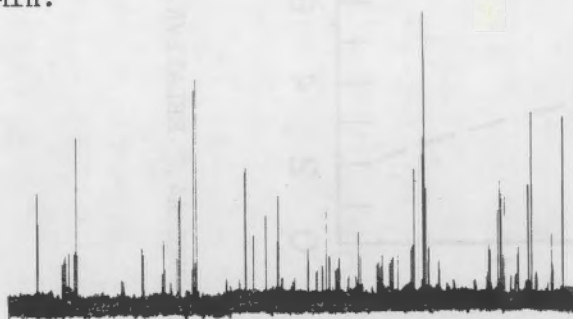
b

9th Min.



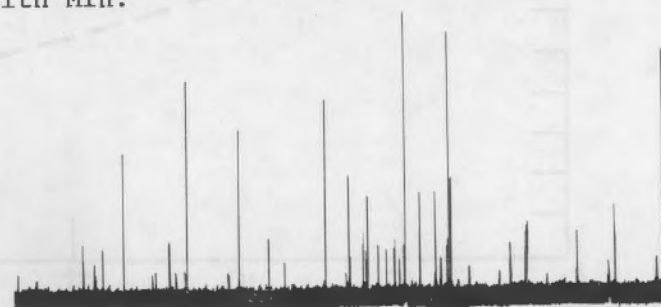
e

5th Min.



c

11th Min.



f

FIGURE A3. RECORDING OSCILLOSCOPE TRACE OF PARTICLE EMISSION RATE

A-5

5

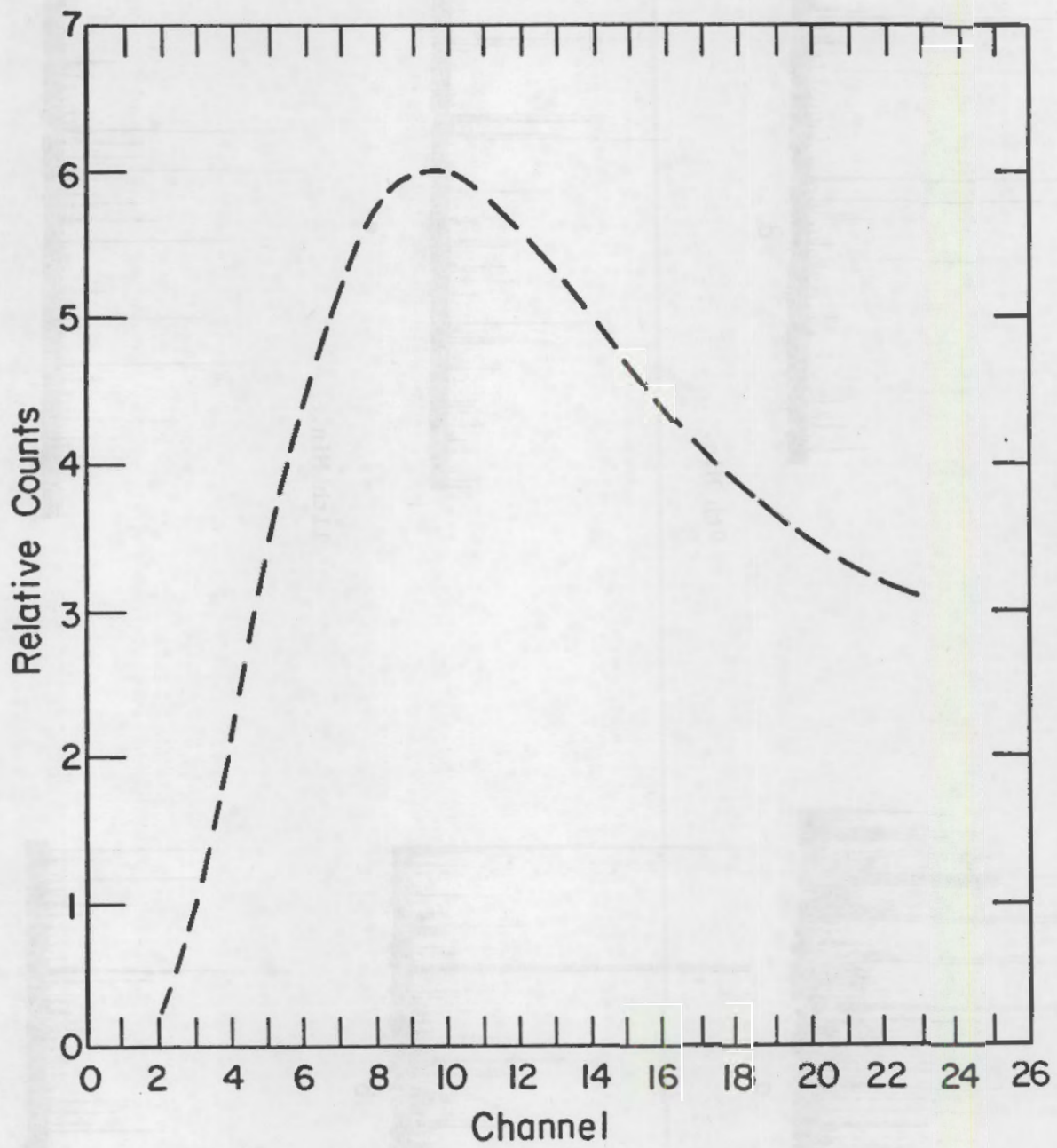


FIGURE A4. RELATIVE COUNTS VS. CHANNEL FOR 8- μm MONODISPersed DOP AEROSOL

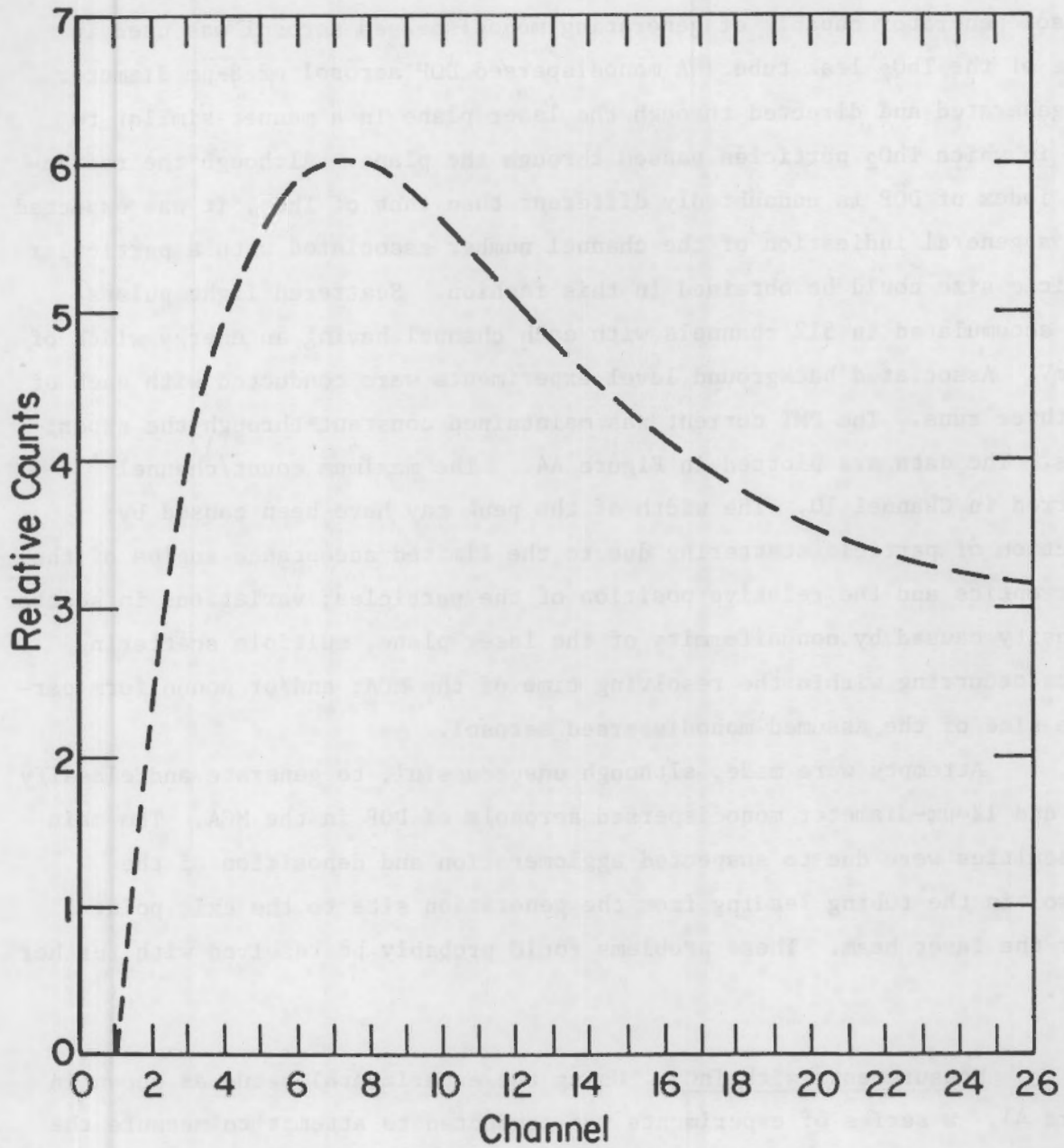


FIGURE A5. RELATIVE COUNTS VS. CHANNEL FOR ThO_2 TEST AEROSOL

In order to calibrate the MCA, a Berglund-Liu vibrating orifice aerosol generator capable of generating monodispersed aerosol was used in place of the ThO₂ leak tube. A monodispersed DOP aerosol of 8- μ m diameter was generated and directed through the laser plane in a manner similar to that in which ThO₂ particles passed through the plane. Although the refractive index of DOP is undoubtedly different than that of ThO₂, it was expected that a general indication of the channel number associated with a particular particle size could be obtained in this fashion. Scattered light pulses were accumulated in 512 channels with each channel having an energy width of \sim 15 mV. Associated background level experiments were conducted with each of the three runs. The PMT current was maintained constant through the experiments. The data are plotted in Figure A4. The maximum count/channel occurred in Channel 10. The width of the peak may have been caused by: detection of particle scattering due to the limited acceptance angles of the fiber optics and the relative position of the particles; variations in scatter intensity caused by nonuniformity of the laser plane, multiple scattering events occurring within the resolving time of the MCA; and/or nonuniform particle size of the assumed monodispersed aerosol.

Attempts were made, although unsuccessful, to generate and classify 4- μ m and 12- μ m-diameter monodispersed aerosols of DOP in the MCA. The main difficulties were due to suspected agglomeration and deposition of the aerosol in the tubing leading from the generation site to the exit point under the laser beam. These problems could probably be resolved with further study.

Measurements with ThO₂. Using the experimental setup as shown in Figure A1, a series of experiments was conducted to attempt to measure the ThO₂ particle size distribution. Three runs were made of approximately 3-1/2 minutes' duration each, at 500-psig helium. Background measurements were taken before each run. Figure A5 shows the average relative counts/channel for ThO₂. The maximum count/channel occurred in Channel 7. A mean particle size of 7- μ m equivalent diameter had previously been determined by L. Miga of Battelle Columbus Laboratories (December 18, 1976) for the ThO₂. Assuming that DOE and ThO₂ scatter light by a similar mechanism, the maximum

count/channel for ThO_2 should occur in a channel number <10 as is the case. The overall similarity between the DOP peak spread and the ThO_2 peak spread, however, indicate that the attempted particle size distribution measurements were not successful with the present apparatus. Assuming the DOP is truly monodispersed, its peak shape should be considerably different from the peak shape of a material such as ThO_2 which is composed of particles ranging from $\sim 0.2 \mu\text{m}$ to $\sim 20 \mu\text{m}$. Additional refinement of the apparatus is required before useful particle size distribution data can be obtained.

Discussion

The experiments have shown the usefulness of the LOPMS as a monitoring tool to detect relative particulate leak rates. Thus, this technique, when used to monitor a particulate leak rate under given conditions, can measure general trends such as plugging and unplugging of the leak crack. Furthermore, relative amounts of particulate leaked for different conditions may be measured and comparisons drawn using this technique.

In order to use the LOPMS as a quantitative counting tool, a particulate detection efficiency calibration would be necessary. There are no assurances that every leaked particle crossed the laser plane nor that all which did resulted in detectable scattered light. Inherent in the system is a limited "probe volume" from which the scattered light can be detected. This limitation is due to the limited solid angle of the fiber bundle. Also, no correction for the effect of multiple scatters (more than one particle in the probe volume at one time) was made. This calibration could be accomplished by comparing simultaneously LOPMS particle counts with that of another calibrated counting instrument such as a commercially available optical particle counter. Such a calibration was not conducted during the current program.

The size distribution measurement experiments demonstrated the limited use of the LOPMS as a sizing instrument. The results show the need for further system development to reduce and define the peak width. To relate such measurements to an absolute size distribution would require

calibration by another sizing technique such as a cascade impactor. Even if such a calibration were made there are several problems associated with the LOPMS technique for sizing. The relation between particle size and relative scattering intensity must be known. Such a relationship is dependent in part on refractive index, thus the calibration aerosol must have the same or relatable refractive index as the test aerosol. Furthermore, once a calibration is made, care must be taken to maintain the identical probe volume/fiber detecting head configuration. These considerations made the LOPMS a tedious system to operate for size distribution measurement. There are also problems in interpreting intensity (and thus size) measurements due to multiple simultaneous scattering incidents, partial scattering incidents (only part of a particle passing through the probe volume), and nonuniformity of the laser plane.

Conclusions

- The laser system described can monitor in real time the relative amounts of particles leaked and trends in particle leak rate.
- The technical feasibility of the LOPMS as a counting instrument has been demonstrated; however, further experimentation is needed before this use can be demonstrated quantitatively.
- Such a system requires additional development before real quantitative particle size distributions can be measured.

APPENDIX B

TABULATION OF LEAK RATE EXPERIMENTS DATA

TABLE B1. SUMMARY OF ROOM-TEMPERATURE PuO₂ LEAK RATE EXPERIMENTS USING A SIMULATED CRACK;^(a)
 HELIUM FLOW RATE EQUAL TO 11.4 cc/sec

| Run Number | Tube Position | Helium Pressure, psi | Vibration | Helium Leak Rate(c) scc/sec | Total Helium Flow scc(e) | Quantity of PuO ₂ Detected, μg ^(b) | | Mass Flow Ratio μg/cc |
|------------|---------------|----------------------|-----------|-----------------------------|--------------------------|--|--------------------------|-----------------------|
| | | | | | | Total | Net Total ^(d) | |
| Pu 46b | Up | 1000 | No | 7.8 | 4680 | 0.0023 | -0.0002 | -4.3E-08 |
| Pu 46c | Up | 1000 | No | 7.4 | 4440 | 0.0011 | -0.0014 | -3.2E-07 |
| Pu 47b | Up | 1000 | Yes | 7.8 | 4680 | 0.0013 | -0.0012 | -2.6E-07 |
| Pu 47c | Up | 1000 | Yes | 7.4 | 4440 | 0.0017 | -0.0008 | -1.8E-07 |
| Pu 48d | Down | 1000 | No | 7.8 | 4680 | 0.0008 | -0.0017 | -3.6E-07 |
| Pu 48e | Down | 1000 | No | 7.4 | 4440 | 0.0015 | -0.0010 | -2.3E-07 |
| Pu 49d | Up | 500 | Yes | 3.0 | 1800 | 0.0025 | 0.0000 | 0.0000 |
| Pu 49e | Up | 500 | Yes | 2.6 | 1560 | 0.0007 | -0.0007 | -4.5E-07 |
| Pu 49g | Up | 500 | Yes | 2.6 | 1560 | 0.0019 | -0.0006 | -3.8E-07 |
| Pu 50b | Down | 500 | Yes | 2.2 | 1320 | 0.0028 | 0.0003 | 2.3E-07 |
| Pu 50c | Down | 500 | Yes | 2.2 | 1320 | 0.0028 | 0.0003 | 2.3E-07 |
| Pu 51d | Up | Ambient | Yes | - | - | 0.0035 | 0.0010 | |
| Pu 51e | Up | Ambient | Yes | - | - | 0.0034 | 0.0009 | |
| Pu 52b | Down | Ambient | No | - | - | 0.0019 | -0.0006 | |
| Pu 52c | Down | Ambient | No | - | - | 0.0010 | -0.0015 | |

- (a) The simulated crack has a 220-μm finish perpendicular to the helium flow. The helium leak rate was initially 11.4 cc/sec at 920 psig. All runs were for 10 min
- (b) Based on a specific activity of 0.096 Ci/g for the PuO₂ powder.
- (c) The leak rate was determined by the pressure decay method at the midpoint of the run.
- (d) The net total is the amount above the average containment box background of 0.0025 μg.
- (e) Best estimate of total flow in standard CM³ standard conditions: 1 atm 25°C.

TABLE B2. SUMMARY OF ROOM-TEMPERATURE PuO₂ LEAK RATE EXPERIMENTS USING A SIMULATED CRACK;^(a)
INITIAL HELIUM FLOW RATE EQUAL TO 9.8 cc/sec AT 1000 psi

| Run Number | Tube Position | Helium Pressure, psi | Vibration | Helium Leak Rate (c), scc/sec | Total Helium Flow (e), scc | Quantity of PuO ₂ Detected, μg ^(b) | | Mass Flow Ratio $\mu\text{g}/\text{cc}$ |
|------------|---------------|----------------------|-----------|-------------------------------|----------------------------|---|---------------|---|
| | | | | | | Total | Net Total (d) | |
| 54a | Up | 1000 | No | 8.7 | 5220 | 0.0054 | 0.0041 | 7.9E-07 |
| 54b | Up | 1000 | No | 8.7 | 5220 | 0.0056 | 0.0043 | 8.2E-07 |
| 57 | Up | 1000 | Yes | 8.7 | 5220 | 0.0098 | 0.0085 | 1.6E-06 |
| 57a | Up | 1000 | Yes | 8.7 | 5220 | 0.0027 | 0.0014 | 2.7E-07 |
| 58 | Down | 1000 | No | 8.7 | 5220 | 0.0037 | 0.0024 | 4.6E-07 |
| 58a | Down | 1000 | No | 7.8 | 4680 | 0.0025 | 0.0012 | 2.6E-07 |
| 59 | Up | 500 | Yes | 2.6 | 1560 | 0.0008 | -0.0005 | -3.2E-07 |
| 59a | Up | 500 | Yes | 2.6 | 1560 | 0.0041 | 0.0028 | 1.8E-06 |
| 59b | Up | 500 | Yes | 2.6 | 1560 | 0.0003 | -0.0010 | -6.4E-07 |
| 53 | Down | 500 | Yes | 3.0 | 1800 | 0.0986 | 0.0973 | 5.4E-05 |
| 53b | Down | 500 | Yes | 3.0 | 1800 | 0.0359 | 0.0346 | 1.9E-05 |
| 55 | Up | Ambient | Yes | - | - | 0.0062 | 0.0049 | |
| 55a | Up | Ambient | Yes | - | - | 0.0019 | 0.0006 | |
| 56 | Down | Ambient | Yes | - | - | 0.0005 | -0.0008 | |
| 56a | Down | Ambient | Yes | - | - | 0.0005 | -0.0008 | |
| 60 | Down | Ambient | No | - | - | 0.0014 | 0.0001 | |
| 60a | Down | Ambient | No | - | - | 0.0005 | -0.0008 | |

(a) The simulated crack has a 220-microinch finish perpendicular to the helium flow. The helium leak rate was initially 9.8 cc/sec at 1000 psi. All runs were for 10 min

(b) Based on a specific activity of 0.096 Ci/g for the PuO₂ powder.

(c) The leak rate was determined by the pressure decay method at the midpoint of the run.

(d) The net total is the amount above the average containment box background of 0.00130 μg .

(e) Best estimate of total flow in standard cm³. Standard conditions: 1 atm, 25°C.

TABLE B3. SUMMARY OF ROOM-TEMPERATURE PuO₂ LEAK RATE EXPERIMENTS USING A SIMULATED CRACK;^(a)
INITIAL HELIUM FLOW RATE EQUAL TO 11.6 cc/sec AT 1000 psi

| Run Number | Tube Position | Helium Pressure, psi | Vibration | Helium Leak Rate(c) scc/sec | Total Helium Flow scc ^(e) | Quantity of PuO ₂ Detected, μg ^(b) | | Mass Flow Ratio μg/cc |
|------------|---------------|----------------------|-----------|-----------------------------|--------------------------------------|--|--------------------------|-----------------------|
| | | | | | | Total | Net Total ^(d) | |
| Pu 61 | Up | 1000 | No | 9.3 | 5580 | 0.5685 | 0.5672 | 1.0E-04 |
| Pu 61a | Up | 1000 | No | 8.5 | 5100 | 0.1384 | 0.1371 | 2.7E-05 |
| Pu 61b | Up | 1000 | No | 6.5 | 3900 | 0.0136 | 0.0123 | 3.2E-06 |
| Pu 61c | Up | 1000 | No | 6.9 | 4140 | 0.0043 | 0.0030 | 7.2E-07 |
| Pu 62 | Up | 1000 | Yes | 7.4 | 4440 | 1.750 | 1.749 | 3.9E-04 |
| Pu 62a | Up | 1000 | Yes | 7.4 | 4440 | 0.0018 | 0.0005 | 1.1E-07 |
| Pu 62b | Up | 1000 | Yes | 6.9 | 4140 | 0.0131 | 0.0118 | 2.9E-06 |
| Pu 62c | Up | 1000 | Yes | 6.9 | 4140 | 0.0028 | 0.0015 | 3.6E-07 |
| Pu 63 | Down | 1000 | No | 6.1 | 3660 | 0.2697 | 0.2684 | 7.3E-05 |
| Pu 63a | Down | 1000 | No | 6.5 | 3900 | 0.4127 | 0.4114 | 1.1E-04 |
| Pu 63b | Down | 1000 | No | 6.9 | 4140 | 0.1445 | 0.1432 | 3.5E-04 |
| Pu 63c | Down | 1000 | No | 6.9 | 4140 | 34.79 | 34.79 | 8.4E-03 |
| Pu 63d | Down | 1000 | No | 6.9 | 4140 | 0.0991 | 0.0978 | 2.4E-05 |
| Pu 63e | Down | 1000 | No | 6.9 | 4140 | 0.0235 | 0.0222 | 5.4E-06 |
| Pu 64 | Up | 500 | Yes | 1.7 | 1020 | 0.0017 | 0.0004 | 3.9E-07 |
| Pu 64a | Up | 500 | Yes | 2.2 | 1320 | 0.0005 | -0.0008 | -6.1E-07 |
| Pu 65 | Down | 500 | Yes | 1.7 | 1020 | 1.742 | 1.741 | 1.7E-03 |
| Pu 65a | Down | 500 | Yes | 1.7 | 1020 | 0.1188 | 0.1175 | 1.2E-05 |
| Pu 65b | Down | 500 | Yes | 2.2 | 1320 | 0.0030 | 0.0017 | 1.3E-06 |
| Pu 65c | Down | 500 | Yes | 2.2 | 1320 | 0.0109 | 0.0096 | 7.3E-06 |
| Pu 66 | Up | Ambient | Yes | - | - | -0.0002 | -0.0015 | - |
| Pu 66a | Up | Ambient | Yes | - | - | 0.0004 | -0.0009 | - |
| Pu 67 | Down | Ambient | No | - | - | 0.0022 | 0.0009 | - |
| Pu 67a | Down | Ambient | No | - | - | 0.0001 | -0.0012 | - |

(a) The simulated crack has a 220-microinch finish perpendicular to the helium flow. The helium leak rate was 11.6 cc/sec at 1000 psi. All runs were for 10 min

(b) Based on a specific activity of 0.096 Ci/g for the PuO₂ powder.

(c) The leak rate was determined by the pressure decay method at the midpoint of the run. Standard conditions 1 atm, 25°C

(d) The net total is the amount above the average containment box background of 0.0013 μg.

(e) Best estimate of total flow in standard cm³. Standard conditions: 1 atm, 25°C.

TABLE B4. SUMMARY OF ROOM-TEMPERATURE PuO₂ LEAK RATE EXPERIMENTS USING A SIMULATED CRACK;^(a)
INITIAL HELIUM FLOW RATE EQUAL TO 13.2 cc/sec AT 1000 psi

| Run Number | Tube Position | Helium Pressure, psi | Vibration | Helium Leak Rate(c) scc/sec | Total Helium Flow scc(e) | Quantity of PuO ₂ Detected, μg ^(b) | | Mass Flow Ratio μg/cc |
|------------|---------------|----------------------|-----------|-----------------------------|--------------------------|--|--------------------------|-----------------------|
| | | | | | | Total | Net Total ^(d) | |
| Pu 68 | Up | 1000 | No | 12.4 | 7440 | 0.1028 | 0.1015 | 1.4E-05 |
| Pu 68a | Up | 1000 | No | 11.3 | 6780 | 0.0064 | 0.0051 | 7.5E-07 |
| Pu 68b | Up | 1000 | No | 9.6 | 5760 | 0.0038 | 0.0025 | 4.3E-07 |
| Pu 68c | Up | 1000 | No | 10.0 | 6000 | 0.0033 | 0.0020 | 3.3E-07 |
| Pu 69 | Up | 1000 | Yes | 11.1 | 6660 | 0.0083 | 0.0070 | 1.1E-06 |
| Pu 69a | Up | 1000 | Yes | 9.3 | 5580 | 0.0050 | 0.0037 | 6.6E-07 |
| Pu 70 | Down | 1000 | No | 9.5 | 5700 | 0.0304 | 0.0291 | 5.1E-06 |
| Pu 70a | Down | 1000 | No | 9.7 | 5820 | 0.0546 | 0.0533 | 9.2E-06 |
| Pu 71 | Up | 500 | Yes | 3.0 | 1800 | 0.0048 | 0.0035 | 1.9E-06 |
| Pu 71a | Up | 500 | Yes | 2.6 | 1560 | 0.0006 | -0.0007 | -4.5E-07 |
| Pu 71b | Up | 500 | Yes | 2.6 | 1560 | 0.0017 | 0.0004 | 2.6E-07 |
| Pu 71c | Up | 500 | Yes | 2.6 | 1560 | 0.0012 | -0.0001 | -6.4E-08 |
| Pu 72 | Down | 500 | Yes | 2.6 | 1560 | 0.6522 | 0.6509 | 4.2E-04 |
| Pu 72a | Down | 500 | Yes | 2.6 | 1560 | 0.4911 | 0.4898 | 3.1E-04 |
| Pu 73 | Up | Ambient | Yes | - | - | 0.0013 | 0.0000 | - |
| Pu 73a | Up | Ambient | Yes | - | - | 0.0000 | -0.0013 | - |
| Pu 74 | Down | Ambient | No | - | - | 0.1471 | 0.1458 | - |
| Pu 74a | Down | Ambient | No | - | - | 0.0022 | 0.0009 | - |
| Pu 74b | Down | Ambient | No | - | - | 0.0019 | 0.0006 | - |
| Pu 74c | Down | Ambient | No | - | - | 0.0013 | 0.0000 | - |

- (a) The simulated crack has a 220-μ in. finish perpendicular to the helium flow. The helium leak rate was initially 13.2 cc/sec at 1000 psi. All runs were for 10 min.
- (b) Based on a specific activity of 0.096 Ci/g for the PuO₂ powder.
- (c) The leak rate was determined by the pressure decay method at the midpoint of the run. Standard conditions: 1 atm, 25°C
- (d) The net total is the amount above the average containment box background of 0.0013 μg.
- (e) Best estimate of total flow in standard cm³. Standard conditions: 1 atm, 25°C.

TABLE B5. SUMMARY OF ROOM-TEMPERATURE PuO₂ LEAK RATE EXPERIMENTS USING A SIMULATED CRACK; (a)
WITH AN INITIAL He FLOW RATE OF 17.3 cc/sec AT 1000 psi

| Run Number | Tube Position | Helium Pressure, psi | Vibration | Helium Leak Rate(c), scc/sec | Total Helium Flow scc(e) | Quantity of PuO ₂ Detected, µg(b) | | Mass Flow Ratio µg/cc |
|------------|---------------|----------------------|-----------|------------------------------|--------------------------|--|--------------|-----------------------|
| | | | | | | Total | Net Total(d) | |
| Pu 75 | Up | 1000 | No | 15.8 | 9480 | 0.0583 | 0.0570 | 6.0E-06 |
| Pu 75a | Up | 1000 | No | 16.3 | 9780 | 0.0287 | 0.0274 | 2.8E-06 |
| Pu 76 | Up | 1000 | Yes | 15.8 | 9480 | 0.2029 | 0.2016 | 2.1E-05 |
| Pu 76a | Up | 1000 | Yes | 16.3 | 9780 | 0.0160 | 0.0093 | 9.8E-07 |
| Pu 76b | Up | 1000 | Yes | 8.25 | 4950 | 0.0137 | 0.0124 | 2.5E-06 |
| Pu 76c | Up | 1000 | Yes | 8.25 | 4950 | 0.0047 | 0.0034 | 6.9E-07 |
| Pu 77 | Down | 1000 | No | 16.3 | 9780 | 0.0260 | 0.0247 | 2.5E-06 |
| Pu 77a | Down | 1000 | No | 16.3 | 9780 | 0.0237 | 0.0224 | 2.3E-06 |
| Pu 78 | Up | 500 | Yes | 2.6 | 1560 | 0.0058 | 0.0045 | 2.9E-06 |
| Pu 78a | Up | 500 | Yes | 2.6 | 1560 | 0.0065 | 0.0052 | 3.3E-06 |
| Pu 79 | Down | 500 | Yes | 2.6 | 1560 | 0.4589 | 0.4576 | 2.9E-04 |
| Pu 79a | Down | 500 | Yes | 2.6 | 1560 | 0.6492 | 0.6479 | 4.2E-04 |
| Pu 80 | Up | Ambient | Yes | - | - | 0.0013 | 0.0000 | |
| Pu 80a | Up | Ambient | Yes | - | - | 0.0016 | 0.0003 | |
| Pu 81 | Down | Ambient | No | - | - | 0.0177 | 0.0164 | |
| Pu 81a | Down | Ambient | No | - | - | 0.0038 | 0.0025 | |

(a) The simulated crack has a 220-µ in. finish perpendicular to the flow of the helium. The helium leak rate was initially 17.3 cc/sec at 1000 psi. All runs were for 10 min.

(b) Based on a specific activity of 0.096 Ci/g for the PuO₂ powder.

(c) The leak rate was determined by the pressure decay method at the midpoint of the run. Standard conditions: 1 atm, 25°

(d) The net total is the amount above the average containment box background of 0.0013 µg.

(e) Best estimate of total flow in standard cm³. Standard conditions: 1 atm, 25°C.

TABLE B6. SUMMARY OF PuO₂ LEAK RATE EXPERIMENTS USING A 20- μ m ORIFICE^(a)

| Run Number | Tube Position | Helium Pressure, psi | Vibration | Helium Leak Rate ^(c) , scc/sec | Total Helium Flow ^(e) , scc | Quantity of PuO ₂ ^(a) Detected, μ g ^(b) | | Mass Flow Ratio μ g/cc |
|------------|---------------|----------------------|-----------|---|--|--|--------------------------|----------------------------|
| | | | | | | Total | Net Total ^(d) | |
| Pu 1 | Down | 1000 | Yes | 5.2 | 3120 | 0.0069 | 0.0039 | 1.3E-06 |
| Pu 1a | Down | 1000 | Yes | 4.3 | 2580 | 0.0428 | 0.0398 | 1.5E-05 |
| Pu 2 | Down | 1000 | No | 5.2 | 3120 | 0.0592 | 0.0562 | 1.8E-05 |
| Pu 2a | Down | 1000 | No | 6.1 | 3660 | 0.0340 | 0.0310 | 8.5E-06 |
| Pu 3 | Sideways | 1000 | No | 2.2 | 1320 | 0.0047 | 0.0017 | 1.3E-06 |
| Pu 3a | Sideways | 1000 | No | 1.8 | 1080 | 0.0630 | 0.0600 | 5.6E-05 |
| Pu 4 | Sideways | 1000 | Yes | 1.4 | 840 | 0.0063 | 0.0033 | 3.9E-06 |
| Pu 4a | Sideways | 1000 | Yes | 1.8 | 1080 | 0.0945 | 0.0915 | 8.5E-05 |
| Pu 5 | Up | 1000 | No | 8.1 | 4860 | 0.1178 | 0.1148 | 2.4E-05 |
| Pu 5a | Up | 1000 | No | 7.1 | 4260 | 0.1777 | 0.1747 | 4.1E-05 |
| Pu 6 | Up | 1000 | Yes | 8.8 | 5280 | 0.1474 | 0.1444 | 2.7E-05 |
| Pu 6a | Up | 1000 | Yes | 7.1 | 4260 | 17.59 | 17.59 | 4.1E-03 |
| Pu 6b | Up | 1000 | Yes | 7.8 | 4680 | 6.00 | 6.00 | 1.3E-03 |
| Pu 7 | Down | 500 | No | 4.4 | 2640 | 0.0838 | 0.0808 | 3.1E-05 |
| Pu 7a | Down | 500 | No | 2.2 | 1320 | 0.4505 | 0.4475 | 3.4E-04 |
| Pu 8 | Down | 500 | Yes | 1.7 | 1020 | 0.0076 | 0.0046 | 4.5E-06 |
| Pu 8a | Down | 500 | Yes | 2.6 | 1560 | 1.620 | 1.617 | 1.0E-03 |
| Pu 9 | Sideways | 500 | Yes | 1.7 | 1020 | 0.2129 | 0.2099 | 2.1E-04 |
| Pu 9a | Sideways | 500 | Yes | 4.3 | 2580 | 0.1058 | 0.1028 | 4.0E-05 |
| Pu 9b | Sideways | 500 | Yes | 3.0 | 1800 | 0.0164 | 0.0134 | 7.4E-06 |
| Pu 14 | Sideways | 500 | No | 8.7 | 5220 | 0.0132 | 0.0102 | 2.0E-06 |
| Pu 14a | Sideways | 500 | No | 3.9 | 2340 | 0.0082 | 0.0052 | 2.2E-06 |
| Pu 10 | Up | 500 | Yes | 4.3 | 2580 | 0.4404 | 0.4374 | 1.7E-04 |
| Pu 10a | Up | 500 | Yes | 3.5 | 2100 | 0.2980 | 0.2950 | 1.4E-04 |
| Pu 10b | Up | 500 | Yes | 7.4 | 4440 | 0.0145 | 0.0115 | 2.6E-06 |
| Pu 10c | Up | 500 | Yes | 4.3 | 2580 | 0.4933 | 0.4903 | 1.9E-04 |
| Pu 15 | Up | 500 | No | 6.5 | 3500 | 0.3238 | 0.3208 | 8.2E-05 |
| Pu 15a | Up | 500 | No | 3.9 | 2340 | 0.0895 | 0.0865 | 3.7E-05 |
| Pu 11 | Down | Ambient | No | - | 0.145 | 0.0302 | 0.0272 | 1.9E-01 |
| Pu 11a | Down | Ambient | No | - | 0.145 | 0.0302 | 0.0272 | 1.9E-01 |
| Pu 11b | Down | Ambient | No | - | 0.145 | 0.0113 | 0.0083 | 5.7E-02 |

TABLE B6. SUMMARY OF PuO₂ LEAK RATE EXPERIMENTS USING A 20- μ m ORIFICE - Continued

| Run Number | Tube Position | Helium Pressure, psi | Vibration | Helium Leak Rate(c), scc/sec | Total Helium Flow scc(d) | Quantity of PuO ₂ Detected, μ g(b) | | Mass Flow Ratio μ g/cc |
|------------|---------------|----------------------|-----------|------------------------------|--------------------------|---|--------------|----------------------------|
| | | | | | | Total | Net Total(e) | |
| Pu 16 | Down | Ambient | Yes | - | 0.145 | 0.0195 | 0.0165 | 1.1E-01 |
| Pu 16a | Down | Ambient | Yes | - | 0.145 | 0.0038 | 0.0008 | 5.5E-03 |
| Pu 12 | Sideways | Ambient | Yes | - | 0.145 | 0.0302 | 0.0272 | 1.9E-01 |
| Pu 12a | Sideways | Ambient | Yes | - | 0.145 | 0.0113 | 0.0083 | 5.7E-02 |
| Pu 12b | Sideways | Ambient | Yes | - | 0.145 | 0.0047 | 0.0017 | 1.2E-02 |
| Pu 17 | Sideways | Ambient | No | - | 0.145 | 0.0095 | 0.0065 | 4.5E-02 |
| Pu 17a | Sideways | Ambient | No | - | 0.145 | 0.0020 | -0.0010 | -6.9E-03 |
| Pu 13 | Up | Ambient | Yes | - | 0.145 | 0.0113 | 0.0083 | 5.7E-02 |
| Pu 13a | Up | Ambient | Yes | - | 0.145 | 0.0189 | 0.0159 | 1.1E-03 |
| Pu 18 | Up | Ambient | No | - | 0.145 | 0.0034 | 0.0004 | 2.8E-03 |
| Pu 18a | Up | Ambient | No | - | 0.145 | 0.0126 | 0.0096 | 6.6E-02 |

(a) Based on a specific activity of 0.096 Ci/g for the PuO₂ powder.

(b) Helium leak rate determined using in-line flow meter. Standard conditions: 1 atm, 25°C.

(c) The net total is the amount above the containment box background of 0.0030 μ g.

(d) The net total is the amount above the average containment box background of 0.0013 μ g.

(e) Best estimate of total flow in standard cm³. Standard conditions: 1 atm, 25°C.

TABLE B7. SUMMARY OF PuO₂ LEAK RATE EXPERIMENTS USING A 10- μ m ORIFICE^(a)

| Run Number | Tube Position | Helium Pressure psi | Vibration | Helium Leak Rate ^(c) , scc/sec | Total Helium Flow scc ^(e) | Quantity of PuO ₂ Detected, μ g ^(b) | | Mass Flow Ratio μ g/cc |
|------------|---------------|---------------------|-----------|---|--------------------------------------|---|--------------------------|----------------------------|
| | | | | | | Total | Net Total ^(d) | |
| Pu 19 | Down | 1000 | No | 2.2 | 1320 | 0.2778 | 0.2748 | 2.1E-04 |
| Pu 19a | Down | 1000 | No | 18.6 | 11160 | 0.0251 | 0.0221 | 2.0E-06 |
| Pu 20 | Sideways | 1000 | Yes | 1.3 | 780 | 0.0296 | 0.0266 | 3.4E-05 |
| Pu 20a | Sideways | 1000 | Yes | 2.2 | 1320 | 0.1341 | 0.1311 | 9.9E-05 |
| Pu 21 | Up | 1000 | Yes | 19.3 | 11580 | 0.4233 | 0.4203 | 3.6E-05 |
| Pu 21a | Up | 1000 | Yes | 1.3 | 780 | 0.0088 | 0.0058 | 7.4E-06 |
| Pu 21b | Up | 1000 | Yes | 1.7 | 1020 | 0.0025 | -0.0005 | -4.9E-07 |
| Pu 22 | Down | 500 | Yes | 0.9 | 540 | 0.0119 | 0.0089 | 1.6E-05 |
| Pu 22a | Down | 500 | Yes | 0.4 | 240 | 0.0365 | 0.0335 | 1.4E-04 |
| Pu 23 | Sideways | 500 | Yes | 2.2 | 1320 | 0.0069 | 0.0039 | 1.1E-07 |
| Pu 23a | Sideways | 500 | Yes | 1.7 | 1020 | 0.0088 | 0.0058 | 5.7E-06 |
| Pu 24 | Up | 500 | Yes | 4.3 | 2580 | 0.0069 | 0.0039 | 1.5E-06 |
| Pu 24a | Up | 500 | Yes | 0.4 | 240 | 0.0094 | 0.0064 | 2.7E-05 |
| Pu 25 | Down | Ambient | No | - | 0.036 | 0.0151 | 0.0121 | 3.4E-01 |
| Pu 25a | Down | Ambient | No | - | 0.036 | 0.0522 | 0.0492 | 1.4 |
| Pu 26 | Up | Ambient | Yes | - | 0.036 | 0.0069 | 0.0039 | 1.1E-01 |
| Pu 26a | Up | Ambient | Yes | - | 0.036 | 0.0044 | 0.0014 | 3.9E-02 |
| Pu 27 | Sideways | Ambient | Yes | - | 0.036 | 0.0025 | -0.0005 | -1.4E-02 |
| Pu 27a | Sideways | Ambient | Yes | - | 0.036 | 0.0044 | 0.0014 | 3.9E-02 |

(a) Based on a specific activity of 0.096 Ci/g for the PuO₂ powder.

(b) Helium leak rate determined using in-line flow meter. ²Standard conditions: 1 atm, 25°C.

(c) The net total is the amount above the containment box background of 0.0030 μ g.

(d) The net total is the amount above the average containment box background of 0.0013 μ g.

(e) Best estimate of total flow in standard cm³. Standard conditions: 1 atm, 25°C.

TABLE B8. SUMMARY OF PuO₂ LEAK RATE EXPERIMENTS USING A 5- μ m ORIFICE^(a)

| Run Number | Tube Position | Helium Pressure, psi | Vibration | Helium Leak Rate ^(c) , scc/sec | Total Helium Flow ^(e) , scc(e) | Quantity of PuO ₂ Detected, μ g ^{(a)2} | | Mass Flow ratio μ g/cc |
|------------|---------------|----------------------|-----------|---|---|--|--------------------------|----------------------------|
| | | | | | | Total | Net Total ^(d) | |
| Pu 28 | Down | 1000 | No | 7.4 | 4440 | 0.0113 | 0.0083 | 1.9E-06 |
| Pu 28a | Down | 1000 | No | 2.6 | 1560 | 0.0063 | 0.0033 | 2.1E-06 |
| Pu 37* | Down | 1000 | No | 5.5 | 19800 | 0.0038 | -0.0113 | -1.9E-07 |
| Pu 38* | Down | 1000 | No | 0.9 | 3240 | 0.0107 | -0.0043 | -3.3E-06 |
| Pu 29 | Sideways | 1000 | Yes | 1.3 | 780 | 0.0145 | 0.0115 | 1.5E-05 |
| Pu 29a | Sideways | 1000 | Yes | 14.9 | 8940 | 0.0038 | 0.0008 | 8.9E-08 |
| Pu 30 | Up | 1000 | Yes | 3.5 | 2100 | 0.0050 | 0.0020 | 9.5E-07 |
| Pu 30a | Up | 1000 | Yes | 6.1 | 3660 | 0.0009 | -0.0021 | -5.7E-05 |
| Pu 31 | Down | 500 | Yes | 0.4 | 240 | 0.0069 | 0.0039 | 1.6E-05 |
| Pu 31a | Down | 500 | Yes | 1.3 | 780 | 0.0101 | 0.0071 | 9.1E-06 |
| Pu 32 | Sideways | 500 | Yes | 1.3 | 780 | 0.0050 | 0.0020 | 2.6E-06 |
| Pu 32a | Sideways | 500 | Yes | 0.4 | 240 | 0.0044 | 0.0014 | 5.8E-06 |
| Pu 33 | Up | 500 | Yes | 1.3 | 780 | 0.0044 | 0.0014 | 1.8E-06 |
| Pu 33a | Up | 500 | Yes | 4.8 | 2880 | 0.0082 | 0.0052 | 1.8E-06 |
| Pu 34 | Down | Ambient | No | - | 0.009 | 0.0044 | 0.0014 | 1.6E-01 |
| Pu 34a | Down | Ambient | No | - | 0.009 | 0.0082 | 0.0052 | 5.8E-01 |
| Pu 35 | Up | Ambient | Yes | - | 0.009 | 0.0017 | -0.0013 | -1.4E-01 |
| Pu 35a | Up | Ambient | Yes | - | 0.009 | 0.0018 | -0.0012 | -1.3E-01 |
| Pu 36 | Sideways | Ambient | Yes | - | 0.009 | 0.0164 | 0.0134 | 1.5 |
| Pu 36a | Sideways | Ambient | Yes | - | 0.009 | 0.0113 | 0.0083 | 9.2E-01 |

(a) Based on a specific activity of 0.096 Ci/g for the PuO₂ powder.

(b) Helium leak rate determined using in-line flow meter. Standard conditions: 1 atm, 25°C.

(c) The net total is the amount above the containment box background of 0.0030 μ g.

(d) The net total is the amount above the average containment box background of 0.0013 μ g.

(e) Best estimate of total flow in standard cm³. Standard conditions: 1 atm, 25°C.

TABLE B9. SUMMARY OF PuO₂ LEAK RATE EXPERIMENTS USING A 5- μ m ORIFICE(a)

| Run Number | Tube Position | Helium Pressure, psi | Vibration | Helium Leak Rate(b) scc/sec | Total Helium Flow scc(e) | Quantity of PuO ₂ Detected, μ g(a) ² | | Mass Flow Ratio μ g/cc |
|------------|---------------|----------------------|-----------|-----------------------------|--------------------------|--|--------------|----------------------------|
| | | | | | | Total | Net Total(d) | |
| Pu 82 | Up | Ambient | No | - | 0.009 | 0.0042 | 0.0029 | 0.32 |
| Pu 82a | Up | Ambient | No | - | 0.009 | 0.0059 | 0.0046 | 0.51 |
| Pu 83 | Down | Ambient | Yes | - | 0.009 | 0.0095 | 0.0082 | 0.91 |
| Pu 83a | Down | Ambient | Yes | - | 0.009 | 0.0168 | 0.0155 | 1.72 |
| Pu 83b | Down | Ambient | Yes | - | 0.009 | 0.1000 | 0.0987 | 10.97 |
| Pu 83c | Down | Ambient | Yes | - | 0.009 | 0.0064 | 0.0051 | 0.57 |
| Pu 84 | Up | 1000 | No | 0.4 | 240 | 0.0009 | -0.0004 | -1.7E-06 |
| Pu 84a | Up | 1000 | No | 0.4 | 240 | 0.0008 | -0.0005 | -2.1E-06 |
| Pu 85 | Down | 1000 | Yes | 0.4 | 240 | 0.0028 | 0.0015 | 6.3E-06 |
| Pu 85a | Down | 1000 | Yes | 1.7 | 1020 | 0.0042 | 0.0029 | 2.8E-06 |
| Pu 86 | Down | 1000 | No | 3.9 | 2340 | 0.0134 | 0.0121 | 5.2E-06 |
| Pu 86a | Down | 1000 | No | 0.9 | 540 | 0.0020 | 0.0007 | 1.3E-06 |
| Pu 86b | Down | 1000 | No | 0.4 | 240 | 0.0024 | 0.0011 | 4.6E-06 |
| Pu 86c | Down | 1000 | No | 0.4 | 240 | 0.0005 | -0.0008 | -3.3E-06 |

(a) Based on a specific activity of 0.096 Ci/g for the PuO₂ powder.

(b) Helium leak rate determined using in-line flow meter. Standard conditions: 1 atm, 25°C.

(c) The net total is the amount above the containment box background of 0.0030 μ g.

(d) The net total is the amount above the average containment box background of 0.0013 μ g.

(e) Best estimate of total flow in standard cm³. Standard conditions: 1 atm, 25°C.

TABLE B10. SUMMARY OF PuO₂ LEAK RATE EXPERIMENTS USING A 10- μ m ORIFICE^(a)

| Run Number | Tube Position | Helium Pressure, psi | Vibration | Helium Leak Rate(c), scc/sec | Total Helium Flow scc(e) | Quantity of PuO ₂ Detected, μ g ^(b) | | Mass Flow Ratio μ g/cc |
|------------|---------------|----------------------|-----------|------------------------------|--------------------------|---|--------------|----------------------------|
| | | | | | | Total | Net Total(d) | |
| Pu 87 | Down | 500 | Yes | 0.4 | 240 | 0.0071 | 0.0058 | 2.4E-05 |
| Pu 87a | Down | 500 | Yes | 0.4 | 240 | 0.0019 | 0.0006 | 2.5E-06 |
| Pu 87b | Down | 500 | Yes | 0.4 | 240 | 0.0019 | 0.0006 | 2.5E-06 |
| Pu 87c | Down | 500 | Yes | 0.4 | 240 | 0.0066 | 0.0053 | 2.2E-05 |
| Pu 88 | Down | 500 | No | 0.4 | 240 | 0.0066 | 0.0053 | 2.2E-05 |
| Pu 88a | Down | 500 | No | 0.4 | 240 | 0.0052 | 0.0039 | 1.5E-05 |
| Pu 88b | Down | 500 | No | 0.4 | 240 | 0.0003 | -0.0010 | -4.2E-06 |
| Pu 88c | Up | 500 | No | 0.4 | 240 | 0.0012 | -0.0001 | -4.2E-07 |
| Pu 89 | Up | 500 | No | 0.8 | 480 | 0.0117 | 0.0104 | 2.5E-05 |
| Pu 89a | Up | 500 | No | 0.8 | 480 | 0.0024 | 0.0011 | 2.3E-06 |
| Pu 89b | Up | 500 | No | 0.8 | 480 | 0.0026 | 0.0013 | 2.7E-06 |
| Pu 89c | Up | 500 | No | 0.8 | 480 | 0.0009 | -0.0004 | -8.3E-07 |

- (a) Based on a specific activity of 0.096 Ci/g for the PuO₂ powder.
 (b) Helium leak rate determined using in-line flow meter. Standard conditions: 1 atm, 25°C.
 (c) The net total is the amount above the containment box background of 0.0030 μ g.
 (d) The net total is the amount above the average containment box background of 0.0013 μ g.
 (e) Best estimate of total flow in standard cm³. Standard conditions: 1 atm, 25°C.

TABLE B11. SUMMARY OF PuO₂ LEAK RATE EXPERIMENTS USING A 8- μ m ORIFICE^(a)

| Run Number | Tube Position | Helium Pressure, psi | Vibration | Helium Leak Rate ^(c) , scc/sec | Total Helium Flow scc ^(e) | Quantity of PuO ₂ Detected, μ g ^(b) | | Mass Flow Ratio μ g/cc |
|------------|---------------|----------------------|-----------|---|--------------------------------------|---|--------------------------|----------------------------|
| | | | | | | Total | Net Total ^(d) | |
| Pu 98 | Up | 1000 | Yes | 5.2 | 3120 | 0.1113 | 0.1100 | 3.5E-05 |
| Pu 98a | Up | 1000 | Yes | 3.0 | 1800 | 0.0082 | 0.0069 | 3.8E-06 |
| Pu 98b | Up | 1000 | Yes | 23.7 | 14220 | 0.0020 | 0.0007 | 4.9E-08 |
| Pu 98c | Up | 1000 | Yes | 1.1 | 660 | 0.0019 | 0.0006 | 9.1E-07 |
| Pu 99 | Down | 1000 | Yes | 0.87 | 520 | 0.0684 | 0.0671 | 1.3E-04 |
| Pu 99a | Down | 1000 | Yes | 1.1 | 660 | 0.0014 | 0.0001 | 1.5E-07 |
| Pu 99b | Down | 1000 | Yes | 1.1 | 660 | 0.0012 | -0.0001 | -1.5E-07 |
| Pu 99c | Down | 1000 | Yes | 2.2 | 1320 | 0.0057 | 0.0044 | 3.3E-06 |
| Pu 100 | Sideways | 1000 | Yes | 1.1 | 660 | 0.0016 | 0.0003 | 4.5E-07 |
| Pu 100a | Sideways | 1000 | Yes | 1.1 | 660 | 0.0021 | 0.0008 | 1.2E-06 |
| Pu 100b | Sideways | 1000 | Yes | 2.2 | 1320 | 0.0024 | 0.0011 | 8.3E-07 |
| Pu 100c | Sideways | 1000 | Yes | 2.2 | 1320 | 0.0017 | 0.0004 | 3.0E-07 |
| *Pu 101 | Down | 1000 | No | 1.3 | 4680 | 0.0654 | 0.0641 | 1.4E-05 |
| *Pu 101a | Down | 1000 | No | 4.8 | 17280 | 0.0082 | 0.0069 | 4.0E-07 |
| +Pu 102 | Down | 1000 | No | 1.1 | 7920 | 0.0024 | 0.0011 | 1.4E-07 |
| +Pu 102a | Down | 1000 | No | 7.8 | 56160 | 0.0030 | -0.0017 | -3.0E-08 |
| Pu 103 | Up | 1250 | Yes | 24.8 | 14880 | 0.0033 | 0.0020 | 1.3E-07 |
| Pu 103a | Up | 1250 | Yes | 1.3 | 780 | 0.0009 | -0.0004 | -5.1E-07 |
| Pu 104 | Down | 1250 | Yes | 2.2 | 1320 | 0.0008 | -0.0005 | -3.8E-07 |
| Pu 104a | Down | 1250 | Yes | 6.9 | 24840 | 0.0018 | 0.0005 | 2.0E-08 |
| *Pu 105 | Down | 1250 | No | 1.3 | 4680 | 0.0008 | -0.0005 | -1.1E-07 |
| *Pu 105a | Down | 1250 | No | 1.7 | 12240 | 0.0035 | 0.0022 | 1.8E-07 |
| +Pu 106 | Down | 1250 | No | 2.2 | 15840 | 0.0017 | 0.0004 | 2.5E-08 |
| +Pu 106a | Down | 1250 | No | 10.9 | 78480 | 0.0013 | 0.0000 | 0.0000 |

(a) Based on a specific activity of 0.096 Ci/g for the PuO₂ powder.

(b) Helium leak rate determined using in-line flow meter. ²Standard conditions: 1 atm, 25°C.

(c) The net total is the amount above the containment box background of 0.0030 μ g.

(d) The net total is the amount above the average containment box background of 0.0013 μ g.

(e) Best estimate of total flow in standard cm³. Standard conditions: 1 atm, 25°C.

DISTRIBUTION

No. of
Copies

No. of
Copies

OFFSITE

| | | | |
|----|--|-----|---|
| | A. A. Churm DOE Patent Division 9800 S. Cass Avenue Argonne, IL 60439 | | William H. Lake NRC Office of Nuclear Material Safety & Safeguards Transportation Branch Washington, DC 20555 |
| | J. J. Davis Office of Nuclear Regulatory Research Division of Safeguards, Fuel Cycle and Environmental Research NRC Division of Research Washington, DC 20555 | 261 | NRC Division of Technical Information and Document Control Washington, DC 20555 |
| 10 | W. Lahs Office of Nuclear Regulatory Research Division of Safeguards, Fuel Cycle and Environmental Research NRC Division of Research Washington, DC 20555 | | Donald R. Hopkins NRC Division of Standards Washington, DC 20555 |
| | Frank Swanberg, Jr. Office of Nuclear Regulatory Research Division of Safeguards, Fuel Cycle and Environmental Research NRC Division of Research Washington, DC 20555 | 2 | DOE Technical Information Center U.S. Department of Energy P.O. Box 62 Oak Ridge, TN 37830 |
| | Charles E. MacDonald NRC Office of Nuclear Material Safety & Safeguards Transportation Branch Washington, DC 20555 | | John A. Andersen Sandia Laboratories Albuquerque, NM 87115 |
| | C. Ross Chappell NRC Office of Nuclear Material Safety & Safeguards Transportation Branch Washington, DC 20555 | | J. K. Cole Sandia Laboratories Albuquerque, NM 87115 |
| | | | M. Pobereskin Battelle Memorial Institute 505 King Avenue Columbus, OH 43201 |
| | | 25 | W. J. Madia Battelle Memorial Institute 505 King Avenue Columbus, OH 43201 |
| | | | E. W. Schmidt Battelle Memorial Institute 505 King Avenue Columbus, OH 43201 |

No of
Copies

J. D. Yesso
Battelle Memorial Institute
505 King Avenue
Columbus, OH 43201

ONSITE

50 Pacific Northwest Laboratory

T. J. Bander
C. E. Elderkin
R. K. Hadlock
J. W. Johnston
J. Mishima (35)
P. C. Owzarski
L. C. Schwendiman
S. L. Sutter
R. K. Woodruff
Publishing Coordination (2)
Technical Information (5)

| | | | | | |
|---|--|--|--|---|------------------|
| NRC FORM 335 (7-77) | | U.S. NUCLEAR REGULATORY COMMISSION BIBLIOGRAPHIC DATA SHEET | | 1. REPORT NUMBER (Assigned by DDC) NUREG/CR-1302 PNL-3278 | |
| 4. TITLE AND SUBTITLE (Add Volume No., if appropriate) Study of Plutonium Oxide Powder Emissions From Simulated Shipping Container Leaks | | | | 2. (Leave blank) | |
| 7. AUTHOR(S) *J.D. Yesso, W.J. Madia, G.H. Beatty, E.W. Schmidt **L.C. Schwendiman, J. Mishima | | | | 5. DATE REPORT COMPLETED MONTH May YEAR 1980 | |
| 9. PERFORMING ORGANIZATION NAME AND MAILING ADDRESS (Include Zip Code) *Battelle Columbus Laboratories 505 King Avenue Columbus, Ohio 43201 **Pacific Northwest Laboratory Richland, WA 99352 | | | | DATE REPORT ISSUED MONTH August YEAR 1980 | |
| 12. SPONSORING ORGANIZATION NAME AND MAILING ADDRESS (Include Zip Code) Office of Nuclear Regulatory Research U.S. Nuclear Regulatory Commission Washington, DC 20555 | | | | 6. (Leave blank) | |
| | | | | 8. (Leave blank) | |
| | | | | 10. PROJECT/TASK/WORK UNIT NO. | |
| | | | | 11. CONTRACT NO. FIN No. B2093 | |
| 13. TYPE OF REPORT | | | PERIOD COVERED (Inclusive dates) | | |
| 15. SUPPLEMENTARY NOTES | | | | 14. (Leave blank) | |
| 16. ABSTRACT (200 words or less) To provide data to facilitate the predictions of PuO ₂ emissions through leaks in PuO ₂ shipping containers under accident conditions, a series of experiments was conducted using PuO ₂ powder and an experimental system designed to simulate a shipping container leak. Over two hundred experiments were completed. The experimental parameters investigated were the leak size/type, internal system pressure, agitation of the apparatus, leak orientation with respect to the powder location and the run time. No single parameter appeared to have any observable effect on the quantities of PuO ₂ emitted. However, there was an apparent dependency on the interaction between the orifice area and the internal pressure. The dependency took the form of a function of $A\sqrt{P}$. Although this functional form was suggested by the data, the data were not sufficient to allow a more detailed function to be determined. The results of experiments in which the run time was variable produced the observation that changes in the run time did not result in changes in the quantities of PuO ₂ emitted. This observation led to the conclusion that the majority of PuO ₂ observed is emitted during the initial pressurization of the leak tube. | | | | | |
| 17. KEY WORDS AND DOCUMENT ANALYSIS | | | 17a. DESCRIPTORS | | |
| 17b. IDENTIFIERS/OPEN-ENDED TERMS | | | | | |
| 18. AVAILABILITY STATEMENT Unlimited | | | 19. SECURITY CLASS (This report) Unclassified | | 21. NO. OF PAGES |
| | | | 20. SECURITY CLASS (This page) | | 22. PRICE S |

BIBLIOGRAPHIC DATA SHEET

STUDY OF FUEL CONTAINER LEAKS
 AND THE EFFECT OF FUEL CONTAINER LEAKS ON THE
 RELEASE OF RADIOACTIVE MATERIALS FROM SIMULATED
 FUEL CONTAINERS

U.S. Nuclear Regulatory Commission
 Washington, D.C. 20555
 Office of Nuclear Regulatory Research
 P.O. Box 217
 Bethesda, Maryland 20814

U.S. Nuclear Regulatory Commission
 Washington, D.C. 20555
 Office of Nuclear Regulatory Research
 P.O. Box 217
 Bethesda, Maryland 20814

| | |
|--|-----------------|
| REPORT NUMBER (NUREG-0038) | DATE (MAY 1980) |
| REPORT TITLE (STUDY OF FUEL CONTAINER LEAKS...) | MONTH (MAY) |
| REPORT AUTHOR (U.S. NUCLEAR REGULATORY COMMISSION) | YEAR (1980) |
| REPORT NUMBER (NUREG-0038) | DATE (MAY 1980) |
| REPORT TITLE (STUDY OF FUEL CONTAINER LEAKS...) | MONTH (MAY) |
| REPORT AUTHOR (U.S. NUCLEAR REGULATORY COMMISSION) | YEAR (1980) |

The purpose of this study is to provide data to facilitate the prediction of fuel container leak rates in fuel storage containers under accident conditions. A series of experiments was conducted using a powder and an experimental system designed to simulate a shipping container leak. The experimental results were compared with the theoretical leak rates calculated from the powder leak rate to the powder location and the time to empty the container. It was observed that the leak rate from the powder location was significantly higher than the theoretical leak rate. This discrepancy is attributed to the fact that the powder location was not a simple point source but a distributed source. The results of the experiments indicate that the leak rate varies with the powder location and the powder location is not a simple function of the powder location. In the quantitative analysis, the powder location is a function of the powder location. The powder location is a function of the powder location. The powder location is a function of the powder location. The powder location is a function of the powder location.

| | |
|---------------------------------------|------------------------|
| U.S. NUCLEAR REGULATORY COMMISSION | WASHINGTON, D.C. 20555 |
| OFFICE OF NUCLEAR REGULATORY RESEARCH | P.O. BOX 217 |
| BETHESDA, MARYLAND 20814 | |